National Aeronautics and
Space Administration

A Resilient Future for the Jet Propulsion Laboratory

Environmental Risks, Infrastructure Vulnerabilities, and Strategic Adaptation

Jet Propulsion Laboratory,
California Institute of Technology

The research was carried out at the Jet Propulsion Laboratory, California Institute of Technology, under a contract with the National Aeronautics and Space Administration (80NM0018D0004).

Jet Propulsion Laboratory
California Institute of Technology

Index

Preface

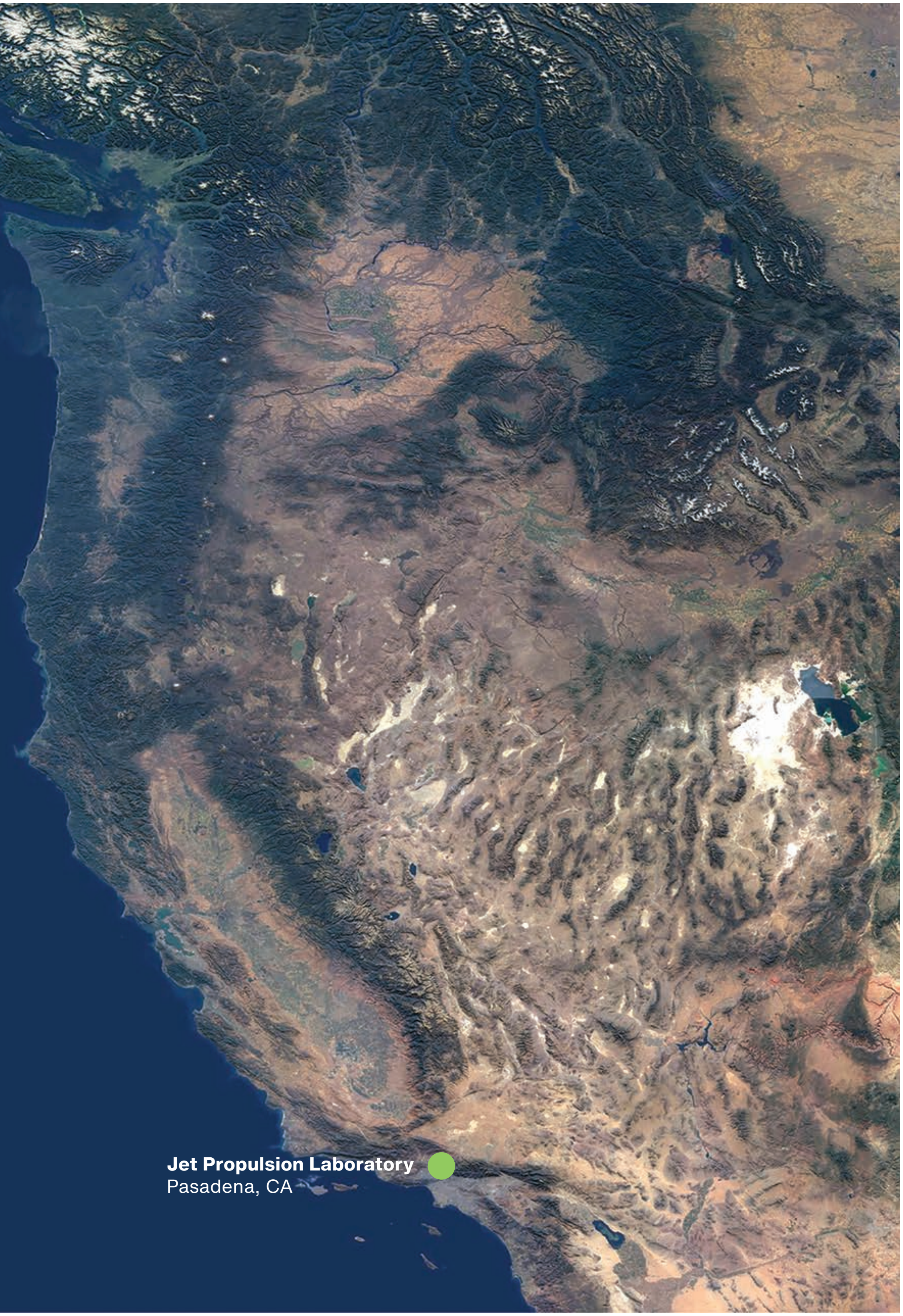
Jet Propulsion Laboratory
Pasadena, CA

About This Report

This environmental risks, infrastructure vulnerabilities and strategic adaptation report, the first for NASA's Jet Propulsion Laboratory (JPL), has been produced by an ad hoc collaborative JPL and NASA team (see Page 10). Its objective is to help characterize JPL's and the surrounding region's vulnerabilities to climate variability and environmental pressures and to support decision-makers preparing for, adapting to, and mitigating these vulnerabilities. It represents both a contribution to, and an outcome from, NASA's Climate Adaptation Science Investigators (CASI) Workgroup, a partnership between NASA's Earth Science Division (ESD) and Office of Strategic Infrastructure (OSI) to provide science-based information to support NASA's efforts to characterize potential environmental impacts at each NASA center and develop associated adaptation and mitigation plans (Appendix A). Moreover, the report is intended to represent a contribution to NASA ESD's Earth Science to Action (ES2A) strategic focus/paradigm, particularly toward ES2A's Objective 2—deliver trusted information to drive Earth resilience activities. Finally, the report and associated activities to develop it contribute to several of JPL's Lab-wide, Earth Science and Technology Directorate, and Science Division strategic plans and goals, including helping to address two of the five goals of JPL's Climate Science Plan: Goal 4—inform adaptation, resilience, and mitigation decisions—and Goal 5—increase the visibility of JPL's leadership in Earth science.

The main audiences for this report include the JPL, California Institute of Technology (Caltech), and NASA leadership who are concerned with the overall resilience and sustainability of JPL in the face of ongoing and anticipated climate and environmental challenges. To help inform these concerns and support decision-making, this assessment addresses not only JPL grounds and spaces but also the Greater Los Angeles region where the bulk of the JPL workforce lives. In addition, this report provides considerations for JPL's four additional locations—the Table Mountain Facility and the three Deep Space Network (DSN) locations (Canberra, Australia; Goldstone, California; Madrid, Spain; Appendix C). The report leverages CASI-developed Earth system and environmental change research and analysis results, combines it with additional NASA airborne and satellite remote-sensing products and other integrated Earth/environmental products, and puts the results in the context of the Laboratory's Master Planning needs, which are driven in large part by NASA's OSI. While providing direct guidance and recommendations to entities outside of NASA and JPL, for example to Los Angeles County and the cities of Los Angeles, La Cañada Flintridge, and Pasadena, is not the explicit target for this report, its authors hope that some of the information highlighted here might be useful to the resilience and sustainability efforts for other civic and nongovernment organizations in the surrounding area.

Dedication

This report is dedicated to the hundreds of JPL colleagues and thousands in surrounding communities who experienced significant loss as a result of the **January 2025 Southern California wildfires**, some of the most destructive in the state's history.

We also express our immense gratitude to the brave first responders, including those at JPL, for their extraordinary efforts to protect people and property through this crisis, as well as those colleagues who kept critical mission and Lab operations on track.

Our hope is that this report will be a trusted resource to help better understand and mitigate the impacts of events like this and other key environmental risks so that we at JPL, in concert with Caltech and NASA, may continue building a more resilient and sustainable future together.

Report Writing Team and Contributors

JPL Report Coordinators	*Duane Waliser (8000, Directorate Scientist)
	*Charlie Chen (8000, Intern/UC Davis Graduate Student)
JPL Facilities and Logistics Business Operations Office	*Diana Chen (2842, Environmental Sustainability Administrator)
	Maia Durant (2842, Group Supervisor, Facilities Strategic Planning & Real Estate)
	Paulina Natera (2813, Engineering and Design)
	Michael Uyeki (2812, Architectural Design Project Administrator)
NASA's CASI Team	Cynthia Rosenzweig (CASI Science Lead, NASA GISS)
	*Nick Pelaccio (CASI Science Support, Columbia University)

Team Members

Alex Ruane (GISS)	***Paul Stackhouse** (LaRC)	**Chris Potter** (ARC)
Brent Roberts (MSFC)	***Bradley Hegyi** (LaRC)	**Matthew Strauser** (JSC)
***Duane Waliser** (JPL)	**Patrick Taylor** (LaRC)	**John Murray** (LaRC)
Sujay Kumar (GSFC)	**Laura Iraci** (ARC)	***Benjamin Hamlington** (JPL)
Ben Cook (GISS)	**Elizabeth Wiggins** (LaRC)	

JPL Report Team **Advisory Group**

Stephanie Granger (398P)	**Daniel Limonadi** (8000)	**Jessica Neu** (3200)
Benjamin Hamlington (329C)	**Charles Miller** (329G)	**David Schimel** (329G)
Cathleen Jones (334G)	**Kimberley Miner** (398P)	**Diana Chen** (2842)

JPL REPORT TEAM

Contributors—Narrative, Environmental Information, GIS and Analysis Support

Ashley Agapep (329G), Extreme Heat Imagery

*__David Bekaert__ (3340), LULC

Carmen Boening (3290), GIS Innovation Hub

Kerry Cawse-Nicholson (329G), Extreme Heat

*__Steven Chan__ (334D), LULC

Adam Chlus (382B), Ecosystems, Albedo

Eric Fielding (329A), Earthquakes

Renato Frasson (329F), Water, LULC

*__Michelle Gierach__ (329F), Coastal Water Quality

Rob Green (382B), VSWIR, Albedo

*__Bin Guan__ (329J/JIFRESSE), Atmospheric Rivers

*__Benjamin Hamlington__ (329C), Sea Level Rise

*__Alexander Handwerger__ (334H), Landslides, LULC

Simon Hook (3200), Extreme Heat

*__Sina Hasheminassab__ (398P), Air Quality

*__Glynn Hulley__ (329G), Extreme Heat

Olga Kalashnikova (329J), Air Quality, Wildfire

Felix Landerer (329C), Groundwater

*__Christine Lee__ (329F), Inland Water Quality

*__Hugo Lee__ (398L), Fire Weather, Winds

*__Paul Lundgren__ (329A), Earthquakes

Anastasia Menshikova, GIS Innovation Hub

*__Charles Miller__ (329G), GHG, Carbon

*__Noah Molotch__ (329F / U. Colorado), Snowpack

Jessica Neu (3200), Air Quality

*__Nicholas Parazoo__ (329G), GHG/Carbon

*__Madeleine Pascolini-Campbell__ (329F), Wildfire

Annemarie Peacock (334F), GIS Innovation Hub

*__JT Reager__ (329F), Water Supply, Drought

Stanley Sander (3200), GHGs Monitoring

David Schimel (329G), Ecosystems, GHG/Carbon

*__Felix Seidel__ (329J), Wildfire

Andrew Thorpe (382B), GHG Plumes

Abhishek Chatterjee (329G), GHG

Report Production, Communications, and Review

Kimberley Rizzo (1832)

Graydon Manzke (1872)

Margaret Srinivasan (398P)

Mejs Hasan (1865)

Jocelyn Argueta (1865)

Grace Wilk (1830)

*__Jane Lee__ (1821)

Wing Sze Lui-Small (3219)

External Data and Resource Contributors

Esri—GIS and Societal Layer Information Support

*__CoreLogic__—Hazard Indices for JPL Buildings and Structures

* Lead authorship contributions in a given topical area.

Acknowledgments and Resources

The report's writing team and contributors would like to acknowledge NASA ESD's Research & Analysis and ES2A programs for their support of CASI, which provided core elements of the Earth system projection information utilized in this report, a portion of the funding that supported the writing team, and a valuable interface to NASA's OSI. Additionally, this report and its writing leverage a wide range of valuable resources and support from several JPL internal programs, organization elements, and funding sources, as well as NASA missions and projects. These include:

JPL Elements

- Earth Science and Technology Directorate
  - Center for Climate Sciences
  - GIS Innovation Hub
- Engineering and Science Directorate
  - Science Division
  - Communications Tracking and Radar Division
  - Mission Systems and Operations Division
  - Mechanical Systems Engineering, Fabrication and Test Division
- Facilities and Logistics Division
- National Partnerships Office
- Communications and Education Division
- Legislative and Government Affairs

NASA Integrated Model and Analysis Projects

- NASA Earth Exchange (NEX) Global Daily Downscaled Projections (GDDP)
- Socioeconomic Data and Applications Center (SEDAC)
- Observational Products for End-Users from Remote Sensing Analysis (OPERA)
- Global Land Data Assimilation System (GLDAS)
- National Land Data Assimilation System (NLDAS)
- Moderate Resolution Imaging Spectroradiometer (MODIS) Snow Cover products
- Modern-Era Retrospective analysis for Research and Applications, Version 2 (MERRA-2)

NASA Satellite Projects and Products

- ECOsystem Spaceborne Thermal Radiometer Experiment on Space Station (ECOSTRESS)
- Earth Surface Mineral Dust Source Investigation (EMIT)
- Gravity Recovery and Climate Experiment Follow-On (GRACE-FO)
- NASA-ISRO Synthetic Aperture Radar (NISAR)
- Orbiting Carbon Observatory 3 (OCO-3)
- Landsat
- Multi-Angle Imager for Aerosols (MAIA)

NASA Airborne Projects

- Hyperspectral Thermal Emission Spectrometer (HyTES)
- Airborne Visible / Infrared Imaging Spectrometer (AVIRIS)
- Uninhabited Aerial Vehicle Synthetic Aperture Radar (UAVSAR)
- Landslide Climate Change Experiment (LACCE) EVS-4

Executive Summary

Motivation and Background of this Report

Environmental extremes and other risks present critical challenges to the sustainability and resilience of JPL and its surrounding areas, impacting infrastructure, operations, and the well-being of the workforce. This report—developed under NASA's CASI program (Appendix A)—provides JPL's first comprehensive assessment of local environmental hazards, highlighting the complexity and urgency of these challenges. In addition to long-term shifts in temperature and precipitation associated with climate variability, JPL/NASA also faces a range of environmental hazards and extreme events—including heat waves, poor air quality, severe storms, and wildfire, which together can have immediate and lasting impacts.

The report's primary goal is to characterize JPL's vulnerabilities to environmental extremes while supporting adaptation and resilience planning. It examines hazards such as rising temperatures, deteriorating air quality, precipitation extremes, and wildfire risks, all of which impact JPL's facilities, operations, and surrounding communities. By integrating state-of-the-art Earth observations with actionable insights, this report provides a framework for addressing these challenges and serves as a potential model for other NASA centers.

Aligned with NASA's ES2A strategy, an additional goal of this report is to support the resilience efforts of civic and nongovernment organizations in the Greater Los Angeles area. Los Angeles County, the most populous county in the United States, has also been identified by the Federal Emergency Management Agency (FEMA 2023) as the highest-risk county in the nation for environmental hazards. The potential for significant loss was underscored by the January 2025 Eaton and Palisades Fires (Section 4), highlighting the need for coordinated mitigation and response strategies. By proactively addressing these issues, JPL not only ensures its operational integrity but also contributes to regional sustainability efforts.

Earth Science to Action

NASA's Earth Science to Action develops and leverages remote-sensing technology to advance science that can support civic and commercial decision-making, as well as NASA facilities and infrastructure planning.

Key Environmental Risks

Section 2 highlights the most pressing environmental risks faced by JPL and its surrounding communities. These include but are not limited to:

Rising Temperatures and Extreme Events	Projected increases in average and extreme temperatures pose risks to public health, operational costs, and ecological stability. Heat waves are becoming more frequent and intense, exacerbated by the urban heat island effect. In addition to direct health impacts, such as heat stress, elevated temperatures can disrupt energy systems due to greater air-conditioning demands and threaten sensitive infrastructure.
Santa Ana Wind Conditions	Known for intensifying and driving wildfires, Santa Ana winds (SAWs) pose significant threats to both natural and urban areas. The combination of dry, fast-moving air and low humidity can transform small brush fires into raging infernos within a matter of hours. Moreover, these winds often degrade air quality in the Los Angeles region by carrying particles, pollutants, and debris into the air, increasing particulate matter (PM) levels.
Wildfires	Increased wildfire activity can be driven by drought, changing wind patterns, and higher temperatures, threatening JPL's infrastructure, air quality, and surrounding natural resources. Events like the January 2025 wildfires underline the importance of fire-resistant infrastructure and emergency preparedness. Beyond immediate damage, post-fire effects, such as soil erosion, debris flow, and clean-up impacts on air quality, can create lasting environmental and operational challenges.
Air Quality	Persistent air pollution, aggravated by wildfires and regional emissions, can undermine workforce safety and productivity. While advancements in monitoring and mitigation have reduced certain pollutants, wildfire smoke and rising temperatures are likely to exacerbate air quality issues, making this an ongoing concern for public health.
Precipitation, Atmospheric Rivers, and Flooding	Modest increases seen in the frequency of atmospheric river (AR) events elevate the likelihood of flash flooding and infrastructure stress, requiring enhanced water management and storm preparation systems. Moreover, the increasing severity and frequency of drought conditions in the southwestern United States pose risks to consistently meeting water needs in the Greater Los Angeles area.
Water Supply and Drought	Projected decreases of the Sierra Nevada snowpack, a critical source of water for the Los Angeles region, will pose challenges for water management and necessitate the development of strategies to mitigate potential shortages. By 2050–2074, the snowpack could decrease by 40%–60% from historical averages, directly impacting water availability during the dry seasons.

Water Quality	Environmental and human-driven factors affect the quality of both inland and coastal waters. Warm temperature events, land use and land cover (LULC) change, and water management practices are driving up freshwater harmful algal blooms (FHABs) across Southern California with significant impacts on water quality, public health, and ecosystem stability. Meanwhile, water quality variations along the Los Angeles County coast are shaped by ocean temperature variations, urban runoff, wildfire debris, and harmful algal blooms.
Sea Level Rise	Rising sea level, coupled with storm surges, threaten critical coastal infrastructure within the region. As these events become more frequent, strategic coastal defense measures and adaptive urban planning are essential to mitigate risks.
Earthquakes and Landslides	Southern California, and thus JPL, is subject to impacts from earthquakes, with catastrophic consequences for an extreme event. Moreover, earthquakes can be a major driver for landslides in areas of steep topography. Moreover, heavy precipitation, particularly over areas denuded by fire, can significantly increase the potential of debris flow and landslides. Therefore, JPL's location astride the frontal toe of the San Gabriel mountains makes it susceptible to a variety of hazards and their cascading effects, including both large and local earthquakes as well as landslides and debris flows.
Land Use and Land Cover Change	Over the past two decades, the LA region has undergone significant LULC changes driven by both anthropogenic activities, such as urban expansion, and natural processes, such as wildfires. In the years following a significant wildfire, such as the Station Fire in 2009, vegetation increases and, during dry seasons, becomes wildfire fuel. The dynamic forest ecosystem where this cycle has been observed is situated a few miles north of JPL and poses risk to the Laboratory and the surrounding residential areas.
Carbon and Greenhouse Gas Considerations	JPL/NASA instruments—land-based[1], airborne[2], and spaceborne[3]—identify, quantify, and help to attribute variations and trends in methane and carbon dioxide contribution from individual sectors in the Los Angeles region. JPL's tools and data records for Los Angeles are now sufficiently mature to inform commercial, city, county, and regional emission reduction goals.

1. For example, California Laboratory for Atmospheric Remote Sensing (CLARS)
2. For example, AVIRIS and AVIRIS-NG
3. For example, Earth Surface Mineral Dust Source Investigation (EMIT) and Orbiting Carbon Observatory-2 (OCO-2) and OCO-3

JPL Infrastructure Vulnerabilities and Impacts

A minor flood, earthquake, or wildfire that inflicts limited damage to utility infrastructure could result in outages of power, gas, potable water, and wastewater services, with repairs achievable within hours to days. If they are severe enough, these disruptions could lead to the shutdown of the Lab and remote work for staff. In the case of a severe earthquake, wildfire, or flood, outages may extend for a considerably longer period, and of course the Lab itself could sustain significant damage. These vulnerabilities, explained in depth in **Section 3, are summarized here:**

Electricity	JPL primarily depends on external third-party energy suppliers for its electricity needs and lacks the on-site power-generation capabilities to meet all the Lab's energy demands. A power outage lasting a few hours would cause data centers to shut down. One lasting several days could cause significant delays in project timelines.
Natural Gas	Buildings at JPL are mostly heated by natural gas, and JPL relies on a single provider for this resource. A disruption in the sole connection to this individual provider could impact overall functionality.
Potable Water	A dependable supply of potable water is essential for upholding operational integrity and safety, as it is essential for cooling the Lab's facilities. A 24-hour outage would suspend activities in clean rooms, test chambers, and simulators. Water in sprinkler systems is also essential to ensuring Lab safety and the ability to respond to emergencies.
Wastewater	JPL does not possess its own wastewater treatment operations but instead relies on an external treatment facility for this essential service. The dependence on this connection highlights the vulnerabilities of JPL's infrastructure, as there exists only one line linking the Laboratory to the main off-site wastewater treatment facility.
Communications and Transportation	A disruption in IT communications, such as the DSN, for even an hour could have consequences for NASA's research and mission support capabilities and may lead to the loss of crucial research and mission data or hinder the ability to assist other NASA facilities effectively. An earthquake, fire, or flood could also disrupt the arrivals and deliveries of special instruments essential for space missions, posing a risk to the overall functioning and preparedness of NASA facilities.

- **Liquid and Gaseous Nitrogen** — Gaseous nitrogen, which is supplied through a third-party vendor, is a crucial component that supports the day-to-day activities and testing procedures conducted at the facility. Any interruptions in the supply of either liquid nitrogen or gaseous nitrogen could have a significant impact on the testing chamber work, potentially delaying important experiments and projects.
- **Cooling and Heating** — One important consequence of the warming temperatures anticipated at JPL is the change in energy needed to heat and cool buildings. Across most emission scenarios, cooling systems will need to be larger in future buildings at JPL, and the increasing frequency, intensity, and duration of heat waves will also add additional strain on cooling systems.

Adaptation and Sustainability Considerations

Section 3 outlines JPL's approach to resilience and sustainability:

- **Infrastructure Adaptation** — Investments in drainage improvements, cooling systems, and fire-resistant designs are essential to reduce vulnerabilities. For example, pilot projects that incorporate reflective materials and sustainable landscaping have already shown promise in mitigating heat impacts and enhancing resilience.
- **Workforce Resilience** — Proactive initiatives, such as workforce education on environmental risks, emergency drills, and support for workers who bike, walk, or ride public transit, ensure staff preparedness and safety. Programs designed to offer flexible remote work options during extreme weather events also enhance resilience while maintaining productivity.
- **Sustainable Practices** — Efforts to increase renewable energy sources, such as solar photovoltaics, and to achieve net-zero greenhouse gas (GHG) emissions highlight JPL's leadership in sustainability. By adopting water conservation measures and green infrastructure, the Laboratory mitigates its environmental footprint while promoting regional environmental health.
- **Technology Integration** — Advanced monitoring tools, such as air quality sensors and predictive analytics systems for wildfire risks, could be integrated into operational decision-making to enhance situational awareness and readiness.

Recommendations and Next Steps

Outlined in more detail in **Section 5**, the recommendations for enhancing Laboratory resilience include:

Enhanced Collaboration	Strengthening partnerships with NASA's CASI program, civic leaders, and state agencies to support regional sustainability goals. Regular dialogues and joint initiatives can ensure that adaptation strategies are comprehensive and aligned across all stakeholders. Engaging local universities and colleges with Earth science, environmental, and sustainability programs (e.g., Caltech; University of California, Los Angeles [UCLA]; University of Southern California [USC], California State University [CSU]) to augment research collaborations, student training, and data-sharing efforts that can enhance future assessments and expand their impacts.
Data-Driven Decision-Making	Expanding the use of airborne and spaceborne assets to acquire detailed environmental data and refine predictive models for heat, flood, and wildfire risks. These technologies enable precise monitoring of evolving conditions and inform proactive responses.
Regular Assessments	Establishing periodic reassessment cycles to align adaptation strategies with evolving Earth System projections and technological advancements. These updates ensure that JPL remains at the forefront of resilience planning.
Community Integration	Coordinating with the City of Los Angeles, Los Angeles County, and local stakeholders to create joint plans for emissions reduction, sustainable infrastructure, and disaster preparedness. Collaborative efforts can amplify the impact of JPL's resilience strategies on the broader community.
Convening Earth, Environment, Space, and Decision-Support Communities	In alignment with JPL's recently developed Strategic Imperative "Expand JPL's role as a convenor, host, and promoter of Earth- and space-science communities aligned with NASA's missions," integrate the enhanced collaborations, regular assessment updates, and growing collaborative efforts into a structured framework for sustained engagement and knowledge exchange. These efforts can both leverage and contribute to NASA's ES2A program to facilitate forums, workshops, and discussions that enhance resilience planning across NASA centers and the broader communities in which they are located.

Earth Science to Action Value

NASA's ES2A initiative underscores the transformative value of Earth observations in enhancing resilience to regional climate variations and environmental risks as well as their associated impacts. Leveraging spaceborne and ariborne remote sensing assets, this report exemplifies the application of NASA's Earth science capabilities to actionable insights for local and regional environmental challenges. In addition, these assets are poised to enable:

- High-resolution monitoring of land surface temperatures, atmospheric conditions, and water resource variability. Observational data provide detailed insights into emerging climate and environmental risks, such as intensifying heat waves and time-varying precipitation patterns.
- Development of predictive models that integrate remote-sensing data with ground-based observations. These models allow for scenario-based planning and informed decision-making.
- Empowerment of decision-makers through tools that translate complex Earth system and environmental data into practical adaptation strategies. NASA's Earth science research and information are positioned to enhance decision-makers' ability to respond effectively to environmental risks, benefiting JPL, NASA, and the surrounding community.

This pathfinding report helps establish a model for NASA's environmental resilience planning, integrating new technologies with institutional collaboration to address the multifaceted risks associated with Earth system variations and environmental hazards. An intention with this report is to not only to help safeguard JPL's mission-critical operations but also to enhance the sustainability of its surrounding community, reinforcing NASA's role as a global leader in Earth science for the benefit of society.

Introduction

01

Extreme weather events in the United States present significant risks and challenges. Heat waves can be intense and prolonged, leading to health impacts and increasing the potential for wildfires that threaten infrastructure and degrade air quality. In California, drought conditions have varied in frequency and duration over the last few decades, influencing the severity of heat waves and the occurrence of extreme storms such as ARs. These weather patterns together contribute to fluctuations in freshwater supplies, risks of flooding and landslides, and broader environmental and infrastructure concerns. Moreover, as noted in the Fifth National Climate Assessment (USGCRP 2023), these types of environmental extremes are becoming more variable and, in some cases, more frequent, influencing both short- and long-term environmental stability.

These extremes pose challenges for both the Greater Los Angeles region (see the Los Angeles County Climate Assessment), home to a majority of the JPL workforce, and NASA's JPL facilities. For example, the Station Fire of August–October 2009 burned more than 250 square miles in Los Angeles County and reached within a meter of JPL's main campus. Beyond immediate air quality impacts, the fire altered the local landscape, increasing the risk of debris flows during subsequent heavy precipitation events. Los Angeles County spent approximately $70 million to remove 1.3 million cubic yards of sediment from the Arroyo Seco watershed, just behind the Devil's Gate Dam, to enhance flood protection and improve natural habitat and recreational areas near JPL. More recently, the tragic impacts of the January 2025 Eaton and Palisades Fires serve as a reminder that extreme weather events—such as heat, drought, wind, poor air quality, and wildfires—can have profound effects on JPL and its workforce. (See Section 4 for a more in-depth discussion of the recent fires and their impacts.)

With more than $1.6 billion of constructed assets and about 5,500 employees and contractors living in the surrounding Los Angeles region (Appendix B), JPL's exposure to weather and environmental hazards is significant. Moreover, JPL has supporting facilities that are subject to their own unique environmental risks. These include the three DSN facilities in Goldstone, California; Canberra, Australia; and Madrid, Spain, as well as the Table Mountain Facility, about 30 miles to the northeast of JPL in the Angeles National Forest. The Bridge Fire started on September 8, 2024, burned 55,000 acres, and came within very close proximity of the facility before full containment in October (Hill 2024). It destroyed 81 structures, including over 15 homes in the nearby town of Wrightwood, home to several JPL / Table Mountain Facility employees.

In all cases, climate variations and environmental hazards pose risks to the natural, human, and infrastructure resources associated with JPL, and thus Caltech and NASA, and could have deleterious effects on JPL's ability to deliver on its mission to support NASA (Section 3). These risks could impact space mission planning, satellite mission development, spacecraft operations, ground systems, training, and testing and data analysis facilities. Potential impacts could be: 1) direct, physical impacts on JPL infrastructure and employee residences, 2) those that arise from shifting reliability and/or increasing costs of water and energy, 3) changes in safety and workforce operations related to extreme events, such as wildfire, droughts, floods, and poor air quality, and 4) from recommended or mandated GHG and carbon accounting and mitigation efforts.

To enhance resilience to environmental hazards/extremes and climate variations at its facilities, NASA established the CASI Workgroup in 2009 (Rosenzweig, Horton et al. 2011). CASI is a collaboration between NASA's ESD and OSI, supported by ESD's Research and Analysis and ES2A programs. Its mission is to strengthen resilience against environmental hazards, including extreme weather events and other risks that could impact NASA operations, while also incorporating the latest scientific research on climate variability and change. The first iteration of CASI (2009–2014) fostered collaboration among Earth scientists, applications researchers, and institutional stewards. Relaunched in 2021, CASI now builds on earlier outcomes while expanding guidance outside the boundaries of NASA centers where available and useful. By bridging Earth science expertise with NASA's risk management culture, CASI helps facilities managers adapt to evolving environmental challenges effectively. For more information on CASI, see Appendix A.

Where feasible, NASA's JPL strives to increase energy and water efficiency, reduce waste and pollution, achieve sustainable acquisition and procurement, meet sustainable supply chain efforts, reduce GHG emissions, transition to electricity that reduces carbon pollution, transition to a low-to-zero-emissions fleet and achieve near-zero emissions buildings. JPL, NASA's only federally funded research and development center (FFRDC), supports not only NASA's overall mission of innovation and development related to space-based science and technology but also NASA's goal of meeting federally mandated sustainability requirements. Specifically, as of this writing, federal facilities are required to meet The National Energy Conservation Policy Act (NECPA), Energy Policy Act of 2005 (EPAct), and the Energy Independence and Security Act of 2007 (EISA).

This report was developed in concert with the CASI program to support JPL and its managing and sponsoring institutions—Caltech and NASA, respectively—in addressing the concerns and mandates outlined above. Specifically, this report—a first of a kind for JPL—aims to serve as an example for other NASA centers through the CASI program. Key elements of this prototype report include a focus not only on the NASA center itself (i.e., JPL) but also the surrounding region where the JPL workforce lives. (See Appendix B for logistic and geographic descriptions of JPL and the Greater Los Angeles region.) In addition, the report augments the traditional, downscaled, model-based Earth system change projection information with NASA airborne and satellite remote-sensing products and other integrated Earth science and environmental information products that are becoming increasingly available and actionable.

This report represents a significant contribution to two of of the five goals of the JPL Climate Science Strategic Plan (JCSSP). These include Goal 4—inform adaptation, resilience, and mitigation decisions, and Goal 5—increase the visibility of JPL's leadership in Earth science. For Goal 4, the strategic objectives are to 1) generate the scientific basis for accurate and actionable information relevant to scientific basis for the causes, risks and solutions to environmental changes, and 2) actively engage and partner with end users and decision-making entities to maximize the societal benefit of JPL's Earth science endeavors. For Goal 5, the strategic objectives are to 1) improve internal JPL communication to better inform and engage engineers, technologists, and data scientists in Earth sciences, as well as to bring together scientists across disciplines, and 2) improve our ability to communicate our scientific findings to NASA HQ, the science community, and the public.

This report is structured as follows: Section 2 presents an overview of the climate and environmental hazards currently affecting JPL as well as how those are anticipated to change in the future. Section 3 examines JPL's resilience and sustainability perspectives, highlighting critical infrastructure vulnerabilities, providing detailed adaptation recommendations, and addressing sustainability considerations relevant to Laboratory operations, workforce sustainability, and long-term environmental goals. Section 4 summarizes the January 2025 Los Angeles wildfires and their associated impacts to the Laboratory and its workforce. Finally, Section 5 summarizes the report's key findings, emphasizing the urgency and complexity of climate and environmental challenges faced by JPL, alongside actionable recommendations for resilience and sustainability. It concludes with a roadmap for innovation, collaboration, and regional partnerships to establish JPL as a leader in climate science and adaptation strategies.

02

Environmental Risks

02

This section highlights the potential environmental and climate risks affecting JPL and the broader Los Angeles region across various geophysical factors, including temperature, precipitation, wind, air quality, wildfires, water availability, sea level rise, earthquakes, landslides, land use, and GHG emissions. A key consideration is that these factors can be coupled together, leading to compounded impacts that can be more severe than those associated with any one factor alone. Such coupling should be considered when developing mitigation and adaptation strategies for the Laboratory. The data for these quantities come from a wide range of airborne and spaceborne remote-sensing systems, Earth system model projections, and other composite information products. For the quantities and discussions that can utilize Earth system model projections (e.g., temperature, winds, precipitation), the results are typically based on an ensemble of models from the Climate Model Intercomparison Project 6 (CMIP6) that have been downscaled by NASA's Earth Exchange (NEX) team , and further processed into the forms shown here by the CASI project. To account for the uncertainty associated with future GHG emission scenarios, the Intergovernmental Panel on Climate Change (IPCC) developed a set of five shared socioeconomic pathways (SSPs) that range from a very low-emissions, sustainable pathway to a very high-emissions scenario, with low-, medium-, and high-emissions scenarios in between. For this report, the projection information from the NEX-downscaled (and CASI-processed) model data refer to low-emissions (SSP1.26), medium-emissions (SSP2.45), and high-emissions (SSP3.70) scenarios. Further information on the model projection data, SSPs, NEX downscaling, and CASI processing is given in Appendix D. In addition, although the Earth projection data are available out to 2100, most of the analysis and illustrations will focus on the next 10–20 years for near- and mid-term facility planning purposes.

2.1 Rising Temperatures and Extreme Events

Global warming has led to rising temperatures worldwide, with urban areas such as the greater Los Angeles region particularly vulnerable due to its large population, economic activity, and geographic location. Over the past century, Southern California has experienced increases in average, maximum, and minimum temperatures (He and Gautam 2016). As temperatures continue to rise, the Los Angeles region faces significant challenges, impacting the local environment, public health, economy, and urban infrastructure. Heat waves, wildfires, and water scarcity are highly coupled and are expected to become more frequent and severe, placing considerable strain on the region's resources. Public health will also likely suffer, with an increase in heat-related illnesses, while the local economy may struggle with rising energy costs. These impacts come as Los Angeles is already grappling with an increase in the severity and frequency of heat waves, limited water supply, and continued poor air quality punctuated by extreme events, typically from wildfires.

The public health implications of rising temperatures are particularly concerning. Extreme heat is one of the most serious health impacts of climate change, particularly for the Los Angeles area. Heat stress is the leading cause of weather-related deaths and can increase the risks of heat-related illness, such as cramps, exhaustion, and heat stroke, while also exacerbating underlying conditions such as cardiovascular disease, diabetes, mental health, and asthma. Additionally, extreme heat can heighten the risks of accidents and the spread of some infectious diseases (Hall, Berg et al. 2018). Vulnerable populations, such as the elderly, children, and people with pre-existing health conditions, are especially at risk.

As temperatures rise, so does the demand for energy, particularly for air-conditioning. This increased demand can strain the power grid, potentially leading to blackouts or the need for rolling outages, as seen during the 2020 California heat wave. Residents and businesses in the Los Angeles region will likely experience higher energy bills as they rely more heavily on air-conditioning to stay cool during increasingly hot days. The increased energy demand also has environmental consequences as most of the energy consumed in the Los Angeles region is still produced from fossil fuels. This creates a feedback loop in which higher energy consumption leads to increased carbon emissions, further accelerating rising temperatures.

2.1.1 Heat Waves

One of the most direct consequences of rising temperatures is the increasing frequency, intensity, and duration of heat waves in the Los Angeles region. A heat wave is commonly defined as a period of at least three consecutive days exceeding a regional air temperature threshold based on daily and monthly climatological percentiles (Meehl, Tebaldi et al. 2009). Perkins and Alexander (2013) identified three main heat wave definitions in the climate science literature: (1) the excess heat factor (EHF), which is based on three-day averaged daily mean temperature, (2) CTX90pct, defined as the calendar day 90th percentile of maximum air temperature (Tmax) based on a 15-day window centered on a given day, and (3) CTN90pct, defined as the threshold in the calendar day 90th percentile of minimum air temperature (Tmin). Heat waves generally result from either large-sale high-pressure systems, also known as blocking highs, or synoptic scale ridging, which generates warm and dry descending air (Hulley, Dousset et al. 2020). Due to its geographical location, the Los Angeles region is particularly vulnerable to more intense and frequent heat waves. Rising temperatures, shifts in weather patterns, and the urban heat island effect (discussed below) all exacerbate the risks associated with heat waves in the region.

The Los Angeles region has experienced a noticeable increase in the number of extreme heat days, defined as days with temperatures exceeding 95°F (35°C). If global warming continues, the frequency and severity of heat waves are expected to rise further. Hulley, Dousset et al. (2020) examined heat waves from 1950 to 2020 using three heat wave severity metrics and found an increase in the number of heat waves per year across inland urban, coastal urban, and rural areas in Southern California (Figure 2-1). Although all areas showed an increase in the number of heat waves, inland urban areas experienced stronger increases than coastal urban areas, demonstrating that heat waves affect different locations in distinct ways due to local climate variations and differences in vegetation. In addition, the urban heat island effect plays a significant role in intensifying heat waves in the Los Angeles region. This occurs when urban areas, with their abundance of asphalt, concrete, and buildings, absorb and retain more heat than surrounding rural areas. In densely populated areas, the urban heat island effect can cause temperature differences of several degrees compared to outlying areas, resulting in higher daytime and nighttime temperatures, and thus reduced overnight cooling.

Climate change is also leading to prolonged high-pressure systems known as heat domes. These heat domes trap heat in a particular area for days or even weeks, creating extended periods of higher temperatures as cooler air is prevented from moving in. Due to its location, situated between the Pacific Ocean and the desert, the Los Angeles region is particularly susceptible to heat domes. Recent studies have also shown that the probability of a heat dome settling over the Los Angeles region and remaining in place for longer periods has increased due to changes in the jet stream caused by warming in the Arctic. As weather patterns continue to shift, the Los Angeles region may experience more frequent and intense heat domes in the future, resulting in more severe heat waves.

Furthermore, heat waves contribute to longer and more intense drought periods in the Los Angeles region. As temperatures rise, evaporation rates increase, depleting local water supplies, including rivers, reservoirs, and aquifers. The Los Angeles region is heavily reliant on imported water from sources such as the Colorado River and the Sierra Nevada snowpack, both of which are vulnerable to the effects of heat waves and droughts. Reduced water availability during prolonged heat waves can have severe consequences for both the natural environment and human populations. Higher temperatures and reduced precipitation disrupt local ecosystems, endangering wildlife and plant species that depend on stable environmental conditions. Lastly, longer and more intense heat waves can weaken plant life, making it more susceptible to pests and diseases, which can have cascading effects on local biodiversity. (See Section 2.6 for further discussion on freshwater resources and variability.)

FIGURE 2-1

Heat wave time series and trends from 1950 to 2020 for Southern California (A) inland urban, (B) coastal urban, and (C) rural regions for three heat wave severity metrics: (top) frequency (number/year), (middle) intensity (°C), and (bottom) duration (days). Statistically significant (p < 5%) trend lines and stats are shown for the three different heat wave definitions discussed in the text: EHT, Tmin95, and Tmax95 (Hulley, Dousset et al. 2020).

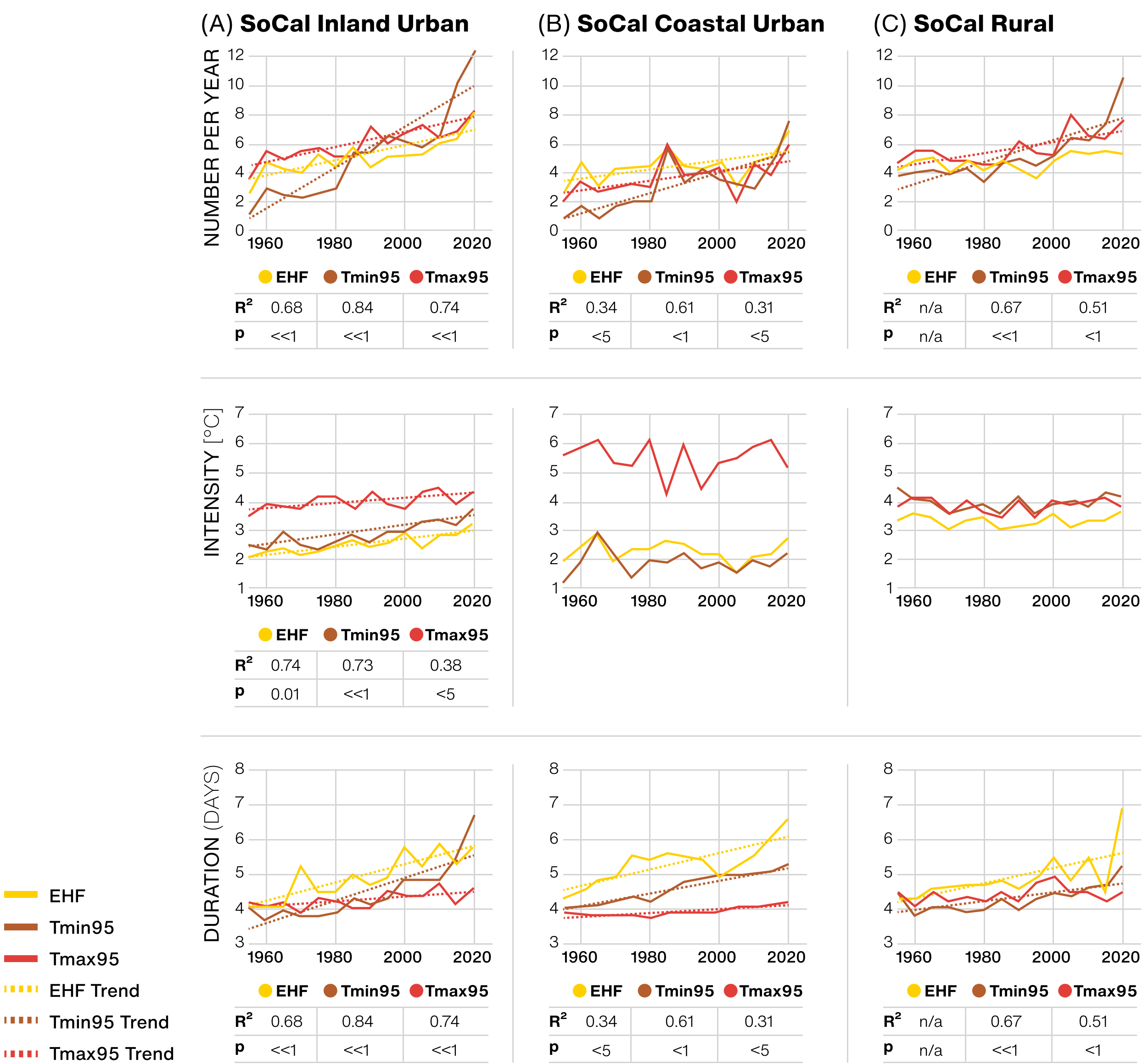

2.1.2 Extreme Heat Maps

To illustrate how extreme heat will manifest in terms of patterns for the Los Angeles region and the Laboratory, Figure 2-2 shows a land surface temperature (LST) image of the Los Angeles region at 70 m resolution retrieved from ECOSTRESS with areas of JPL, downtown Los Angeles, and other local hotspots highlighted on the map. During heat waves, and especially at nighttime, inland urban areas in San Bernardino and Riverside counties experience the hottest temperatures since they are too far inland to benefit from onshore marine breezes that typically cool the coastal areas during heat wave events. Notable in the image are the elevated temperatures over paved surfaces such as roads, freeways, and parking lots, since asphalt surfaces have high heat capacity and retain the heat for longer periods into the night.

ECOSTRESS Land Surface Temperature over Los Angeles

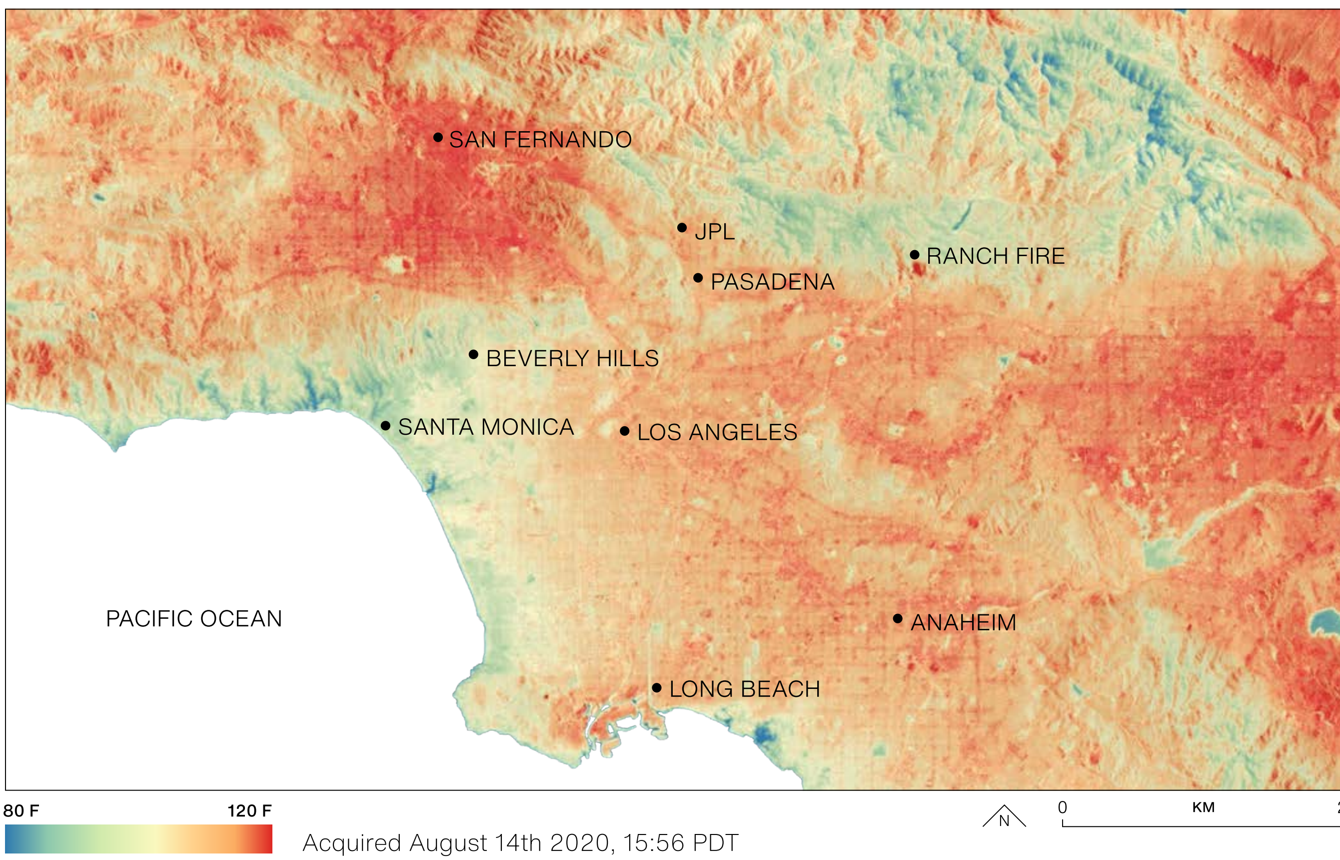

Acquired August 14th 2020, 15:56 PDT

FIGURE 2-2

LST of the Los Angeles region based on satellite observations from the ECOSTRESS thermal infrared remote-sensing instrument on the International Space Station (ISS) for August 14, 2020, at 15:56 PDT.

Figure 2-3 shows a high resolution (5 m) LST image of JPL from HyTES flown on a small utility aircraft on March 26, 2022, at 17:44 PDT. At this spatial resolution, the hotter paved areas, such as the West Lot parking lot and roads within JPL, are clearly visible and are as much as 30°F–50°F (17°C–18°C) hotter than vegetated areas and roofs of buildings that cool down much faster at nighttime. Inset pictures show Mariner Road, which was painted with American Biltrite's DuraShield reflective coating in 2022 to test the efficacy of reflective paint surfaces in cooling road surfaces. The temperatures over Mariner Road in this image show cooling of about 10°F–15°F (6°C–8°C) relative to unpainted roads in the lab.

Jet Propulsion Laboratory: HyTES Land Surface Temperature

March 26, 2022
5:44PM Local TIme

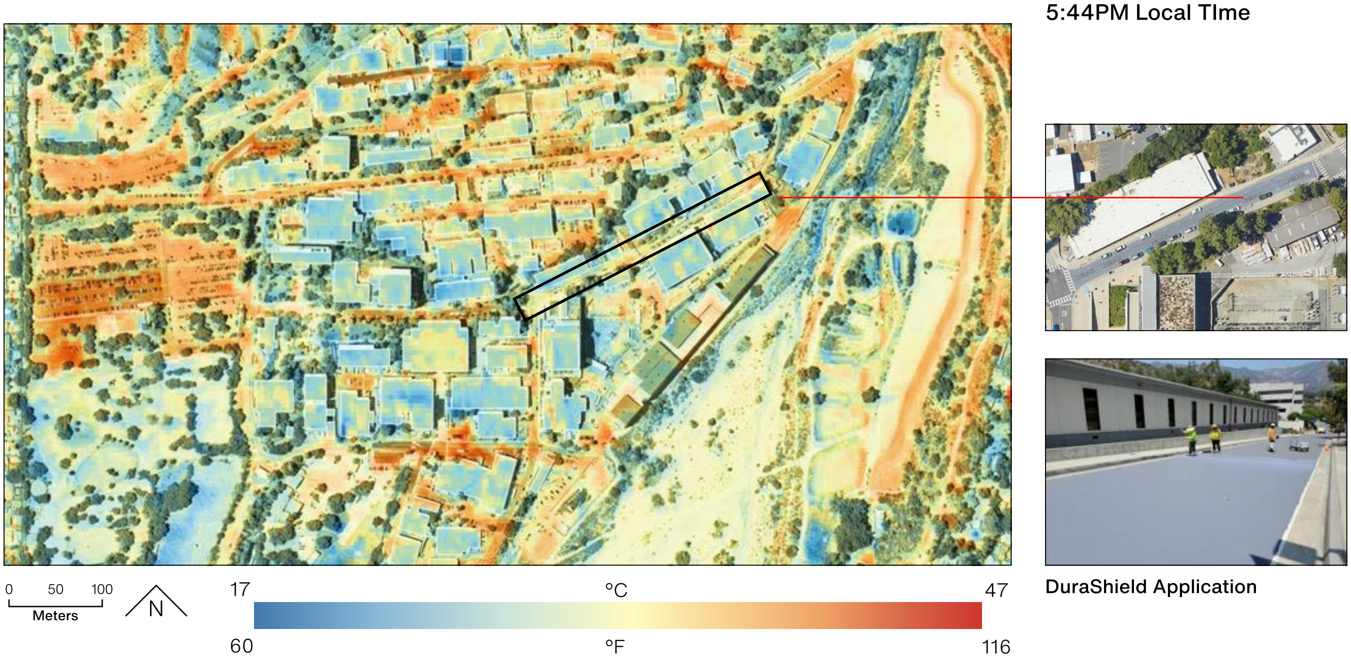

FIGURE 2-3

LST of JPL based on airborne observations from the JPL HyTES thermal infrared remote-sensing instrument on March 26, 2022, at 17:44 PDT. Inset pictures show Mariner Road and the application of American Biltrite's DuraShield reflective coating in May 2021.

Rising temperatures are expected to impact JPL operations moving forward. Historically, outside maximum average air temperature for the Lab ranges from about 88°F (31°C) in the summer to about 67°F (19°C) in the winter. The record daily maximum temperature captured by the weather station installed on the roof of B301 in the JPL Oak Grove campus in March 2021 reached 107°F (41.7°C) on September 4, 2022, while the lowest daily minimum temperature was 35.5°F (1.94°C) recorded on February 26, 2023.

2.1.3 Future Projections

Projections of future climate indicate that the Los Angeles area will experience higher maximum temperatures, more days of extreme heat, and fewer days of frost, independent of the climate-scenario considered. Specifically, projections indicate that the hottest annual temperature will increase by 2.5°F by the year 2045 (Figure 2-4A). The projections also predict the number of hot days per year will increase by about 25 to 33 days (a hot day is defined as a day on which the temperature exceeds the 90th percentile based on the 1995–2014 baseline; Figure 2-4B). Finally, the projections show that the number of "frost" days, when the minimum temperature is below the freezing point of 32°F, will fall from a total of two days in 2005 to only one day by 2045 (Figure 2-4C). These projections are based on historical observations and model simulations for low-emissions (SSP1.26), medium-emissions (SSP2.45), and high-emissions (SSP3.70) climate scenarios (Appendix D).

These changes in temperature extremes are expected to affect the JPL campus in several ways. More frequent "hot" days will increase reliance on air-conditioning for cooling, which will increase annual energy and maintenance costs. Additionally, hotter temperatures and more frequent "hot" days increase the potential for wildfires in the Los Angeles region. Along with the direct physical threat to Laboratory facilities and employee dwellings, wildfires degrade air quality. This, in turn, could negatively affect the health of JPL's employees. Smoke from wildfires can also strain air filtering in some buildings, which could provide problems for clean rooms and other facilities housing mission-critical equipment.

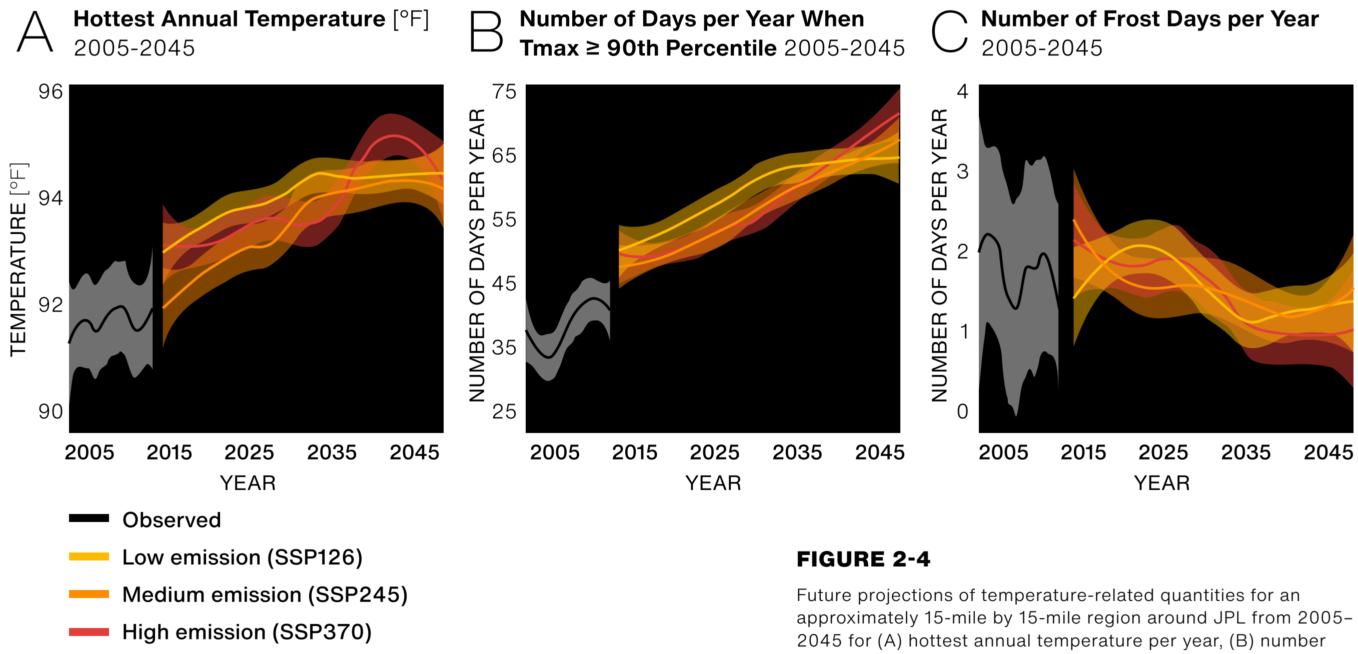

FIGURE 2-4

Future projections of temperature-related quantities for an approximately 15-mile by 15-mile region around JPL from 2005–2045 for (A) hottest annual temperature per year, (B) number of hot days per year, and (C) number of frost days per year. The green, yellow, and red lines show projections for low-, medium-, and high-emissions scenarios, and the gray is based on past observations. Shading represents uncertainty. See Appendix D for source and further information, including an explanation of the gap between the observations and model projections.

2.2 Santa Ana Wind Conditions

In the Los Angeles region, a key environmental change concern is its impact on the SAWs and the wildfires that often accompany them; See Section 4 for a recent and extreme case with significant impacts to JPL and its workforce. SAWs are dry, and often warm, strong winds (~30–60 mph, with severe cases exceeding 70 mph) that typically occur in fall and winter when high-pressure systems form to the east of California, typically over Nevada, Utah, and northern Arizona. These systems create a pressure gradient between this region to the east and the California coastline (Gershunov, Guzman Morales et al. 2021). As SAWs move westward through the Sierra Nevada and other mountain ranges, and then downslope to the Los Angeles Basin, the air heats up and dries due to adiabatic compression. Known for fueling wildfires, SAWs pose significant threats to both natural and urban areas. The combination of dry, fast-moving air and low humidity can transform small brush fires into raging infernos within a matter of hours. SAWs have driven some of Southern California's largest wildfires, including the 1961 Bel Air Fire, the 1993 Laguna Fire, the 2003 Cedar and Old Fires, the 2007 Witch and Canyon Fires, and most recently the Palisades and Eaton Fires (Section 4).

Recent research has identified two types of SAWs—hot and cold—based on Southern California coastal temperatures. Hot SAWs are associated with some of the highest temperatures in the region, while cold SAWs are linked to some of the coldest. Cold SAWs are characterized by the strongest wind speeds, whereas hot SAWs are drier and last longer (Gershunov, Guzman Morales et al. 2021). Wildfires are more commonly associated with hot SAWs (Figure 2-5). From 1948 to 2018, 90% of SAW-driven wildfires and 95% of the burned areas were linked to hot SAWs. Cold SAWs are less likely to trigger wildfires due to higher humidity, shorter duration, and the likelihood of preceding rainfall. In contrast, hot SAWs are longer, drier, and warmer, which increases fire risk (Gershunov, Guzman Morales et al. 2021).

In addition to driving wildfires, SAWs often degrade air quality in the Los Angeles region by carrying particles, pollutants, and debris into the air, increasing PM levels. This can exacerbate respiratory conditions, such as asthma and bronchitis, especially among vulnerable populations, such as children, the elderly, and those with pre-existing health conditions (Corbett 1996).

FIGURE 2-5

(A) Histogram of acres burned by wildfires in coastal Southern California that started during hot (red) and cold (gray) SAW events, and (B) domain map and fire perimeters for wildfires occurring during hot and cold SAW days (Gershunov, Guzman Morales et al. 2021).

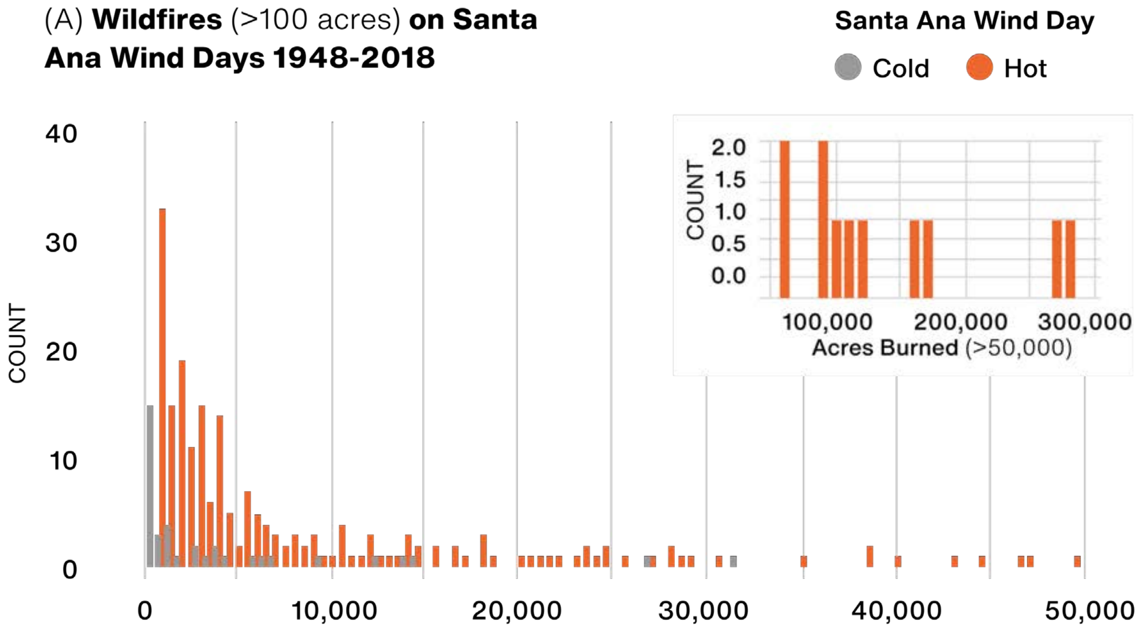

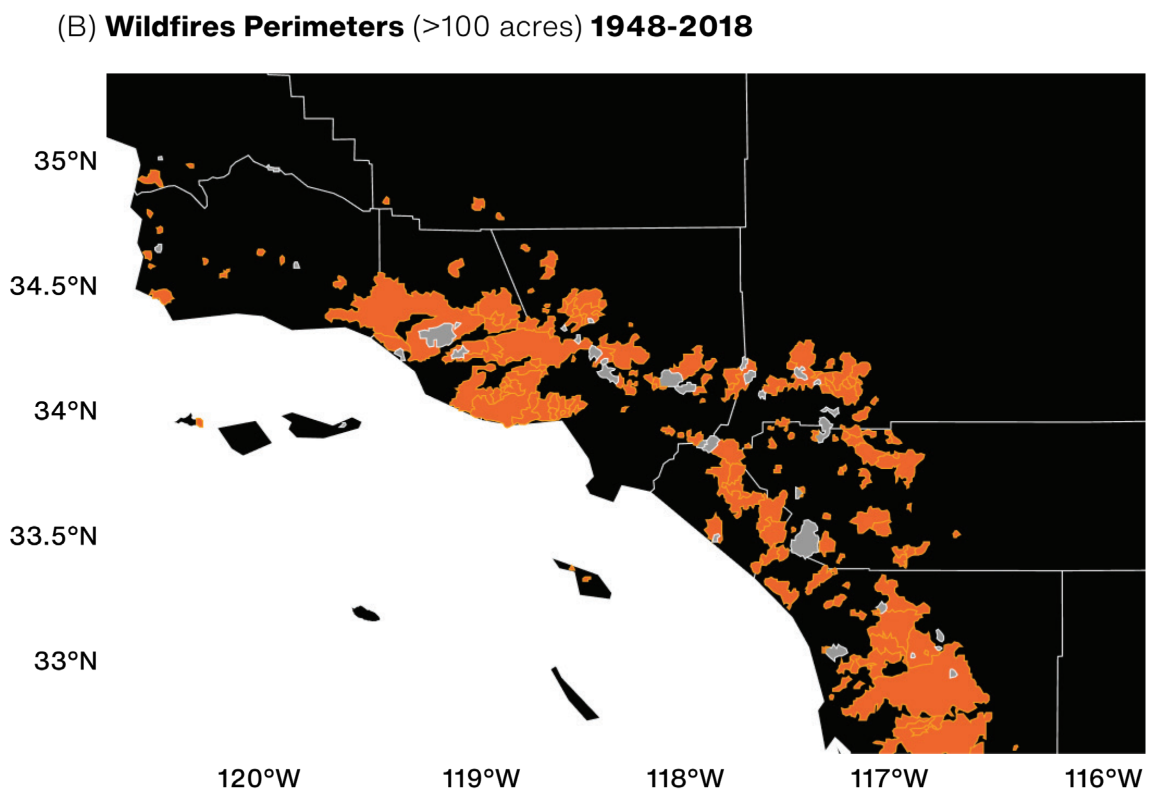

2.2

2.2.1 Future Projections

Climate change is expected to reduce overall SAW activity, primarily by decreasing their frequency rather than their wind speeds. Projections by Guzman-Morales and Gershunov (2019), based on statistical downscaling from eight global climate models, suggest a seasonal decline of 18.5% ± 4.5% in SAW activity by the late 21st century. While SAW frequency is expected to drop significantly, their intensity (wind speed) is projected to decrease to a lesser extent (Guzman-Morales and Gershunov 2019). This reduction in frequency, however, must also be considered in conjunction with the potential changes in the frequency and severity of drought in the region, which increases the potential impact of any given SAW event.

These projections for wind speed indicate a decreasing trend in the number of “high” wind days each year. A high wind day is a day when the projected wind speed exceeds the 95th percentile from a baseline period (2015–2025; Appendix D). Figure 2-6 shows the trend in the number of high wind days from 2015 to 2095 under low-, medium-, and high-emissions scenarios for JPL and the surrounding area.

Number of Days per Year where Wind speed ≥ 95th Percentile

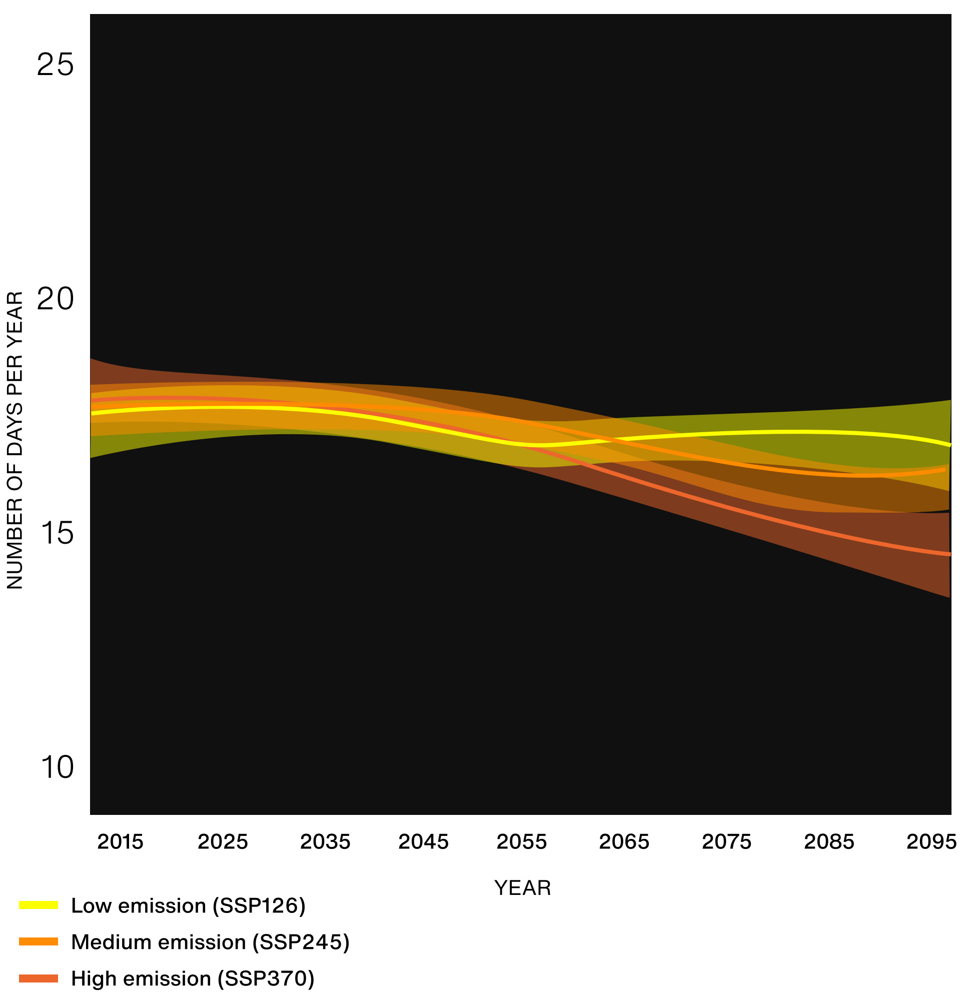

FIGURE 2-6

Projected number of days per year from 2015 to 2095 when wind speed is ≥ 95th percentile from 2015 to 2025 baseline, for low-, medium-, and high-emissions scenarios. See Appendix D for source and further information.

2.3 Wildfires

Wildfires, sometimes referred to as wildland fires, are a natural phenomenon and an inherent component of California's ecosystem and its evolution. Wildfires are influenced by a range of factors, including weather patterns, vegetation, and human activity. Beneficial fires, often referred to as low-intensity or prescribed fires, play a critical role in maintaining healthy ecosystems by reducing excess vegetation, recycling nutrients, and preventing fuel buildup. In contrast, catastrophic wildfires are high-intensity events that can cause widespread destruction to ecosystems, property, and human life. Landscape management, such as controlled burns and other fuel-reduction strategies, is essential to reduce the risk of catastrophic wildfires and restore the natural fire regimes that sustain resilient ecosystems. Los Angeles County has implemented several fuel-management programs, prescribed burns (similar to the historical practices of the area's indigenous people), and community fire protection plans aimed at reducing fuel loads and protecting critical infrastructure. Collaboration between federal, state, and local agencies, as well as community involvement, is key to adapting to an increasingly fire-prone future. JPL's fire response capabilities and how they worked in concert with other agencies during the January 2025 Eaton Fire is discussed in Section 4.

The frequency, intensity, and scale of large wildfires have been steadily increasing in recent decades, and climate change is expected to exacerbate this trend, leading to devastating consequences for the environment, the economy, and communities. Figure 2-7 illustrates that 18 of the largest 20 wildfires (by acres burned) in California over the last century occurred since 2000. This trend is also highlighted in Figure 2-8, which shows that the number of acres burned (in millions) by wildfires each year has increased over time since 1950.

Top 20 Largest California Wildfires
1933-2021

FIGURE 2-7

The top 20 wildfires in California's history by acres burned as of September 10, 2021. From the California Department of Forestry and Fire Protection (CAL FIRE).

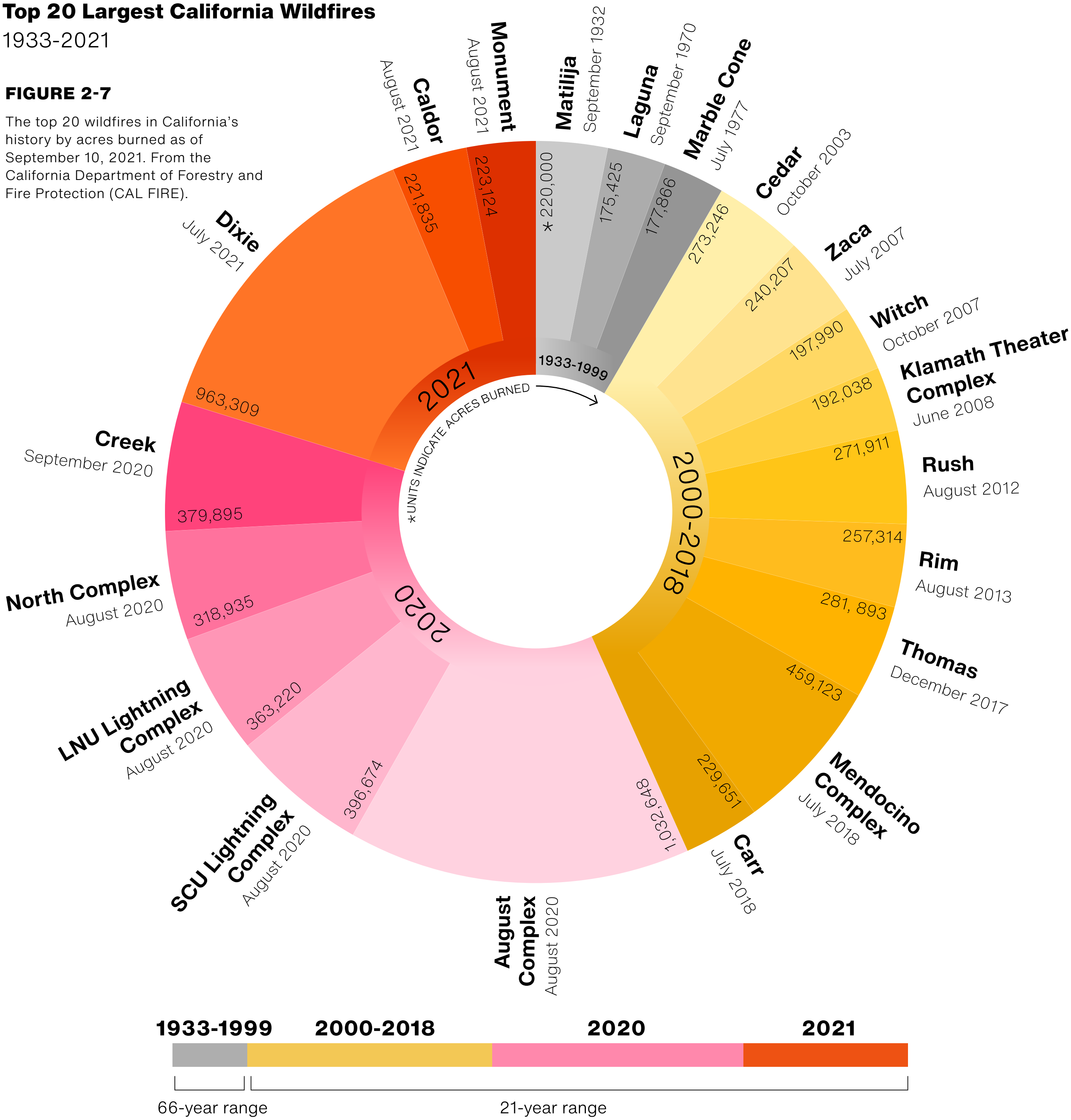

Along with human activity, the occurrence and evolution of wildfires are primarily influenced by three factors: fuel, weather, and topography (Holsinger, Parks et al. 2016). Rising temperatures, extended droughts, and shifting wind patterns can create the perfect conditions for more frequent and intense wildfires (e.g., Section 4). A warmer climate will be more effective at pulling moisture from the soil and vegetation into the air, leaving forests, grasslands, and shrubs dry and highly flammable. In most of California and especially in the Los Angeles region, this drying effect is particularly effective during the summer and fall months, when temperatures can soar and humidity levels typically drop. Such conditions make it easier for flames to spread rapidly and burn for longer periods. As a result, the number of wildfires and the number of acres burned by wildfires has increased since 1950 (Figure 2-7 and Figure 2-8).

As a reminder of the discussion in Section 2.2, another key driver for catastrophic wildfires is dry and gusty SAWs in Southern California. Guzman-Morales and Gershunov (2019) found that climate change is projected to reduce the overall frequency of SAWs, particularly during the early and late parts of the season. However, the core period of Santa Ana activity (November–January) is expected to experience less significant reductions. This shift, coupled with decreasing fall precipitation, could extend the duration of critical fire weather conditions into the winter months. The overlap of drier conditions and sustained wind activity may exacerbate wildfire risks in Southern California, despite the overall decline in SAW frequency.

Statewide Annual Acres Burned
1950-2023

This graph shows the number of acres (in millions) burned by wildfires in California each year.

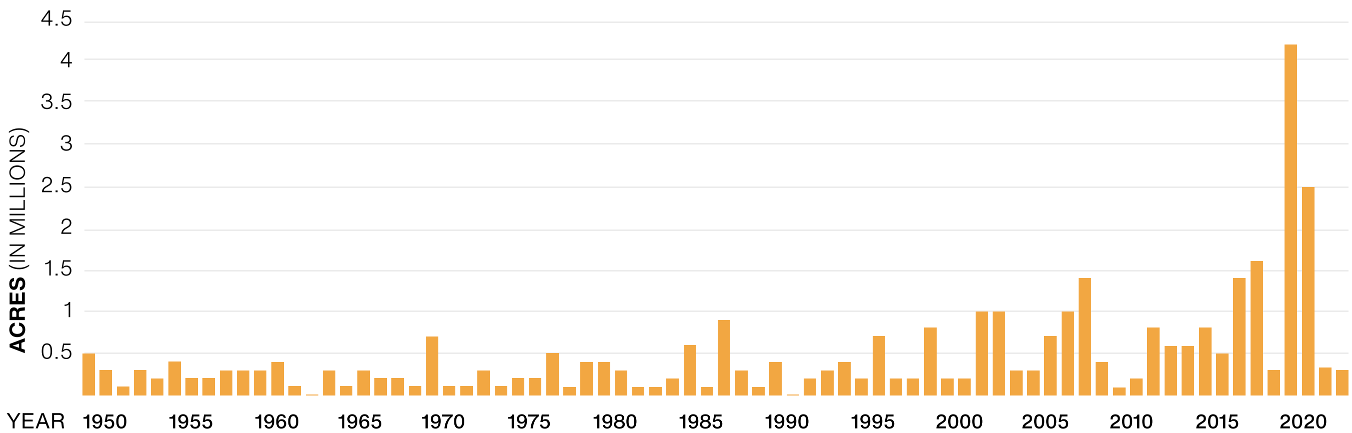

FIGURE 2-8

Number of acres (in millions) burned by wildfires in California each year from 1950 to 2023 (State of California Office of Environmental Health Hazard Assessment, https://oehha.ca.gov/climate-change/epic-2022/impacts-vegetation-and-wildlife/wildfires).

Historically, California's wildfire season has been confined to the summer and fall months, but climate change is altering the timing of these fires. Longer dry spells and hotter temperatures allow fires to start earlier in the year and persist longer into the fall and even winter months. This extended fire season has led to greater challenges for firefighters and emergency management agencies, who must deal with fires in what was previously considered the "off-season."

For JPL, critical infrastructure and workforce safety and viability are vulnerable to wildfires. As mentioned in the introduction, the 2009 Station Fire reached within a meter of JPL, the 2024 Bridge Fire surrounded JPL's Table Mountain Facility, and January 2025 Palisades and Eaton Fires had tremendous impacts on JPL and its workforce (Section 4). The occurrence of wildfires in proximity to JPL and its facilities can lead to power, water, and communications disruptions; workforce impacts; and challenging emergency response efforts and recovery processes. In addition, wildfires can negatively impact employee health due to worsening outdoor air quality, which can result in facility impacts and mandatory telework protocols. The Station Fire in 2009, Bobcat Fire in 2020, and Palisades and Eaton Fires all produced high levels of fine PM, $PM_{2.5}$, which affected JPL employees and facilities. Wildfires also leave a lasting impact on the local environment surrounding the Laboratory. Post-wildfire landscapes are more prone to flooding, mudslides, and debris flows. The JPL Arroyo Seco parking lot, for example, has experienced flooding that extended over portions of the on-Lab parking areas. It is theorized that the flooding was due, in part, to increased sediment flow since the 2009 Station Fire, which covered the bottom of the adjacent Arroyo Seco flood plain (AC Martin Partners Inc. 2012a) but has since been removed, as discussed in the Introduction.

In Southern California, human activity plays a significant role in increasing wildfire risk, particularly in areas where urban development meets wildland ecosystems. Power lines, vehicles, and other human activities can ignite wildfires, especially during critical fire weather conditions. As the population in Los Angeles County grows, managing human-caused ignition sources becomes even more critical.

2.3.1 Future Projections

It is difficult to project the trend in future wildfire occurrence, although a useful construct for this purpose is using a Fire Weather Index (FWI). A FWI is a meteorologically based index to determine whether conditions are right for forest fire ignition and spread by considering variables such as temperature, humidity, wind speed, and dryness of fuels. Developed by the Canadian Forestry Service, these indices are used worldwide to estimate fire danger (EEA 2024).

FWI for the Los Angeles region were estimated for both moderate (N15) and very high wildfire danger (N45) for the projections associated with the low-, medium-, and high-emissions scenarios (Figure 2-9). Analysis shows that the frequency of moderate fire danger in Los Angeles is projected to remain relatively constant through 2045, hovering between 210 and 220 days per year under all climate scenarios. However, the frequency of high fire danger is expected to increase, from about 50–55 days per year to roughly 55–60. These projections show the need to refine fire management, improve early warning systems, and prioritize resources for high-risk areas.

FIGURE 2-9

FWI for (A) moderate (N ≥ 15) and (B) very high danger (N ≤ 45) for the Greater Los Angeles region, for low-, medium-, and high-emissions scenarios. See Appendix D for source and further information, including an explanation of the gap between the observations and model projections.

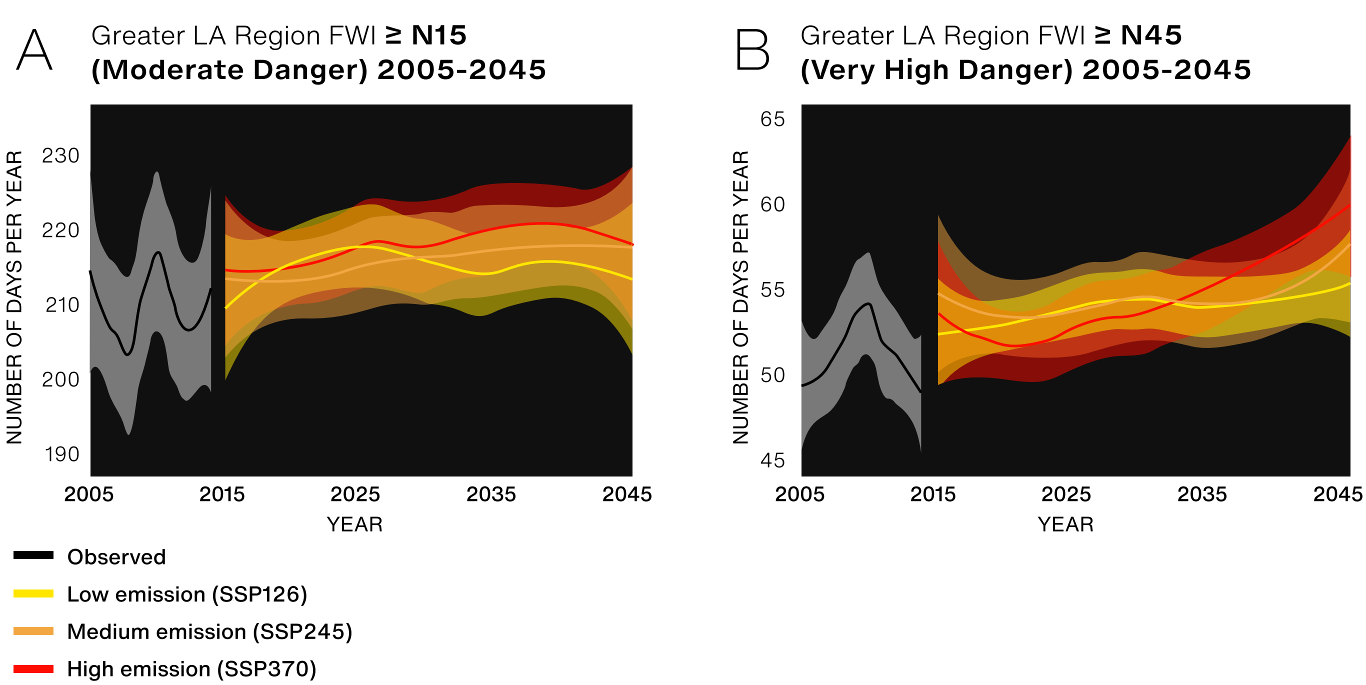

2.4
Air Quality

The Los Angeles region faces significant air quality challenges due to its unique geography, dense population, and diverse pollution sources. Current air quality challenges are primarily driven by emissions from the transportation sector, industrial activities, and wildfires (Section 2.3), as well as by meteorological conditions. Despite significant air quality improvements over the past few decades, the Los Angeles region still exceeds National Ambient Air Quality Standards (NAAQS) maximums for ozone (O_3) and PM with diameter 2.5 µm or less ($PM_{2.5}$; Figure 2-10), experiencing some of the worst air pollution in the nation.

Stringent regulations on mobile sources have played a crucial role in lowering $PM_{2.5}$ and O_3 levels in the region (Hasheminassab, Daher et al. 2014). Heavy-duty diesel trucks, in particular, are significant sources of nitrogen oxides (NOx), a key pollutant that creates ozone, and diesel PM (DPM), the primary contributor to overall air toxics cancer risk in the region (South Coast Air Quality Management District 2021). These regulations have included measures such as retrofitting older vehicles with cleaner technologies and enforcing tighter emissions standards for new trucks. As a result, there have been notable reductions of DPM, a minor but important health-relevant component of $PM_{2.5}$, across the Los Angeles region, with reductions of up to 17% in the vicinity of JPL between 2010 and 2019 (Figure 2-11).

While JPL is situated away from major primary pollution sources, it is usually downwind of the Los Angeles region, particularly during daytime, and thus affected by secondary-formed $PM_{2.5}$ and elevated ozone. The Lab's foothill location also makes it particularly susceptible to wildfire smoke. JPL has an ambient air quality monitoring station equipped with state-of-the-art instruments that continuously monitor outdoor air quality, including various gaseous and PM species. This is complemented by a network of low-cost PurpleAir PM sensors distributed across the Lab, established by the Technical Facility Management (TFM) team, providing continuous monitoring of ambient PM levels (Figure 2-12). Selected measurements from the air monitoring station and PM data from the PurpleAir sensors are seamlessly integrated into an online real-time dashboard (Figure 2-13). JPL's TFM team uses this dashboard to make operational decisions, such as shutting down clean rooms during high-pollution episodes caused by events such as wildfires or fireworks.

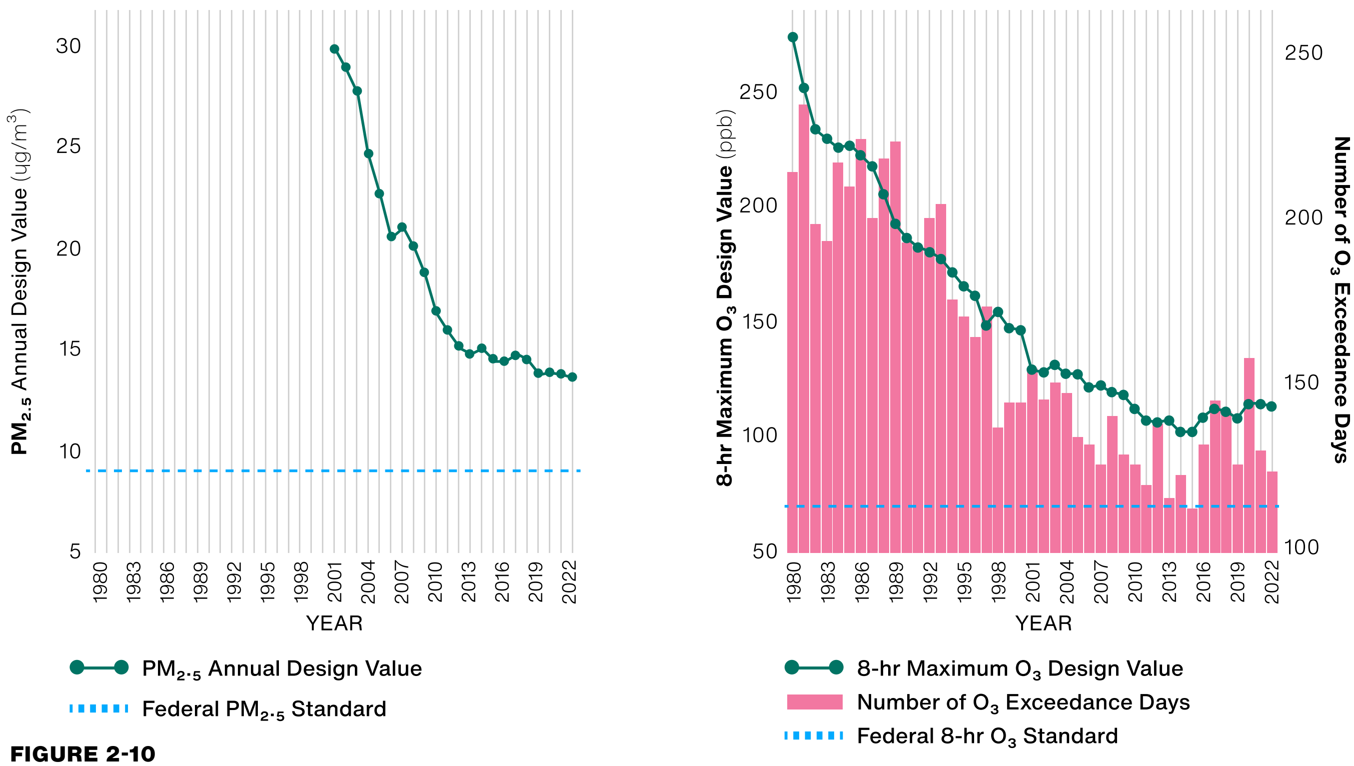

FIGURE 2-10

Historical trends in ozone (O_3) and $PM_{2.5}$ in the South Coast Air Basin. The "design value" is a metric used to assess attainment toward the standards. For O_3, it is defined as the highest daily eight-hour concentration averaged over three years. For $PM_{2.5}$, it is defined as the annual average concentration of $PM_{2.5}$ over three years. Note that routine $PM_{2.5}$ measurements started in 2001. Data sourced from the California Air Resources Board.

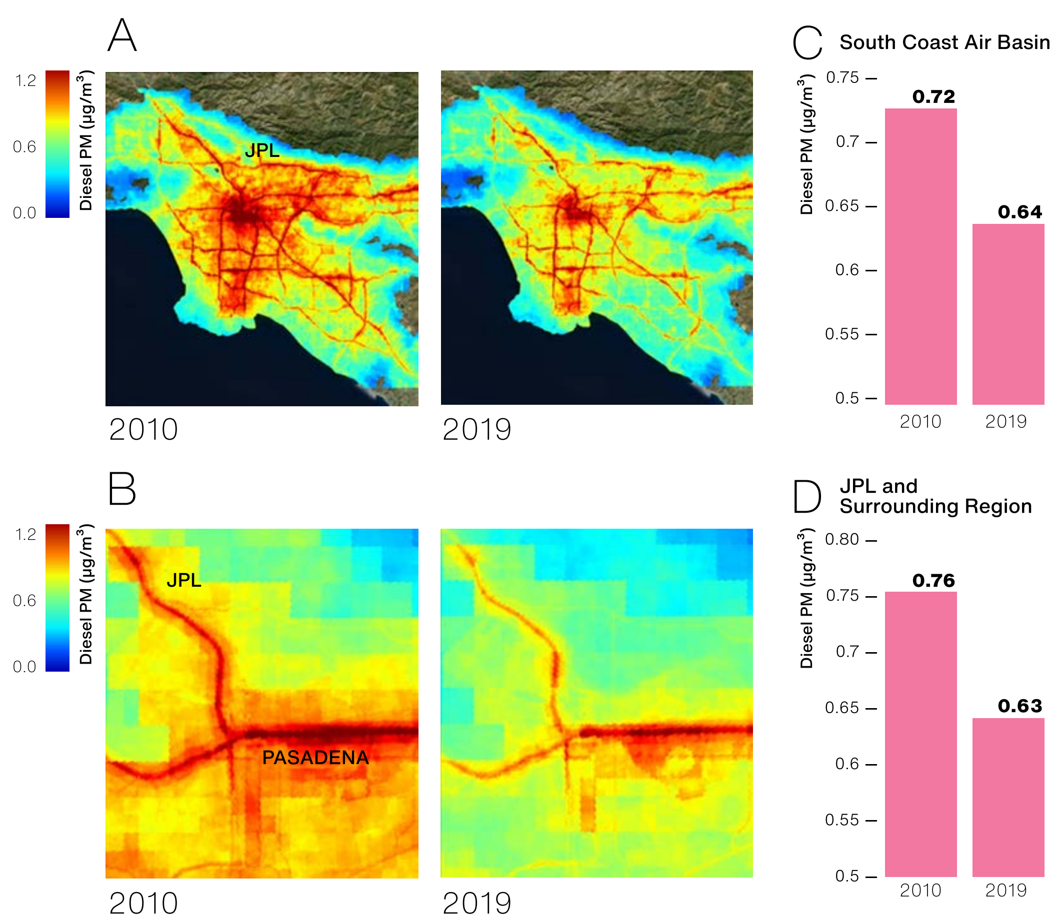

FIGURE 2-11

Changes in ambient DPM concentrations in the South Coast Air Basin from 2010 to 2019. Panels (A) and (B) show spatial distributions of DPM concentrations (in µg/m³) in 2010 and 2019 for the entire South Coast Air Basin and the region surrounding JPL, respectively. Panels (C) and (D) present the average DPM concentrations for the South Coast Air Basin and the area around JPL, respectively, in 2010 and 2019. Modeled elemental carbon (EC) data, sourced from Amini, Danesh-Yazdi et al. (2022), were converted to DPM estimates using an EC/DPM ratio of 0.75, as retrieved from the literature (South Coast Air Quality Management District 2021).

While air quality saw significant improvements with reductions in $PM_{2.5}$ and O_3 until 2010, these levels have remained relatively stagnant in the Los Angeles region (Figure 2-10). For $PM_{2.5}$, this stagnation is attributed to the complexity of its sources, which include secondary formation processes, and contributions from wildfires (Enayati Ahangar, Pakbin et al. 2021). The recent reduction of NAAQS for annual $PM_{2.5}$ from 12 μg/m^3 to 9 μg/m^3 makes it even more challenging for the Los Angeles region to attain the standard. Climate change and increased emissions from volatile chemical products (VCP) and biogenic sources further complicate $PM_{2.5}$ reductions. In the Los Angeles Basin, VCP emissions have a greater impact on $PM_{2.5}$ levels compared to biogenic emissions, owing to their high emission rates in urban environments and their significant contribution to both daytime and nighttime secondary $PM_{2.5}$ formation processes. For O_3, the leveling off is mainly due to the complex chemistry of ozone formation and the changing background photochemical regime. Rising temperatures and increased sunlight enhance O_3 production, while reductions in NOx alone are insufficient without corresponding volatile organic compound (VOC) controls. Studies suggest that even with aggressive emissions-reduction strategies, future levels of $PM_{2.5}$ and O_3 may still be heavily affected by climate-related changes in weather patterns, such as increased temperatures or variations in precipitation, which could alter both the frequency and severity of pollution events (Zhu, Horne et al. 2019).

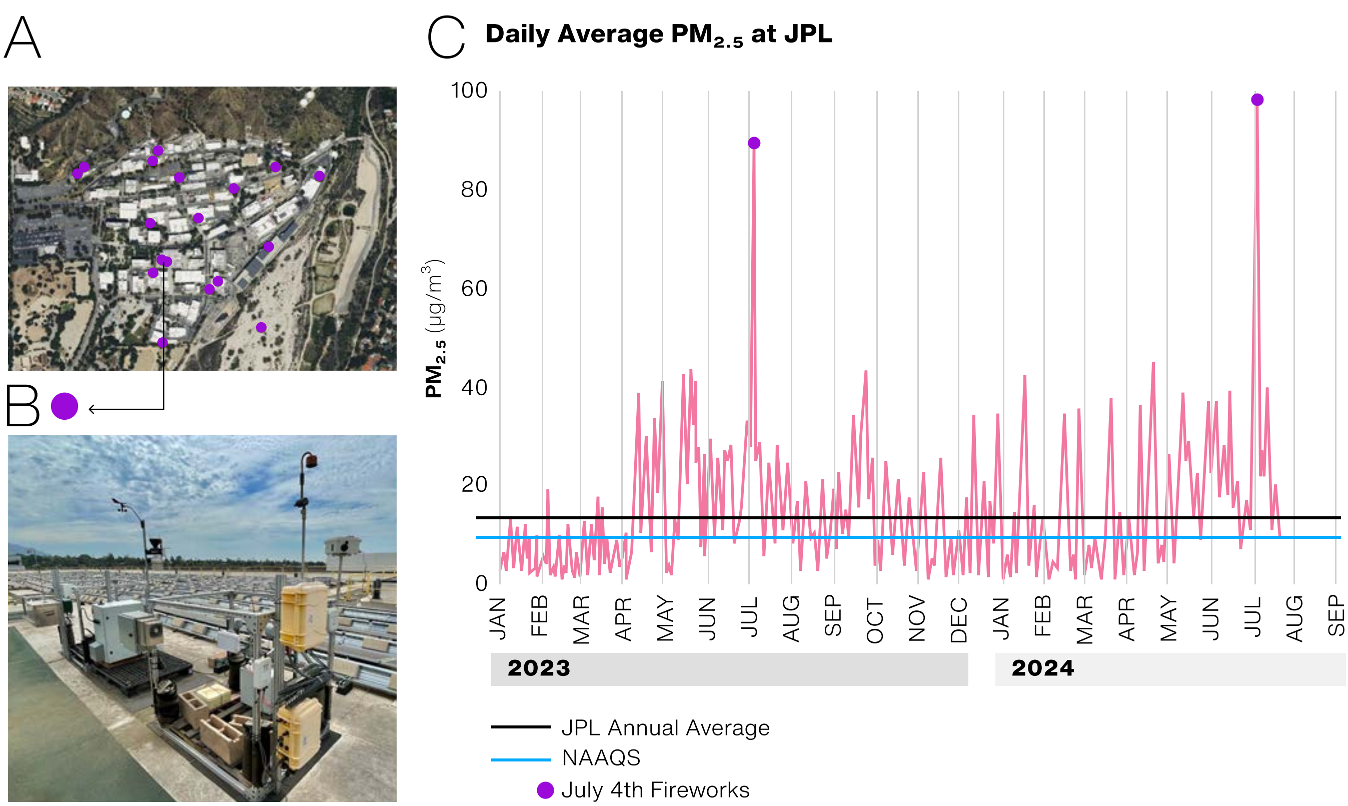

FIGURE 2-12

(A) Map of PurpleAir $PM_{2.5}$ sensors distributed across the JPL campus. (B) Image of the main ambient air monitoring station at JPL. C) Time series of daily averaged $PM_{2.5}$ concentrations at JPL between January 2023 and July 2024, with a comparison against the $PM_{2.5}$ NAAQS.

Projections for future air quality in the Los Angeles region present a mixed outlook. By 2050, despite the anticipated adoption of low-carbon fuels aimed at reducing GHG emissions by 80% and NOx emissions by 25% compared to current levels, O_3 concentrations are expected to remain above the NAAQS (Zhao, Li et al. 2024). This persistence is due to the complex chemistry of O_3 formation, which can result in higher concentrations in urban areas even as traditional combustion sources are phased out. Studies project that further NOx reductions of up to 80%, along with targeted VOC control measures will be needed to meet the O_3 NAAQS (Zhao, Li et al. 2024). Rising temperatures and altered meteorological patterns due to climate change are likely to exacerbate ozone formation, increasing the frequency of high-ozone events and associated health risks (Li, Ravi et al. 2024). Similarly, $PM_{2.5}$ levels are projected to be significantly influenced by climate-driven changes in meteorological conditions. Studies suggest that even with aggressive emissions-reduction strategies, alterations in meteorological conditions, such as higher temperatures, stagnant air, and changes in circulation patterns, could lead to more frequent and intense pollution episodes, potentially resulting in an increase in the number of days exceeding the 24-hour average $PM_{2.5}$ air quality standard by 2035 (Zhu, Horne et al. 2019). Additionally, the increasing frequency and severity of wildfires, driven by climate change, will contribute to higher $PM_{2.5}$ levels and could enhance the formation of ozone.

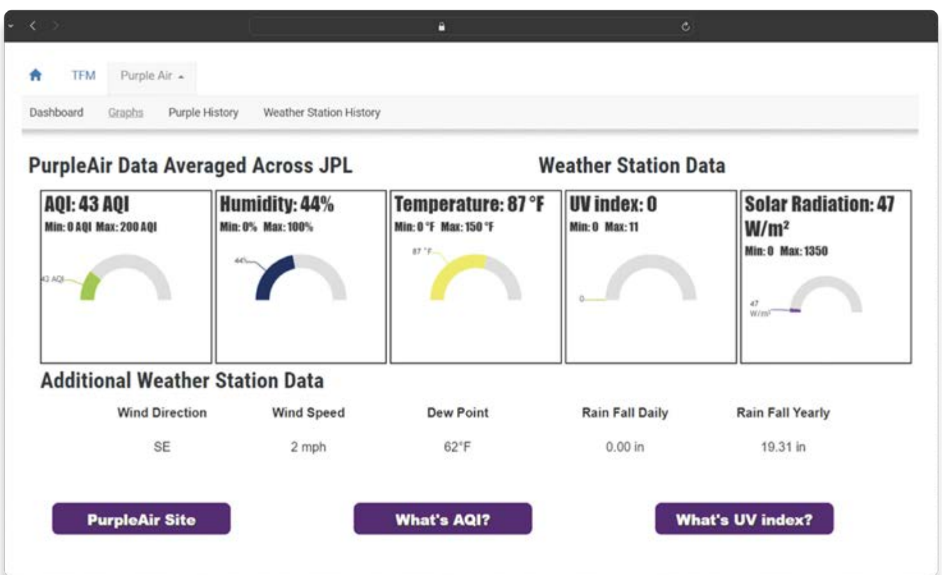

FIGURE 2-13

Screenshot of the online dashboard developed by JPL's TFM, which integrates real-time data from the air monitoring station and the PurpleAir sensor network distributed across the Lab (courtesy of Joshua Garner and Roger Francis).

Poor air quality has direct implications for public health. Exposure to elevated levels of O_3 and $PM_{2.5}$ is associated with adverse health outcomes, including but not limited to respiratory and cardiovascular diseases. Increased incidence of asthma, reduced lung function, and other health issues are expected, potentially impacting workforce attendance and performance. Looking ahead, as pollution levels continue to challenge health standards, the long-term effects could lead to more chronic health conditions and increased healthcare costs. NASA's planned MAIA satellite mission, expected to launch in 2026 in collaboration with the

Italian Space Agency (ASI), is a significant and direct effort to help quantify the amounts, types, and sizes of aerosols effecting urban air quality and to relate them to adverse health outcomes (see https://maia.jpl.nasa.gov/). In addition, satellite observations of trace gases of key air pollutants and their precursors, such as O_3, carbon monoxide (CO), and ammonia (NH_3), have been generated from JPL's TROPESS (see https://tes.jpl.nasa.gov/tropess/) project and integrated into the multi-model multi-constituent chemical (MOMO-Chem) data assimilation framework (Miyazaki, Bowman et al. 2020) to provide information on the distribution and origins of air pollutants at city-to-global scale.

Addressing air quality in the Los Angeles region requires a multifaceted approach combining stringent emissions controls, adoption of clean energy technologies, and adaptation strategies to cope with the impacts of climate change. The South Coast Air Quality Management District (SCAQMD) has indicated that achieving the O_3 NAAQS in the Los Angeles region will require an additional 80% reduction in NOx emissions by 2037, beyond what current rules and regulations mandate (South Coast Air Quality Management District 2022). Achieving such significant emission reductions will require coordinated efforts to cut emissions from both stationary sources, which SCAQMD primarily regulates, and mobile sources such as heavy-duty trucks and ships, which require significant federal action and state-level regulation. The only way to achieve the required NOx reductions is through extensive use of zero-emissions technologies across all stationary and mobile sources (South Coast Air Quality Management District 2022).

At a local level, JPL can implement policies such as indoor air purification, providing health advisories during high-pollution days, and encouraging remote work during peak pollution periods to help mitigate the health impacts of air pollution. Additionally, enhancing air quality monitoring on-site is crucial. JPL can integrate more advanced sensors and real-time data analytics to improve responsiveness to pollution events. Expanding the network of low-cost PM sensors and adding sensors for other pollutants (e.g., black carbon and VOCs) across the Lab will provide comprehensive monitoring coverage. Facility managers can use this enhanced monitoring system to make informed decisions, such as adjusting HVAC systems during high-pollution episodes or shutting down clean rooms during extreme events such as wildfires. Regularly publishing air quality data and trends can also raise awareness and ensure the JPL community stays informed and prepared.

In summary, JPL and the Los Angeles region face persistent and complex air quality challenges that require comprehensive and adaptive strategies. Significant reductions in NOx and $PM_{2.5}$ emissions, coupled with strategic VOC control measures, are crucial to efforts to attain air quality standards in the Los Angeles Air Basin. Additionally, implementing climate change mitigation and adaptation strategies are essential to improving air quality and protecting public health. The intricate interplay between local emissions, regional meteorological conditions, and global climate change necessitates a coordinated effort involving stringent emissions controls and the adoption of advanced, clean technologies. Ensuring these efforts are equitable and affordable will be critical to their success. Furthermore, continuous monitoring, robust regulatory frameworks, and collaborative regional initiatives will play a pivotal role in sustaining long-term air quality improvements and resilience against future environmental changes.

2.5
Precipitation, Atmospheric Rivers, and Flooding

2.5.1
Precipitation

The Los Angeles region receives approximately 15 inches (38 cm) of annual rainfall, with the majority occurring between November and March. This seasonal precipitation is critical for replenishing water supplies and sustaining local ecosystems. However, rainfall patterns in the region are highly variable, with about five storms each year accounting for 50% of total precipitation (Hall, Berg et al. 2018). While historically characterized by arid conditions and extended dry spells, the region has also experienced sporadic episodes of intense rainfall, particularly during climate patterns such as El Niño.

In recent decades, weather variability in the Los Angeles region has increased, reflecting broader global trends. Research by He and Gautam (2016) indicates that annual, winter, and spring precipitation variability has grown over time, with precipitation extremes becoming more frequent. These fluctuations contribute to heightened risks of both drought and flooding, posing challenges for water management and infrastructure resilience.

The projected increase in extreme precipitation is partly driven by stronger linkages between the tropical El Niño-Southern Oscillation (ENSO) phenomenon and mid-latitude weather patterns (Fierro 2014). The natural fluctuations between El Niño (warmer waters in the Pacific Ocean, often leading to wetter conditions in Southern California) and La Niña (cooler waters, associated with drier conditions) significantly influence the Los Angeles region's precipitation patterns. This variability results in longer dry spells interrupted by shorter, more intense rainfall events, heightening the risks of both drought and flood. In the Los Angeles region, this shift likely means extended periods of low or no rainfall punctuated by intense storms that bring flash floods. For example, in February 2024, Southern California was under flash flood advisories and watches, with rainfall totals between 5 inches and 10 inches (12.7 cm to 25.4 cm). This storm was the second one in a few days fueled by an AR (Weber, Antczak et al. 2024). In August 2023, the rare passage of the tropical storm Hilary prompted the National Hurricane Center to issue its first-ever tropical storm watch in Southern California. Rising global temperatures are also a driver of more extreme and irregular precipitation events. For every 1°C (1.8°F) rise in temperature, the atmosphere can hold roughly 7% more water vapor, increasing the potential intensity of rainfall events. This increased atmospheric moisture, combined with shifts in atmospheric circulation patterns, contributes to more frequent and severe precipitation events in many regions. Warmer temperatures also affect the nature of precipitation, reducing the fraction that falls as snow (Knowles, Dettinger et al. 2006), decreasing spring snow accumulation (Mote, Hamlet et al. 2005), and causing earlier snowmelt in spring (Stewart, Cayan et al. 2005).

Increased rainfall intensities present many risks for the Los Angeles region. Urban flooding, where streets, homes, and buildings quickly fill with water, is a particular concern. The Los Angeles region's urban landscape, with its extensive development and low permeability, is especially vulnerable to flooding. Asphalt, concrete, and other impermeable surfaces limit groundwater absorption, causing increased surface runoff. This runoff can overwhelm storm drains, leading to flash floods that can disrupt traffic, damage property, and even endanger lives. Heavy rainfall can also increase the risk of mudslides and landslides, especially in wildfire-affected areas. Without vegetation to anchor the soil, saturated ground is more likely to give way during intense rains, resulting in destructive mudslides that threaten lives, homes, and infrastructure. Additionally, sea level rise, combined with storm surges, increases the risk of coastal flooding in low-lying areas, such as Venice Beach, which are more susceptible to flooding during high-intensity storms.

Changes in precipitation patterns could impact the operations of JPL moving forward. Historically, precipitation near the JPL campus averages about 48 cm to 50 cm (19 inches to 20 inches) per year, primarily from November to March (Table 2-1). More intense precipitation events could result in flooding in certain parts of the JPL Oak Grove campus. The 100-year flood plain upstream from the Devils Gate Dam reaches the 328-meter level, which includes portions of the JPL Arroyo Seco parking lot (AC Martin Partners Inc. 2012a).

2.5

Precipitation Summary for the Oak Grove Campus

Average Annual Precipitation (inches/cm)	20.2/51.4
Record Daily Precipitation (inches/cm)	1.56/3.96

MONTH	JAN	FEB	MAR	APR	MAY	JUN	JUL	AUG	SEP	OCT	NOV	DEC
Average Monthly Precipitation (inches)	4.45	4.57	3.38	1.39	0.43	0.14	0.03	0.09	0.37	0.68	1.67	3.04

TABLE 2-1

Precipitation summary for the Oak Grove campus. Record daily precipitation based on data provided by the weather station installed on the roof of B301 in March 2021; other measurements provided in AC Martin Partners Inc. (2012a).

2.5.1.1 Future Projections

For guidance on how recent trends in precipitation will continue, we provide climate change projection information (Appendix C) for the following variables:

- Number of dry days per year, when precipitation is ≤ .001 inches
- Number of days per year with precipitation greater than the 90th percentile from a baseline period (1995–2014)

FIGURE 2-14

Future projections of precipitation for an approximately 15-mile by 15-mile region around JPL for low-, medium-, and high-emissions scenarios from 2005–2045 for (A) number of dry days (precipitation ≤ 0.001 inches) per year, and (B) number of days per year with precipitation ≥ 90th percentile from a baseline period 1995–2014. In the latter case, the 90th percentile is calculated using all daily precipitation values (dry days excluded) from 1995–2014. See Appendix D for source and further information, including an explanation of the gap between the observations and model projections.

Climate model projections of precipitation over the Los Angeles region show minimal changes through 2045 under the low-, medium-, and high-emissions scenarios for both variables (Figure 2-14). The number of dry days in 2015, for example, was 316; this is projected to increase slightly to 317 under low- and medium-emissions scenarios but is projected to decrease to 313 days under the high-emissions scenario. The number of precipitation days per year that exceed the 90th percentile from the baseline also remains relatively unchanged through 2045. The number of days in 2014 that exceeded the 90th percentile was 5.6; this is projected to change to 4.7, 5.5, and 5.4 days under low-, medium-, and high-emissions scenarios, respectively. Overall, the results from the climate change projections indicate that precipitation trends will remain relatively unchanged through 2045 for the Los Angeles region.

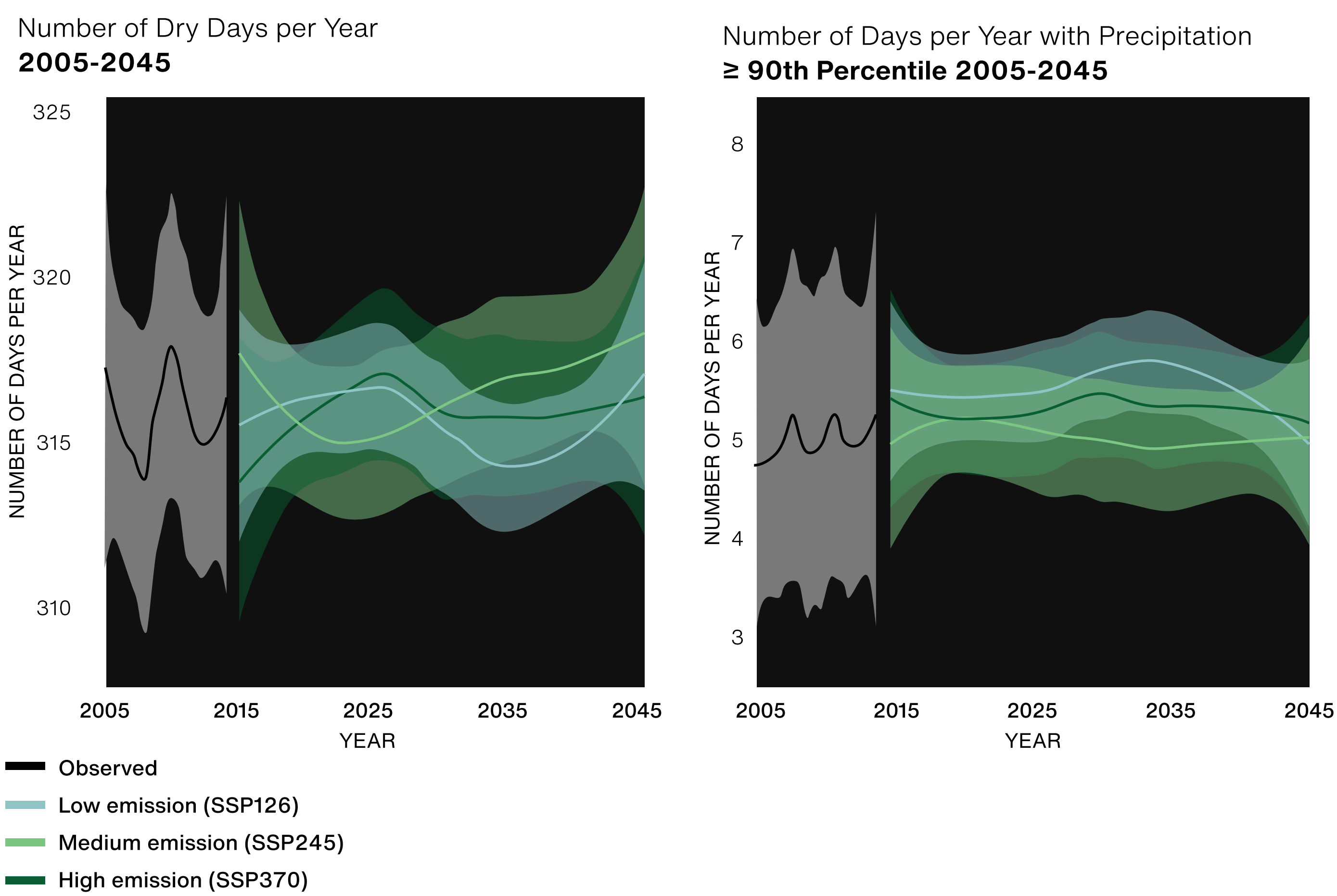

2.5.2 Atmospheric Rivers and Floods

Research has suggested that climate change is likely to increase the severity and risk of the most extreme precipitation events along the Pacific coast and of subsequent severe flood events (Huang, Swain et al. 2020). The main driver behind the projected intensification of extreme precipitation is the increase in the frequency and strength of cool-season ARs—narrow sections of the Earth's atmosphere that typically carry moisture from the Earth's tropics near the equator to the poles.

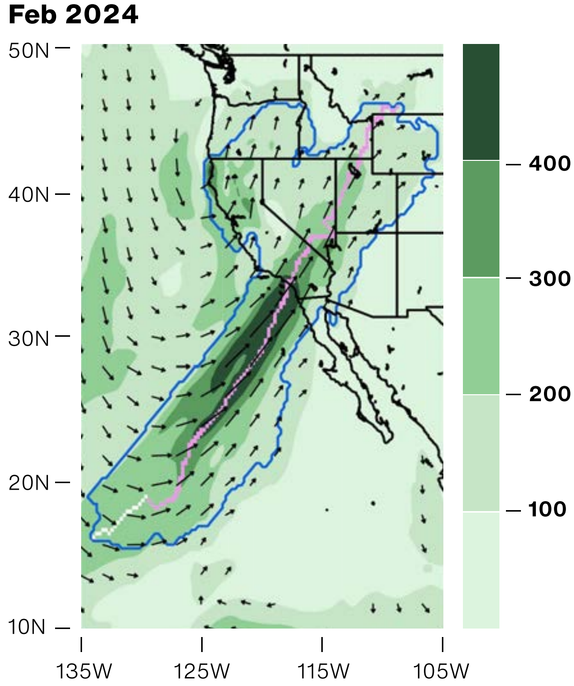

FIGURE 2-15

An AR event in early February of 2024. Shown is a selected time step of the multi-day event. Shading: magnitude of integrated water vapor transport (IVT; kg m−1 s−1). Arrows: vector IVT where magnitude > 100 kg m−1 s−1. Blue: AR shape. Pink/white: AR axis, pink (white) where IVT is poleward (zonal). IVT data are from ERA5. AR shape and axis are based on tARget version 4.

ARs are a key driver of the intraseasonal and interannual variations in precipitation and streamflow in the western United States (Corringham, Ralph et al. 2019). Historically, major flood events in California, including Los Angeles, have been linked to ARs. All seven flood events between 1997 and 2006 on the Russian River in northern California, for example, were linked to ARs (Ralph, Neiman et al. 2006). There are multiple factors that influence ARs' impact, such as duration and spatial extent, temperature and intensity of moisture transport, and antecedent soil moisture and snowpack conditions (Dettinger 2011) (Payne, Demory et al. 2020). For example, an AR event in early February of 2024 (Figure 2-15), which was not particularly intense in terms of the rate of moisture transported but relatively long-lasting, delivered copious precipitation and caused widespread flooding in Los Angeles and surrounding areas (Figure 2-16). A Lab-wide email from the Office of the Director of JPL warning that "An atmospheric river is forecast to hit Southern California over the weekend and through next week" with guidance on hardware and personnel safety went out the day before the event started.

Previous studies have suggested that the increase in the frequency and strength of ARs is due primarily to warming temperatures that drive increases in atmospheric water vapor (Huang, Swain et al. 2020). Although the magnitude is small compared to the interannual variability, an upward trend in historical AR frequency can be seen at JPL over 1940–2023 (Figure 2-17) based on the ERA5 reanalysis and a widely used AR detection algorithm developed at JPL/UCLA (Guan and Waliser 2024). This historical trend, namely 0.75 days per year per

2.5

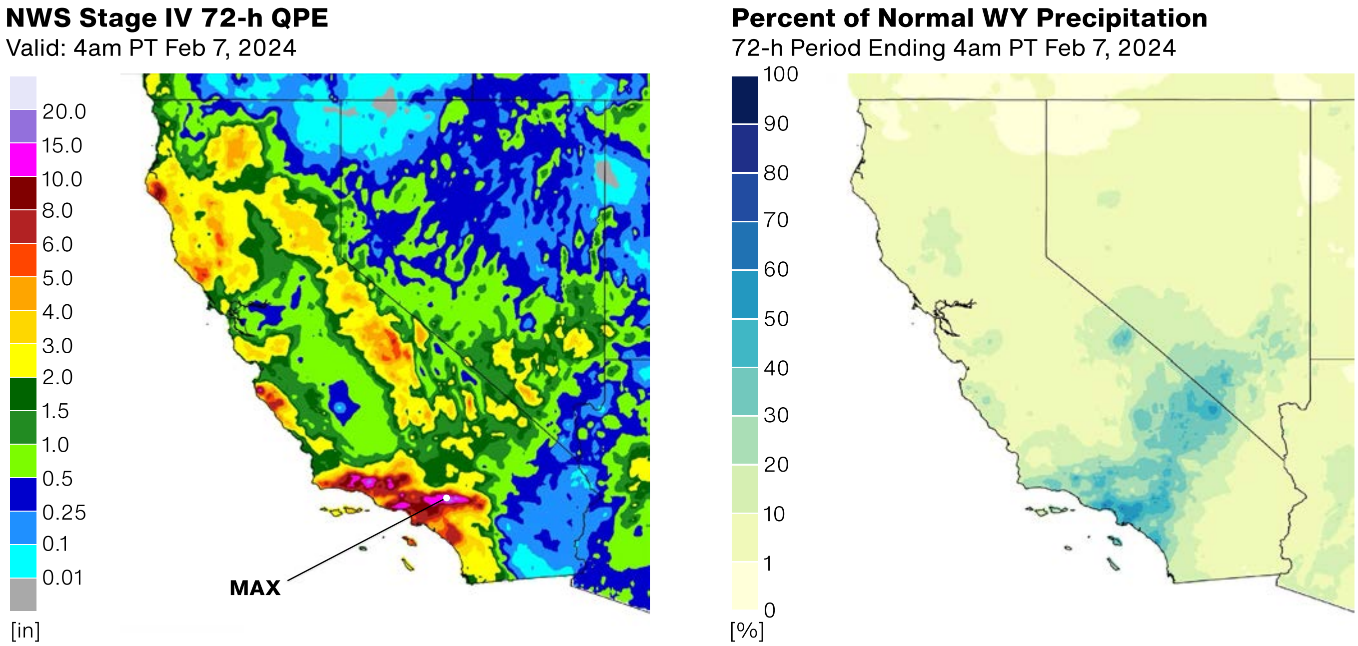

decade (that is, the annual mean on average increases by 0.75 days between two decades), agrees well with the AR frequency trend over the period of 1951–2099 (that is, historical plus future period) estimated by an ensemble of nine CMIP5/6 models, namely 5–10 days per year per century around JPL (O'Brien, Wehner et al. 2022). This trend also suggests that a greater fraction of the extreme precipitation days (which will remain relatively stable as discussed earlier based on 90th percentile events) will be contributed by ARs.

FIGURE 2-16

(A) Accumulated precipitation (in inches) during the AR event in early February of 2024. Shown is NWS Stage IV 72-h quantitative precipitation estimate.
(B) Percentage of normal water-year precipitation delivered during this AR event (Courtesy of UCSD/SIO/CW3E).

ARs can result in substantial socioeconomic damage from landslides (Cordeira, Stock et al. 2019) and flooding (Corringham, Ralph et al. 2019) linked to extreme precipitation. So-called ARkStorm-type ARs have the potential to inundate much of the densely populated coastal plain in the Los Angeles area (Huang and Swain 2022). Additionally, increasing temperatures due to climate change mean more precipitation will fall as rain instead of snow, increasing the likelihood of wintertime flooding and earlier snowmelt, which affects water supply in the dry summer/fall. ARs also frequently occur together with or in close succession after with other natural hazards, such as wildfires, compounding the impact on society and the environment (Payne, Demory et al. 2020).

FIGURE 2-17

Annual AR frequency (days/year; green), the fitted linear trend (light blue), and the long-term mean (dark blue) over 1940–2023 based on the ERA5 reanalysis and the tARget version 4 AR detection algorithm. The trend and mean values are also indicated in the legend.

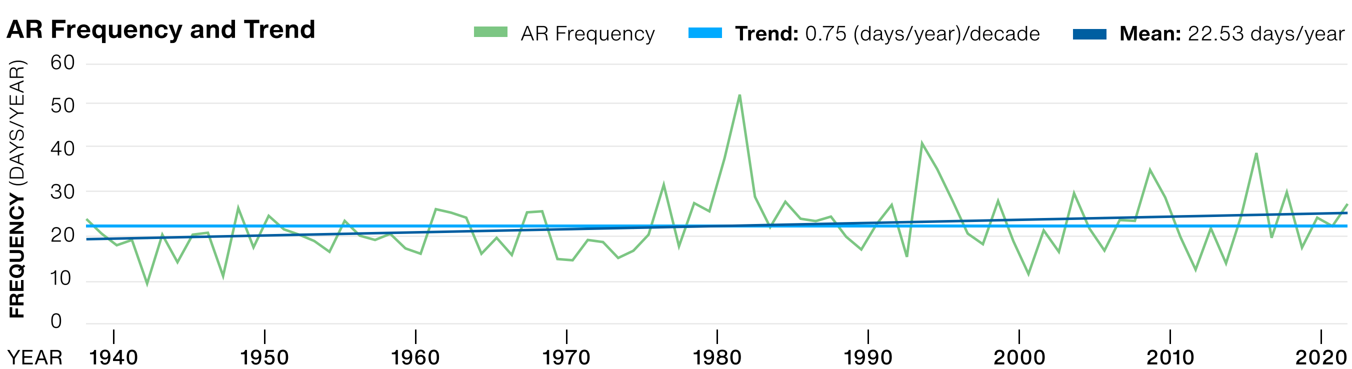

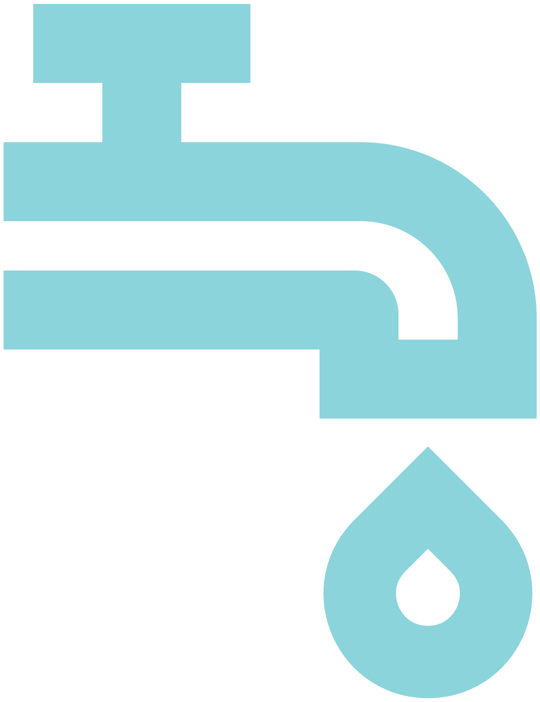

2.6 Water Supply and Drought

Los Angeles and Pasadena are within a semi-arid climate zone where the natural water supply is not consistently sufficient to support local demand and consumptive use, such that typical interannual variability in supply can create challenges for water management. JPL's water resources in Pasadena are managed by the Pasadena Water and Power (PWP) Department, and JPL generally uses the same water resources and water infrastructure as the city of Pasadena. The three major sources of water the PWP uses are local surface water, local groundwater, and imported water from the Metropolitan Water District (MWD) of Southern California (Figure 2-18).

Local surface water sources constitute a small portion of Pasadena's water portfolio, typically around 5% or less, and the majority of that is used to recharge local groundwater. The surface water originates from seasonal rainfall and snowfall in the San Gabriel River watershed surrounding the JPL region and travels through the Arroyo Seco stream seasonally to arrive in a suite of local small reservoirs, including the Devil's Gate reservoir used for flood control immediately adjacent to the JPL Oak Grove facility. These reservoirs may recharge local streams and groundwater but often run dry for long multi-year intervals. Naturally occurring local groundwater is available primarily through natural recharge into the Raymond Basin Aquifer and drawn from a series of wells in Pasadena. Historically, this water resource constitutes about 30%–40% of the city's water portfolio.

Imported water from the Sacramento and San Joaquin River Basins (including snowmelt from the Sierra Nevada mountains) in the central and northern portions of the state of California (i.e., the State Water Project) as well as water from the Colorado River Basin, are managed through the MWD and typically provide the majority of Pasadena water, or about 60%–70% of the total city water supply. Of these two sources making up the MWD water supply, the Colorado River contributes roughly 40%–70% and the State Water Project contributes roughly 30%–60% of the MWD supply, depending on the year. These contributions fluctuate based on natural conditions and the availability of water, precipitation, snowpack, and runoff through the state, and can vary substantially between drought and wet periods, with drought periods drastically reducing the import of water to Southern California as seen in Figure 2-19 during recent drought years (e.g., 2014–2015 and 2019–2021) in the western United States.

FIGURE 2-18

A map showing the sources of water supply for the Greater Los Angeles area, including both local and imported, where "local" is almost entirely composed of groundwater sources within Los Angeles County and "imported" includes deliveries from the State Water Project, the Colorado River Aqueduct, and the Los Angeles Aqueduct (www.lawaterkeeper.org).

Greater Los Angeles County
Water Supply

62%
Imported Water

1%
Local Surface Water and Recycled Water

37%
Groundwater

Note: Percentages fluctuate based on climate conditions

The semi-arid climate of the Greater Los Angeles area makes JPL exceptionally vulnerable to water supply challenges. Major future challenges to the sustainability of JPL's water supply are expected to approach critical thresholds in the 2040–2060 time frame, making JPL water resources a climate consequence of priority. Long-term climate variations could impact JPL water resources in several ways, including: (1) reduced snowpack and runoff from within the San Gabriel watershed and also from the Sierra Nevada mountains, (2) increased and prolonged droughts that can reduce surface water supply and groundwater recharge, (3) increases in extreme weather events, such as heavy rains and flooding (Section 2.5) that can threaten water supply infrastructure and management, and (4) increased evapotranspiration, which can reduce availability from reservoirs and surface water bodies. The water supply risks due to climate change may also be affected by future population growth and/or changing water consumption. Los Angeles county and surrounding regions in Southern California have been one of the fastest growing population centers over the past 100 years.

FIGURE 2-19

The increased use of groundwater when less surface water is available in California (Liu, Famiglietti et al. 2022). (A) Comparison between annual surface water allocations in the aqueducts of the California State Water Project and the federal Central Valley Project, and GRACE-FO-derived groundwater storage anomalies. (B) Comparison between annual surface water deliveries (blue bars; i.e., the total of State Water Project and Central Valley Project) with the GRACE-FO-derived groundwater changes (green and gray bars) in Central Valley.

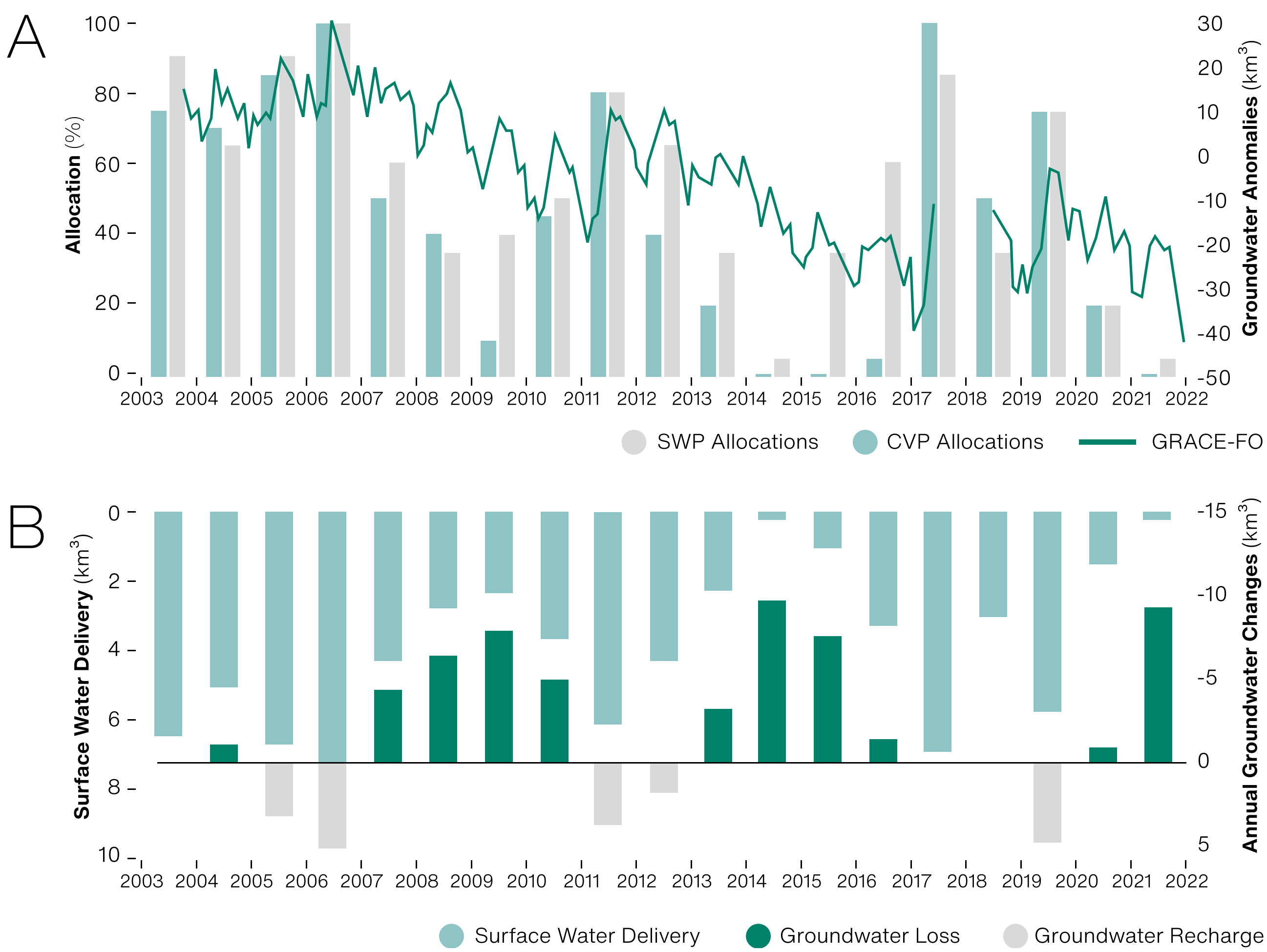

2.6

The sustainability of the water supply at JPL and the greater Los Angeles region is expected to be at critical risk by around the middle of the 21st century. Several sources of information point to this conclusion. Generally, the southwestern United States is projected to experience more frequent and severe droughts in the 2040–2060 time frame. By then, the IPCC indicates that the region may already experience large reductions in snow and altered patterns of precipitation (based on the most probable GHG emissions scenarios, SSP2-4.5; Appendix C). As water shortages intensify, the groundwater contribution will come under further demand and may become exhausted. Compounding these supply/demand challenges, major water infrastructure in Southern California is aging and will require substantial investment, maintenance, and new technology over the next 20–30 years. These combined water supply and infrastructure challenges are expected to stress Pasadena's sustainable access to freshwater as early as 2040. Proactive planning and adaptation efforts are needed to ensure a sustainable water future for JPL.

2.6.1 Sierra Nevada Snowpack

As mentioned above, water supplies in the Los Angeles region and surrounding areas, such as Pasadena, partially depend on natural water storage in the Sierra Nevada snowpack, which stores approximately 14 million acre-feet (~17 km^3) of water annually. Snowmelt from this natural storage fills reservoirs in the Sacramento and San Joaquin River Valleys and serves as the primary water supply for the Los Angeles Aqueduct, which transfers water from the Eastern Sierra Nevada to Los Angeles. Demands on these sources of water storage meet or exceed supply under normal climatic conditions. In this regard, a complex

FIGURE 2-20

Annual time-series of mean 1 April SWE (vertical axis) for California for observations (light blue circles) and variable infiltration capacity (VIC) model (green crosses). Black and blue lines represent a smoothed representation of the data points for VIC (black line) and for observations when 25% of observations were recorded (blue dashed) or 50% or more were recorded (blue solid). For the VIC data, only model cells with an average 1 April SWE > 50 mm are shown (Mote, Li et al. 2018).

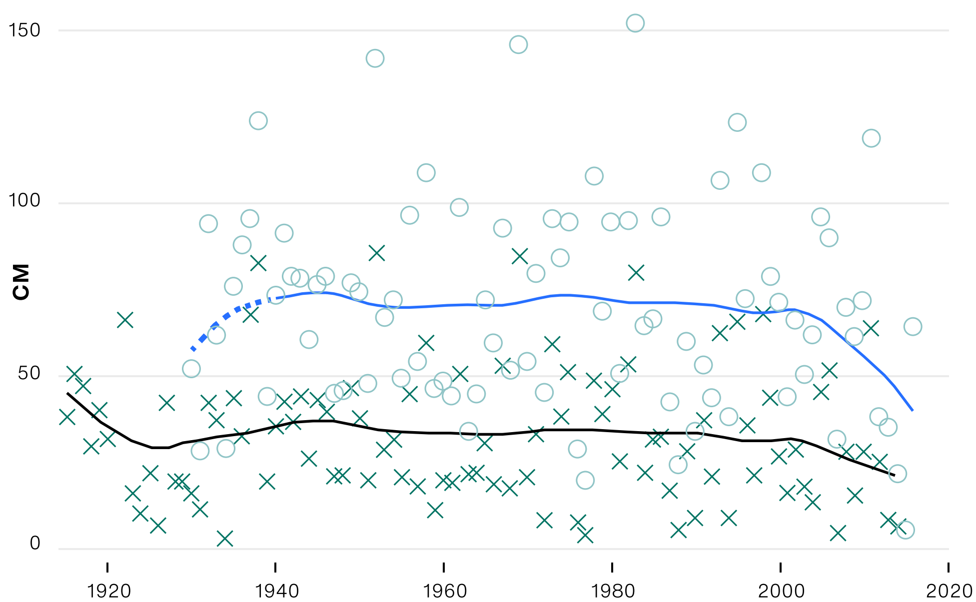

FIGURE 2-21

Ranges of projected 21st century SWE loss for the Sierra Nevada Mountains based on a synthesis of published literature. Projections for near future (2025–2049, green), mid-century (2050–2074, light blue), and end of century (2075–2099, turquoise) are depicted as box plots showing the minimum, maximum, upper and lower quartiles, and median predicted SWE decreases. Percentage decreases in SWE are based on either 1 April, annual maximum SWE, or seasonal SWE. Predictions of future SWE are based on emissions scenarios from IPCC reports and others (see Appendix D). Models used for projecting future SWE include Earth System Models (ESMs; triangles) with and without bias-correction and statistical downscaling (diamonds) and regional climate models (squares). (Figure and caption text adapted from Siirila-Woodburn, Rhoades et al. (2021)).

water conveyance system moves water to the Los Angeles region (Figure 2-18) ensuring relatively efficient allocation to agricultural, municipal, industrial, and hydro-power sectors. The management of this storage and conveyance system and the legal framework governing water allocations is largely enabled by the storage in snowpack and slow release of snowmelt runoff during the spring.

Snowpack conditions in the Sierra Nevada mountains exhibit significant interannual variability with anomalous low-snow years (e.g., snow droughts) (Margulis, Cortés et al. 2016) and high-snow years (e.g., snow deluges) (Marshall, Abatzoglou et al. 2024) significantly complicating management of snow water resources. This variability can lead to significant water supply/demand imbalances, flood risk, and threats to infrastructure that have had profound economic and societal impacts. For example, the 2012–2015 snow drought was the most severe on record with four consecutive years of significantly below-normal snowpack (e.g., < 10% of average in 2015) and above average air temperature (AghaKouchak, Cheng et al. 2014). Conversely, snow deluges in 2017, 2019, and 2023 replenished surface water supplies, partially alleviating water deficits associated with drought. Importantly, model projections into the future estimate that snow deluges in California will decrease by 58% by the end of the century (Marshall, Abatzoglou et al. 2024) and snow droughts will intensify, placing surface water supplies on a trajectory of increased deficit.

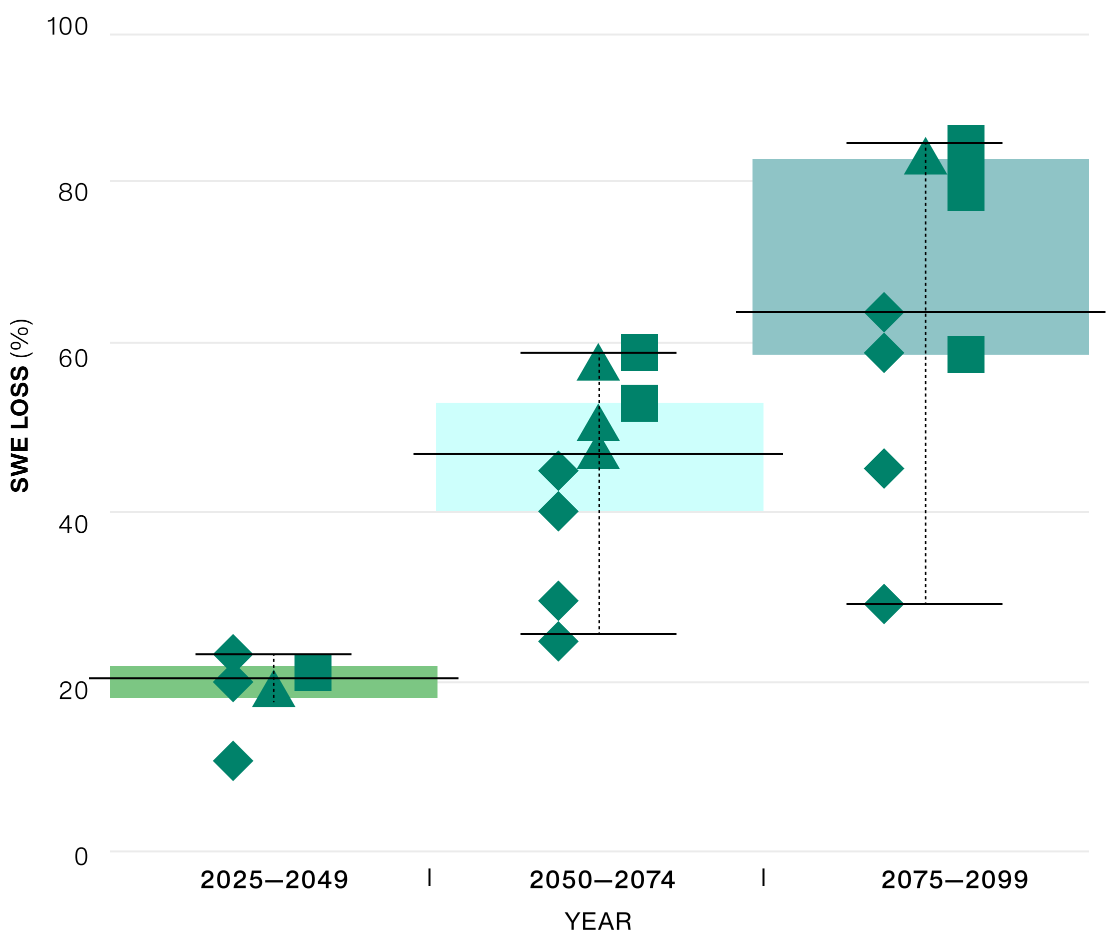

Trend analysis of observations and model-generated data indicate that the widespread declines in snow water equivalent (SWE; a measure of the amount of actual water in the snowpack) across the western United States are particularly acute in California with greater than 90% of observations exhibiting decreases in SWE over at least the past 70 years. Declines in SWE have been particularly notable since 2000, a trend that is partially related to the unprecedented snow drought during 2012–2015 (Figure 2-20) (Mote, Li et al. 2018). Model-based projections of SWE in California's mountains indicate that SWE at the end of the California water year (April 1) will diminish by approximately 50% by midcentury and by over 60% at the end of the century (Figure 2-21) (Siirila-Woodburn, Rhoades et al. 2021). In addition, the spatial extent of areas deemed low- to no-snow will increase from a baseline that from 1950 to 2025 consistently remains below 25% of land area to consistently above 75% after 2060 (Figure 2-22) (Siirila-Woodburn, Rhoades et al. 2021). This suggests that land areas where low to no snowpack conditions exist will increase by approximately 50% by 2060.

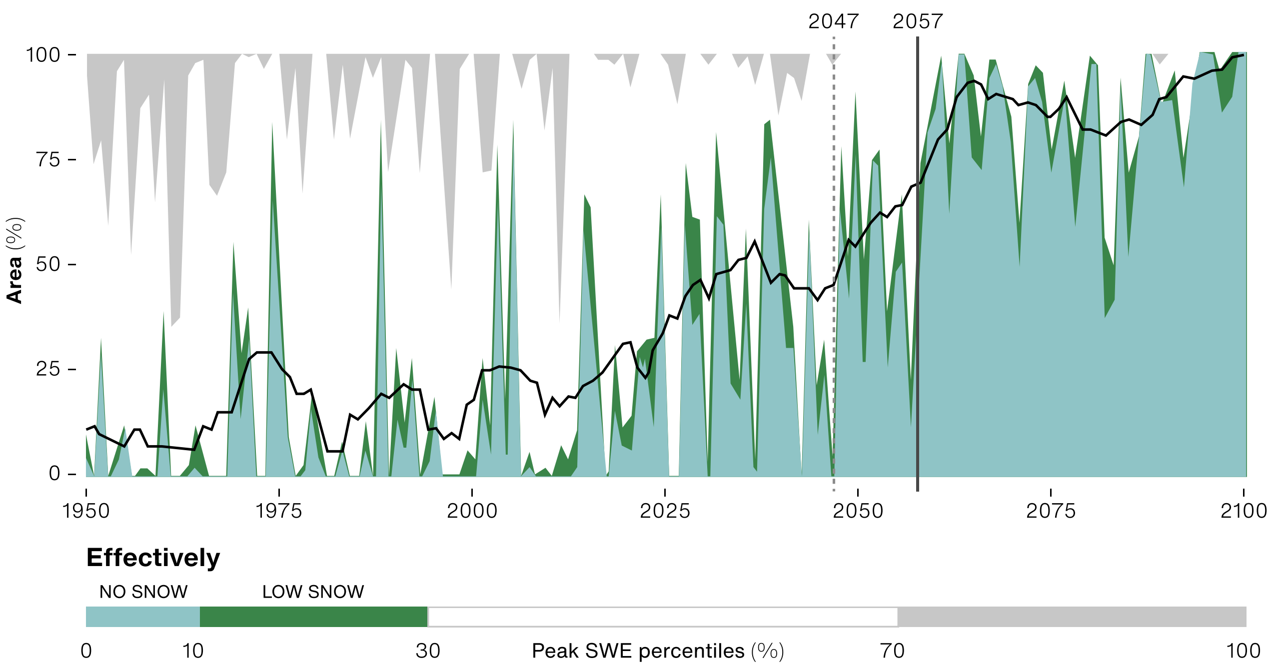

FIGURE 2-22

Time series of maximum annual SWE by percentage of area associated with projected percentiles of future SWE relative to historical SWE for California. The 10-year running average of the area (both snow and non-snow grid cells) at or below the 30th percentile of historical SWE is shown as a black line and represents a low- to no-snow future. Notably, this area increases from approximately 25% in 2025 to 50% by 2050 and to 75% by 2060. These projections are based on the RCP8.5 emissions scenario (see Appendix D) and a single ensemble member of the 20-km-resolution MRI-AGRCM3-2-S ESM (Mizuta, Yoshimura et al. 2012). The dashed and solid vertical lines identify intermittent and consistent low- to no-snow conditions, respectively, which are established as the commencement of five and ten continuous years with low- to no-snow conditions over ≥ 50% of the area. (Figure and caption text adapted from Siirila-Woodburn, Rhoades et al. (2021).)

2.7 Water Quality

2.7.1 Inland

Reliable water quality is essential for JPL's operations, the workforce's well-being, and the surrounding community, particularly given the region's dependence on local reservoirs and imported water sources. Changes in environmental conditions, including temperature fluctuations, extreme weather events, and shifts in precipitation patterns, can influence water quality in ways that directly impact public health and infrastructure. One emerging concern in Southern California is the increasing prevalence of FHABs, which pose risks to water resources, ecosystem stability, and human health.

While water quality encompasses a variety of concerns, including multiple contaminants, FHABs across Southern California's water bodies represent a critical challenge. These blooms now begin earlier in the year and persist longer. Remote sensing provides valuable insights into long-term FHAB trends, helping to track their frequency, duration, extent, and magnitude. Because of the toxins they produce and their other detrimental effects on water resources—such as odor, discoloration, and impacts on water intakes—FHABs require careful monitoring. One approach to mitigating health risks is the establishment of health standards that define FHAB concentrations associated with adverse health effects. A summary of these concentrations is shown in Table 2-2.

FHABs are caused by cyanobacteria, a microscopic organism that can proliferate naturally and produce toxins that are associated with respiratory irritation or illness due to ingestion or skin contact during recreational activities. They can also cause injury to pets, domestic livestock, and wildlife, which may include endangered or vulnerable species. FHABs are also an issue in water bodies that are part of tribal or cultural heritages, or used for subsistence fishing. Even when blooms do not produce toxins, they have other deleterious outcomes, such as foul odor and poor aesthetics, which need to be managed, as well as significant ecosystem impacts such as fish kills.

AUTHORITY	QUANTITY	GUIDELINE VALUE CLASSIFICATION	METHOD
California DWR	< 6 µg/L Microcystis	No Alert	Field Sampling (DWR)
	> 6–19.99 µg/L Microcystis	Alert	
WHO (1999)	≤ 20,000 cyanobacterial cells/ml or < 41 cyanobacteria index	No Alert	MERIS Sentinel-3 (CyAN Products)
	> 20,000 cyanobacterial cells/ml or > 41 cyanobacteria index	Alert	

TABLE 2-2

Summarizes the California Department of Water Resources (DWR) and the World Health Organization (WHO) thresholds for FHABs (credit: B. Lopez Bareto).

Days with heightened FHAB levels are increasing in key reservoirs across Southern California, including the MWD-operated Diamond Valley Lake (about 60 miles southeast of JPL) and the largest treated water supplier in the United States, providing water to over 19 million Southern Californians. These trends underscore the importance of proactive monitoring and response strategies to safeguard water quality for both JPL and the broader region.

FHAB dynamics are rapidly changing due to several factors, including warming temperatures, LULC, and water management practices. Warming temperatures (discussed in Section 2.1) make it easier for algal blooms to form (Ho, Michalak et al. 2019) (Wiley and McPherson 2024) and spread. Second, conversion of land from forested to other land use types, such as urban or agriculture, increases the likelihood that contaminants such as urban runoff and fertilizers reach lakes and reservoirs. Third, as droughts (Lakshmikandan, Li et al. 2024) (discussed in Section 2.6) become more frequent, there may be changes in sources of imported water. The California State Water Resources Control Board has observed that the season for FHABs is getting longer, sometimes extending into winter months, which had not been observed until recently.

FIGURE 2-24

Increasing frequency of FHAB cyanobacteria alerts in California detected using satellite data and the WHO public health threshold; green line simply highlights the trend (credit: B. Lopez Bareto).

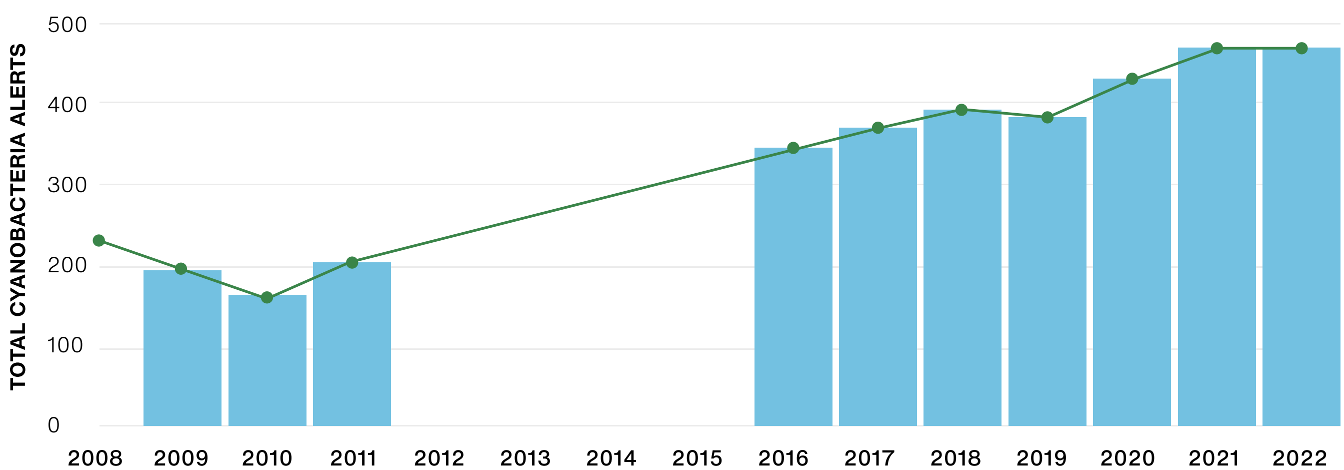

Detection of FHABs in water resources via remote-sensing relies on unique spectral absorption features associated with pigments in the bloom, which can be used to derive a magnitude of cyanobacteria presence. This quantity is then paired with in situ data for validation and evaluation, which can then be used to assess bloom conditions relative to a WHO health risk threshold (Table 2-2).

The remote-sensing record from the European Space Agency Medium Resolution Imaging Spectrometer (MERIS; used to assess 2009–2011) and Sentinel-3 (used to assess 2016–2022), detect a number of blooms above the WHO threshold that has been steadily increasing over time in California (the 2012–2015 represents a gap in the satellite record between MERIS and Sentinel-3; Figure 2-24). Estimates of cyanobacteria index derived from MERIS and Sentinel-3 sensors are related to cell concentrations. If these estimated cell concentrations exceed a certain threshold (Figure 2-24), then the water body is considered likely to pose a health hazard for exposed humans or wildlife.

FIGURE 2-25

This illustration shows how frequently a particular water body is shown to have an FHAB occurring at a level that exceeds the WHO health standard. Several lakes have blooms detected at the WHO threshold in over 50% of imagery acquired from Sentinel-3. Lake Elsinore has a bloom in nearly 100% of Sentinel-3 imagery (credit: B. Lopez Barreto).

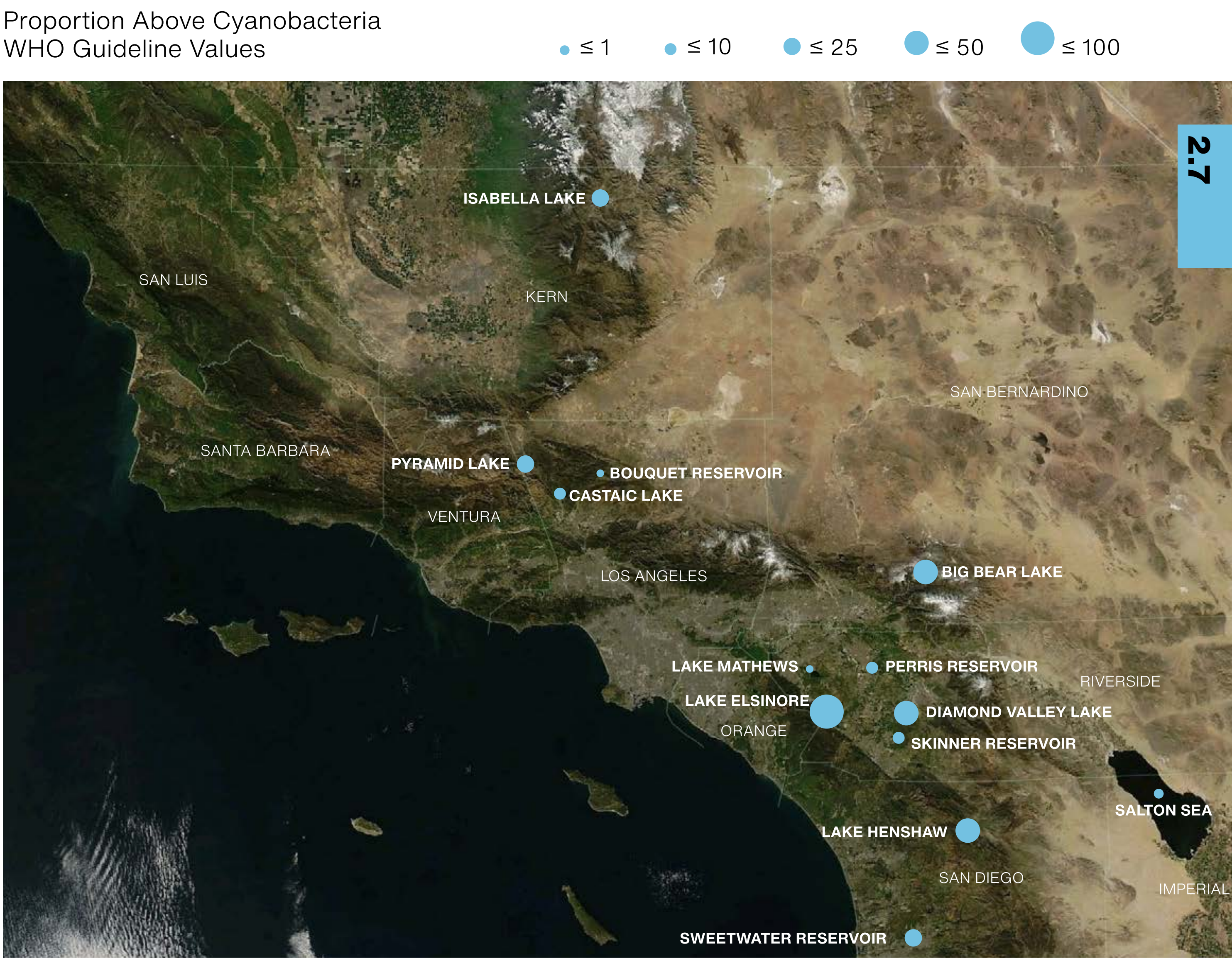

Figure 2-25 leverages the European Space Agency Sentinel-3 Ocean and Land Color Instrument (OLCI) satellite to explore frequency of bloom detection over the satellite record (2016–2022 for various lakes and reservoirs in Southern California). For the lakes where blooms can be monitored by the satellite measurements, the frequency of blooms detected was often high; for example, blooms were detected by satellite in > 50% of the images at Big Bear Lake, Diamond Valley Lake, Pyramid Lake, Lake Henshaw, and Sweetwater Reservoir. Satellite data indicated the presence of blooms for 100% of the imagery at Lake Elsinore. Changes in the timing of cyanobacteria blooms at individual lakes are evident, with a clear contrast between earlier (2008–2012) and later periods (2016–2022). For example, Diamond Valley Lake, a critical reservoir for Southern California, experienced only two FHAB blooms from 2008–2012, compared to over 14 blooms from 2016–2022 (Figure 2-26).

For Diamond Valley Lake, the onsets of the two blooms during the period of 2008–2012 were in October; for the latter period of 2016–2022, blooms were detected starting in May—earlier by approximately 152 days. In addition, the number of days when blooms were observed to exceed the WHO health standard increased from one day between 2008 and 2011 to over 40 days on average between 2016 and 2022. Using Diamond Valley Lake as an example, satellite imagery can be used to better visualize differences in the size and locations of blooms (Figure 2-27) and can be used in conjunction with water sample information, such as the presence of toxins.

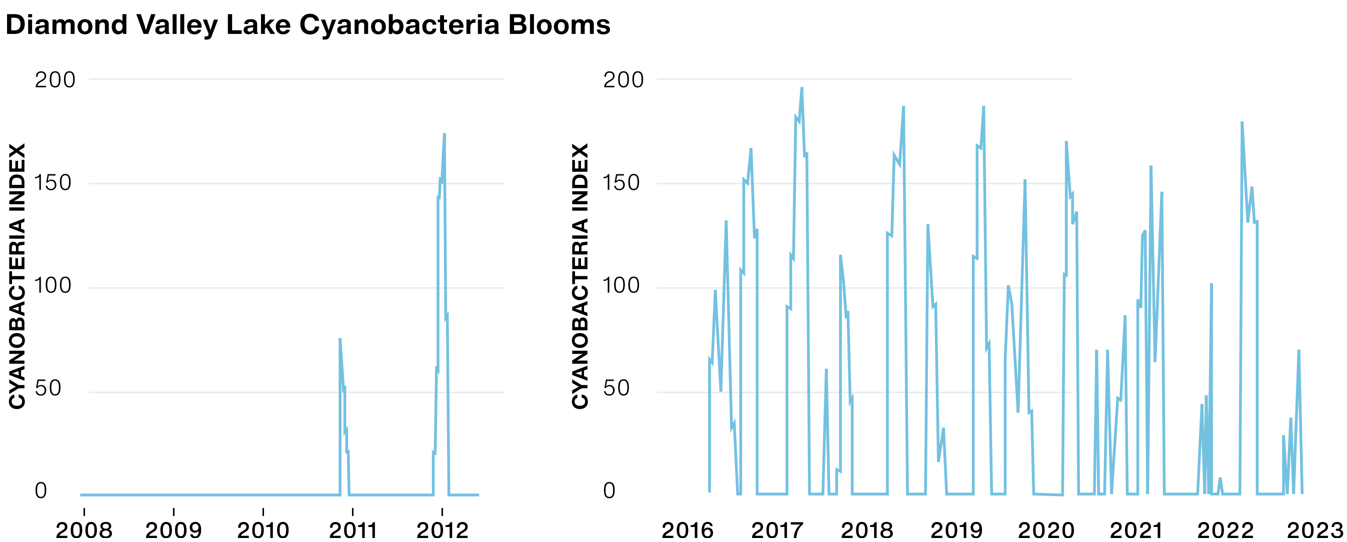

FIGURE 2-26

First time period is 2008–2011, second time period 2016–2022 (credit: B. Lopez Barreto).

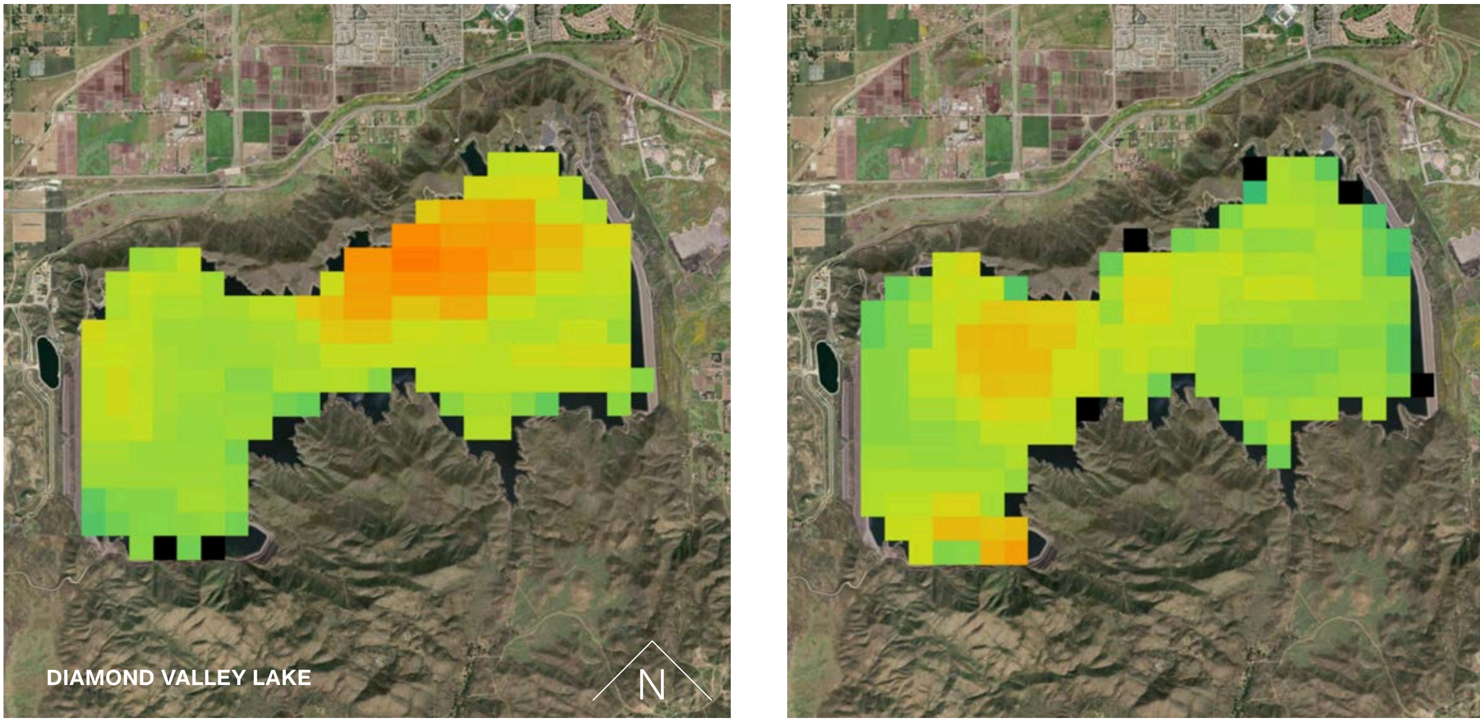

FIGURE 2-27

Snapshots of the FHABs in Diamond Valley Lake, displaying greater bloom intensity in different portions of the reservoir in April 11–May 11, 2024, 10-day pixel max (left) versus June 5–July 5, 2024, 10-day pixel max (right; source: https://fhab.sfei.org/ provisional satellite products).

2.7.2
Coastal

Coastal waters and beaches are vital to Los Angeles County, not only driving regional economic growth and sustaining diverse ecosystems but also providing critical support for mental well-being and serving as a cooling refuge during intensifying urban heat waves for the JPL and Los Angeles communities. Water quality along the Los Angeles County coast is shaped by a range of environmental and human-driven factors, including rising ocean temperatures, urban runoff, wildfire debris, harmful algal blooms, and more. Many sections of the coast generally meet safety standards for recreational use, but conditions can vary widely depending on location, seasonal changes, and weather events. To safeguard public health, agencies monitor water quality parameters (e.g., levels of bacteria and pollutants) to ensure the water is suitable for swimming and other activities.

Following significant rainfall, pollutants from the city's streets and storm drains wash into the ocean, carrying oils, trash, heavy metals, and bacteria that compromise coastal water quality. This runoff is especially concerning after long dry spells, as it contains concentrated levels of pollutants accumulated over time. Rainfall not only drives these pollutants into the ocean but can also prompt local advisories or beach closures due to elevated bacterial levels, especially near river outlets or areas with dense urban populations. Using satellite synthetic aperture radar (SAR) data from 1992 to 2014, Holt, Trinh et al. (2017) illustrated the concentrated distribution and extent of stormwater runoff plumes near river and creek outlets in Santa Monica Bay and the San Pedro Shelf (Figure 2-28A and Figure 2-28B). Beaches in the vicinity of these stormwater runoff hotspots were associated with high levels of bacterial contamination (Figure 2-28C and Figure 2-28D).

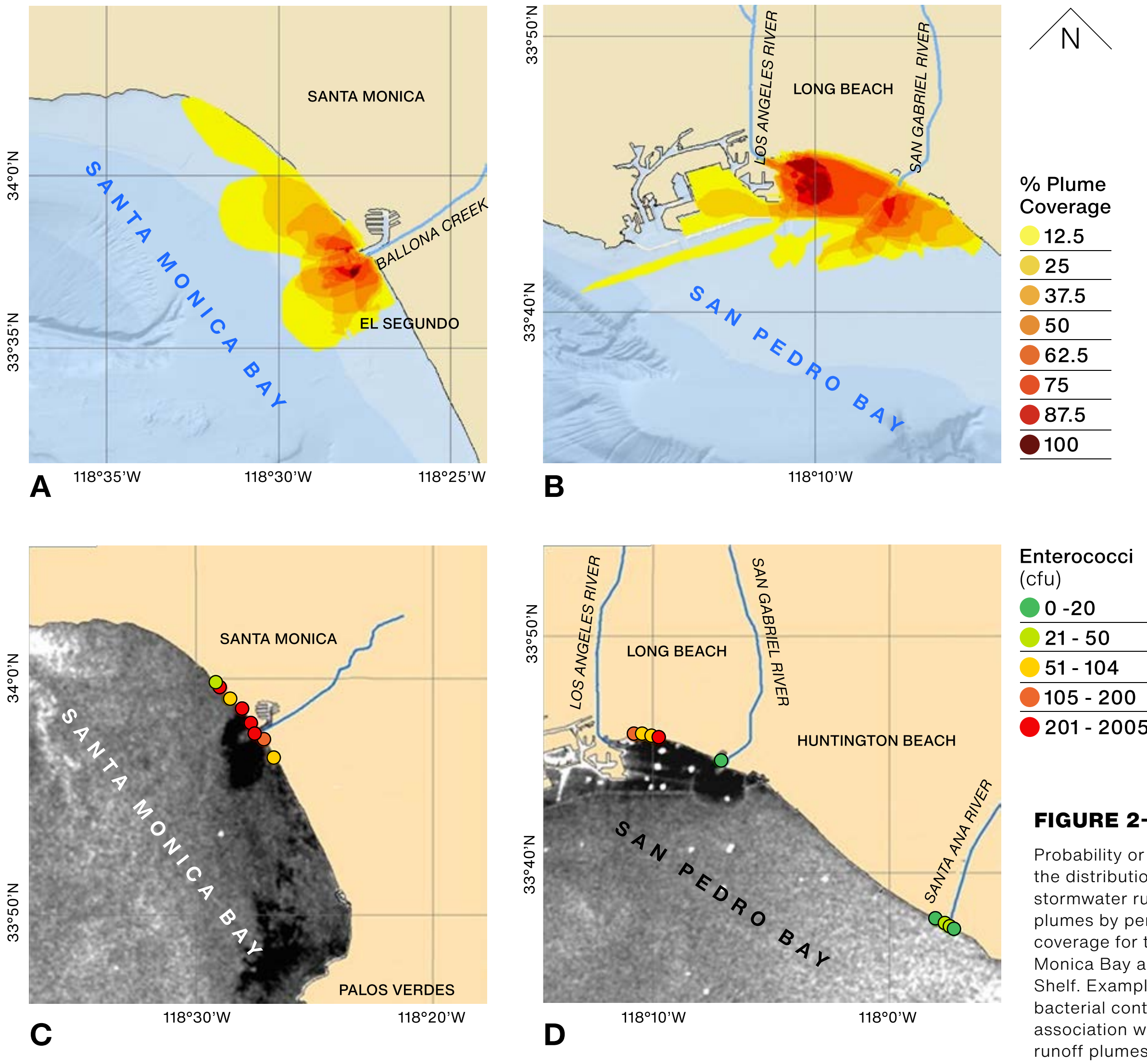

FIGURE 2-28

Probability or heat maps showing the distribution of SAR-detected stormwater runoff surface plumes by percentage of plume coverage for the (A) Santa Monica Bay and (B) San Pedro Shelf. Examples of high levels of bacterial contamination found in association with SAR-detected runoff plumes for (C) Santa Monica Bay and (D) San Pedro Shelf. Exceedance of 104 cfu/100 ml is unsafe for recreational activity (Holt, Trinh et al. 2017).

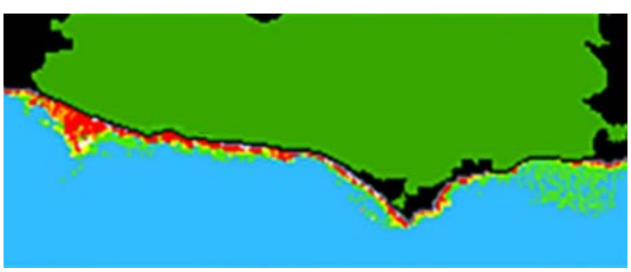

BEFORE WOOLSEY FIRE

2017: Less sediment after rain

Undisturbed vegetation and soil buffers the ocean from run-off.

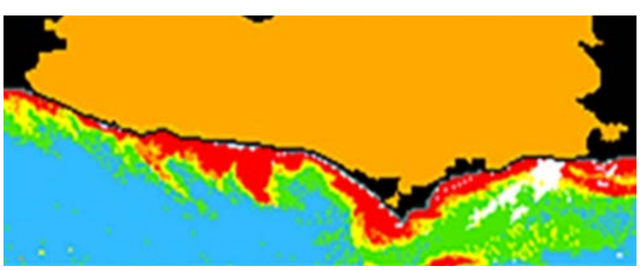

AFTER WOOLSEY FIRE

2018: More sediment after rain

The scalded, bare, burned area erodes quickly during rain.

FIGURE 2-29

Increased sediment load in adjacent waters following the Woolsey Fire (Cira, Bafna et al. 2022).

Heal the Bay's 2023–2024 Beach Report Card reflects the ongoing coastal water quality struggle in Los Angeles County, listing several beaches on its "Beach Bummer" list for water quality issues, including Marina del Rey Mother's Beach, Santa Monica Pier, and Cabrillo Beach Harborside (Wu, Moe et al. 2024). At Santa Monica Pier, recent upgrades, such as stormwater capture systems, have not fully mitigated pollution levels, as continuous urban runoff and ineffective maintenance of bird deterrents contribute to high bacterial counts. Mother's Beach in Marina del Rey, an enclosed beach with poor natural circulation, also has persistent water quality issues despite cleanup efforts. These areas underscore the complex, ongoing challenge of improving water quality in enclosed coastal environments and densely populated areas.

Wildfires introduce another layer of complexity to water quality. Ash, debris, and chemicals from burned areas wash into rivers and streams, altering the physical and chemical quality of receiving waters. Cira, Bafna et al. (2022) documented enhanced turbidity levels and fecal bacteria in recreational marine waters following the 2018 Woolsey Fire (Figure 2-29 and Figure 2-30).

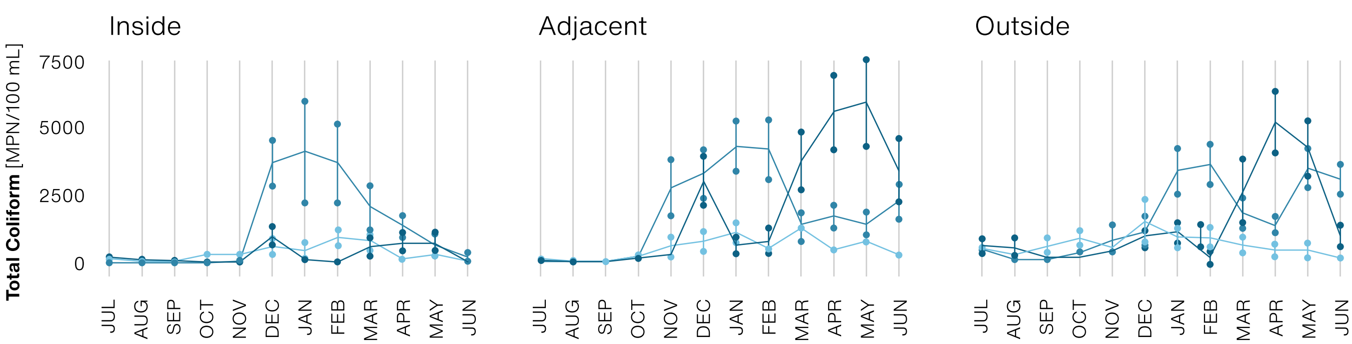

FIGURE 2-30

Fecal bacteria (total coliform, 2008–2020) monthly means and standard errors for the inside region. Fecal bacteria (total coliform) increased in 2018–2019 following the Woolsey Fire (November 8–21, 2018) (Cira, Bafna et al. 2022).

Ocean temperatures off the coast of Los Angeles County have been steadily rising, creating a ripple effect on local ecosystems and water quality (Figure 2-31). Warmer waters can disrupt marine habitats, leading to shifts in fish populations and putting stress on native species, such as kelp forests and marine life that depends on cold water. Higher ocean temperatures also provide ideal conditions for harmful algal blooms. These blooms can release toxins that impact both marine life and human health, leading to beach closures and affecting industries reliant on healthy coastal waters, such as tourism and fishing. For example, the delayed 2015–2016 Dungeness crab season due to a West Coast-wide algal bloom is estimated to have cost over $40 million in lost revenue for the state of California.

The economic implications of poor water quality along Los Angeles County's coast are substantial, impacting tourism, fisheries, and public health costs. Tourism is a major economic driver, generating approximately $34 billion in 2023 (Dean Runyan Associates 2024). Poor water quality, however, can lead to beach closures that deter visitors and Los Angeles County residents, such as the JPL community, reducing revenue for local businesses. Studies indicate that reducing marine debris by 75% at beaches near the Los Angeles River (see Figure 2-28B for the location of the Los Angeles River) could increase visitation by 43%, resulting in an estimated $53 million in economic benefits (Leggett, Scherer et al. 2014). Water quality issues also affect the fishing and seafood industries, which are increasingly vulnerable to environmental changes. Harmful algal blooms and other contaminants can lead to seafood restrictions, affecting commercial fishing and disrupting the local seafood market that serves residents and tourists alike. Furthermore, water quality issues drive up public health costs, as exposure to contaminated water can cause skin infections, respiratory issues, and gastrointestinal illnesses. Together, these challenges create economic ripple effects that reach beyond the coast, underscoring the importance of sustained investment in water quality improvement and environmental resilience to protect Los Angeles County's coastal economy.

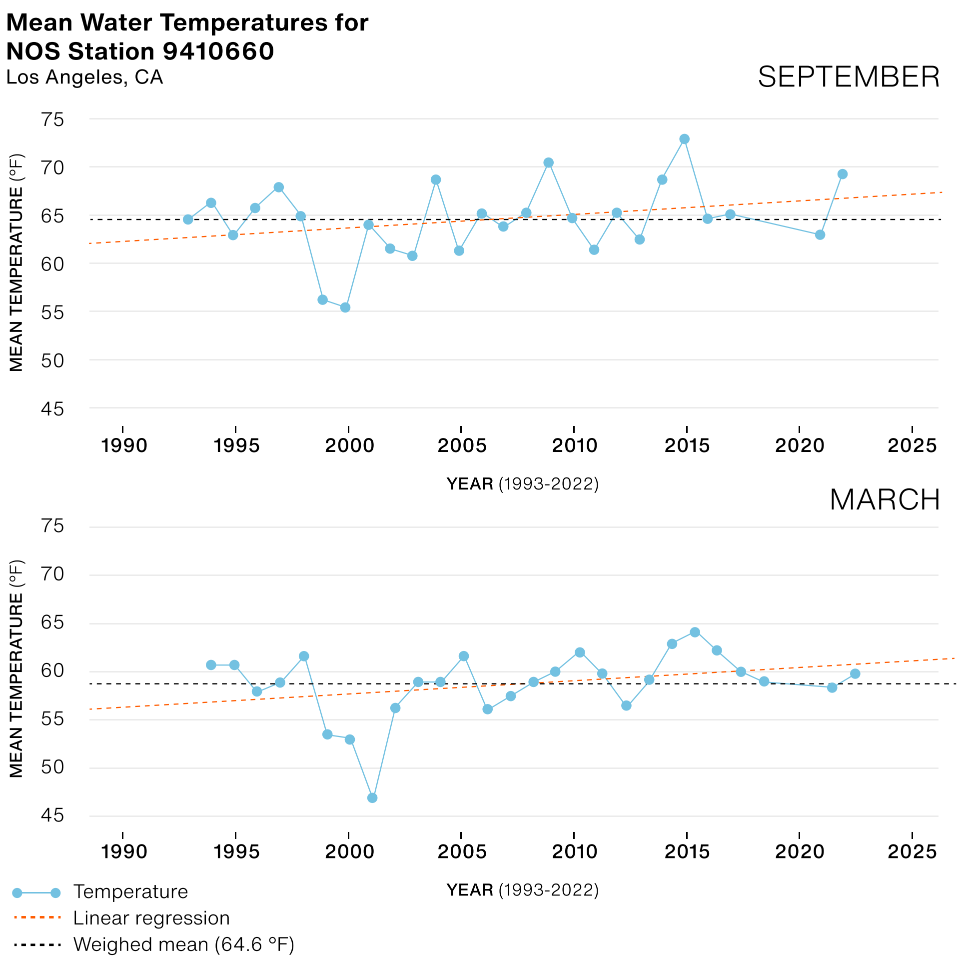

FIGURE 2-31

NOAA National Ocean Service (NOS) mean water temperatures have been increasing over time for Los Angeles station (ID 9410660). Similar trends are observed for all months at this location as well as other coastal locations in Los Angeles County (figure from https://www.ncei.noaa.gov/products/coastal-water-temperature-guide).

2.8 Sea Level Rise

Sea level rise poses significant risks to public infrastructure, health, safety, private property, and natural habitats. In California, around 700,000 people and $250 billion in property could face coastal flood risks this century, especially in vulnerable communities. Rising sea levels will worsen coastal flooding, erosion, and saltwater intrusion into freshwater aquifers as well as make coastal storms more damaging. With rising temperatures globally, these extreme storms are expected to increase in frequency and severity, intensifying the cumulative impacts of rising sea levels.

Using tide gauge observations, the rate of sea level rise along California's coast since 1970 has been lower than the global average for much of this period, largely due to natural variability masking the long-term climate-driven trend. The satellite altimetry data available since 1993 is consistent with the tide gauge data. El Niño events and decadal shifts related to the Pacific Decadal Oscillation have caused significant fluctuations in the rate of sea level rise. In fact, sea level rise was nearly absent in the first half of the record (from about 1970 to 1995) but became pronounced in the second half (from about 1995 to 2024). Figure 2-32 shows monthly variations in both the year-to-year (thin lines) and decade-to-decade (thick lines) changes in average California sea level since 1970. The foundation of sea level has shifted upward over time, although with sizable fluctuations over the course of any given year. Over the full period from 1970 to 2023, California's average sea level rise rate is 0.7 inches (about 1.8 cm) per decade.

The observations in the Los Angeles region from both tide gauges and satellite altimetry support the conclusions drawn from statewide assessments. Tide gauges in Los Angeles (near Long Beach) and Santa Monica both show rates close to the statewide average of 0.9 inches per decade. Both locations show limited amounts of vertical land motion (neither

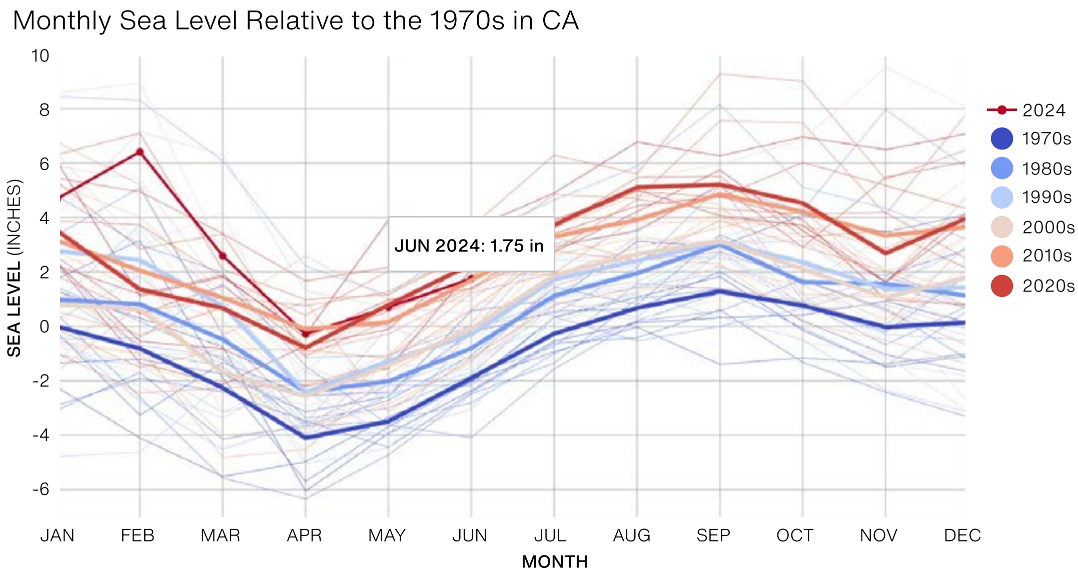

FIGURE 2-32

Change in sea level over time in California relative to the 1970s. Sea level goes up and down throughout the year due to things such as tides and changes in seasons. Some years may also be higher than others due to natural fluctuations from things such as El Niño events. Sea level in California has risen since 1970 as indicated by the upward shift over time. The rate of rise has averaged 0.7 inches/decade since 1970, although this rate has increased over time.

subsidence nor uplift). The Los Angeles area has experienced exceedances of the minor flood threshold over the past few decades, although no substantial increase in more recent years has been seen. The minor flood threshold is defined by NOAA as a level when minor impacts such as road closures, travel delays, or temporary business closures may start to occur. The occurrence of minor flooding is mostly tied to El Niño events that push annual sea levels higher across the coastlines of the Los Angeles area. As seen in Figure 2-33, the two years with the most days with minor flooding since 1970 occurred in 1982–1983 and 2015–2016, both of which had strong El Niño events.

Projections of future sea level rise in the Los Angeles area show that sea level is expected to track to the global average. In the 2022 Interagency Technical Report, five specific scenarios of sea level rise were developed for practical use in the United States using foundational knowledge and projections from the IPCC AR6 (Sweet, Hamlington et al. 2022). The five scenarios are low (0.3 m), intermediate low (0.5 m), intermediate (1.0 m), intermediate high (1.5 m), and high (2.0 m) sea level rise. The scenarios are slightly different than the climate change scenarios used for climate change projections throughout this report. (See Appendix D for additional information about the climate change scenarios used throughout most of this report.) The low-emissions (SSP1-2.6), medium-emissions (SSP2-4.5), and high-emissions (SSP3-7.0) scenarios used throughout this report all fall within the intermediate low to intermediate range in the 2022 Interagency Technical Report's scenarios for sea level rise.

Under the intermediate scenario—a reasonable representation of most likely sea level rise based on the trajectory of recent observations—sea level in Los Angeles is expected to increase 6 inches in the next three decades (Sweet, Hamlington et al. 2022). Beyond 2050, the range of potential sea level rise expands significantly, driven by different future emissions scenarios and the behavior of the Greenland and Antarctic Ice Sheets. By 2100, future sea level rise ranges from 0.6 feet to 6.2 feet across the low to high scenarios. Under the intermediate scenario, the coastal areas of Los Angeles could experience 20 days of minor high tide flooding every year by 2050 and over 250 days of minor high tide flooding every year by 2100 (Figure 2-34).

FIGURE 2-33

The number of days of minor high tide flood exceedances in Los Angeles from 1970 to present. The values of daily sea level are provided relative to mean higher high water (MHHW). The threshold is the minor flood threshold NOAA set for Los Angeles. This threshold indicates when flooding may begin to occur and impacts may start to be felt. The years with the most flooding tend to be driven by the occurrence of significant El Niño events that drive annual sea levels higher across the Los Angeles region.

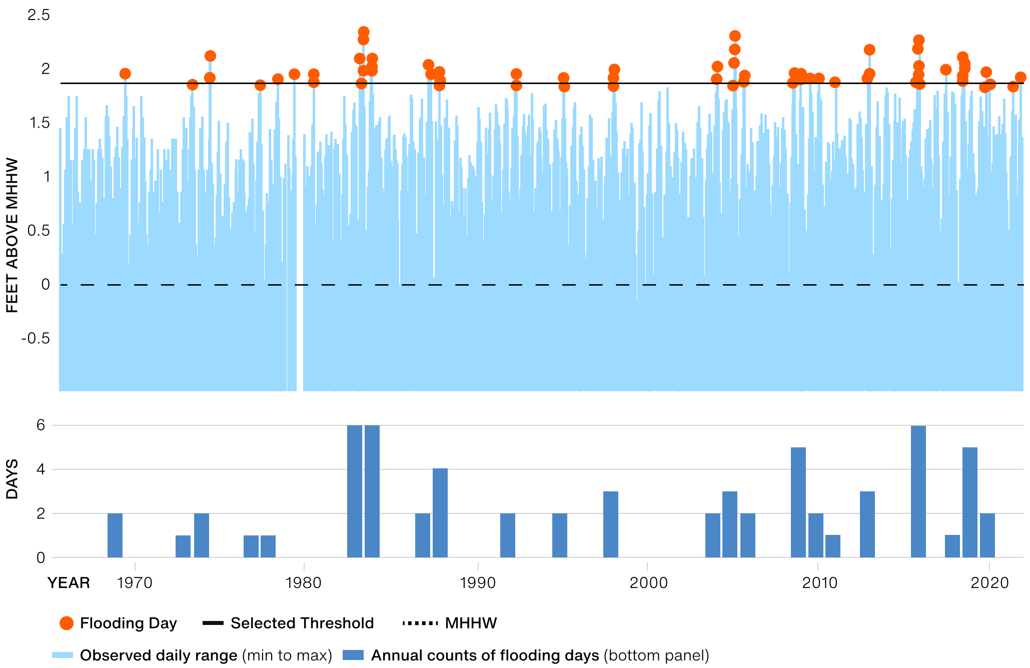

FIGURE 2-34

This bar chart shows the number of minor high tide flood days that are expected during each decade from 2020 to 2100 under different scenarios of sea level rise for Los Angeles. If the number of days reaches 365, the sea level has risen high enough that high tide will exceed the flood threshold every day. The five scenarios have similar sea level change between 2020 and 2050 but vary more after 2050 based on differences in GHG emissions and their impact on sea level rise, such as causing rapid melting of ice sheets.

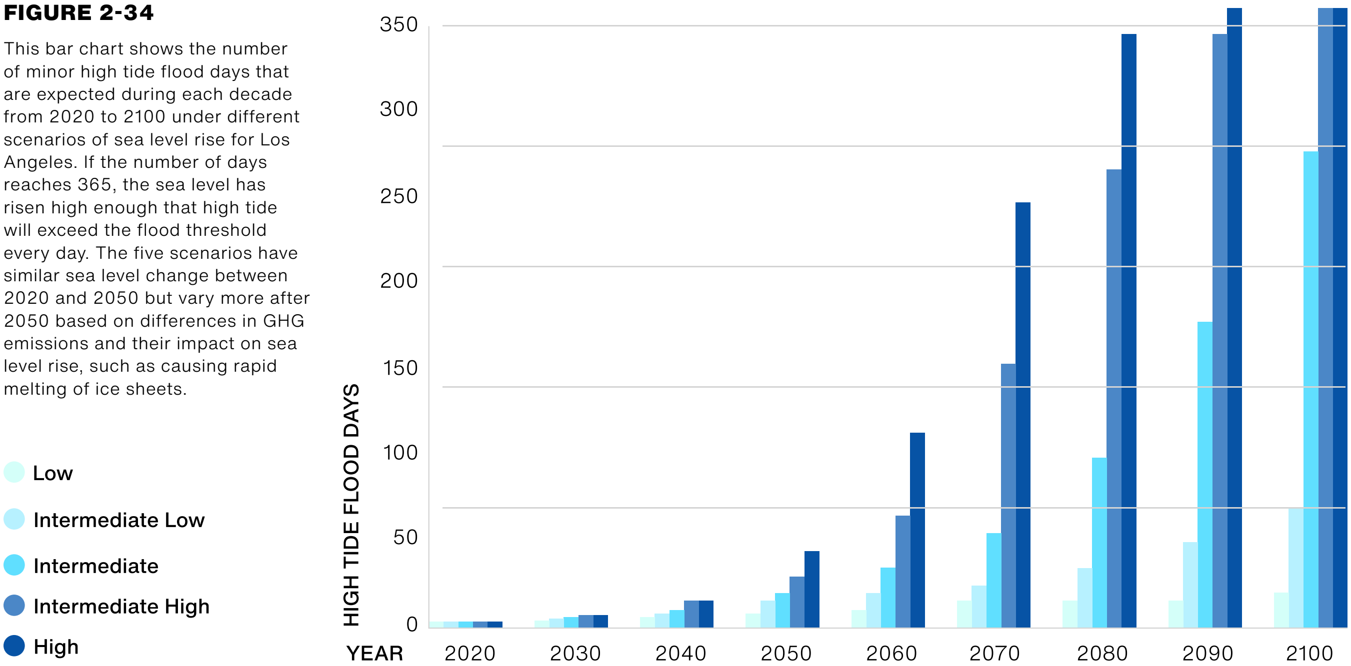

2.8

2.9 Earthquakes and Landslides

Southern California has the highest earthquake hazard in the United States. JPL sits astride the leading edge of the fault system that gives rise to the San Gabriel mountains, an actively rising mountain range that accommodates a convergence component of the section of the San Andreas Fault system north of Los Angeles, the principal plate boundary fault between the North American and Pacific plates. Fault strands of the Sierra Madre-Cucamonga Fault system pass through the main JPL campus. However, there are many other faults spread across Southern California and the Los Angeles region, with every set of hills and smaller mountains (e.g., Santa Monica Mountains, Whittier Hills, Palos Verdes, Baldwin Hills, and Verdugo Hills) resulting from thrust faulting accommodating the deforming plate boundary zone.

Relevant agencies and geophysical organizations, including the United States Geological Survey (USGS) and the Southern California Earthquake Center (SCEC) have assessed earthquake probabilities across the primary faults, such as the UCERF3 report (Field 2015) or as shown in Figure 2-35. In each of these examples, fault earthquake recurrence and magnitude probabilities are based on the historical record, geological estimates, and present-day estimates of fault slip rates and associated models. The underpinnings of these fault slip and acceleration (shaking) estimates are that humans are minor stressors compared to tectonic loading rates. But a recent study (Hill, Weingarten et al. 2023) suggests that variations in water level in the former Lake Cahuilla (where the Salton Sea is now) over hundreds of years

FIGURE 2-35

Number of times per century that shaking from earthquakes will exceed 20% of the acceleration of gravity. Southern California Earthquake Data Center (https://scedc.caltech.edu/earthquake/seismic-hazards.html).

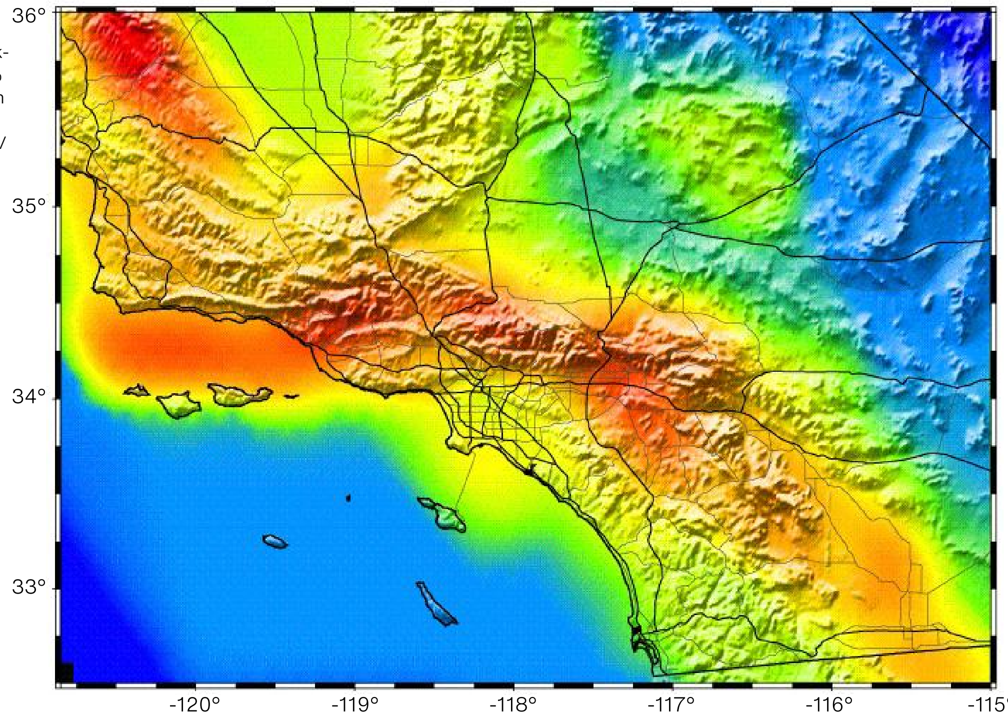

KEY

Number of times per century the shaking from earthquakes exceed 20% the force of gravity. Significant damage to older buildings begins a this level.

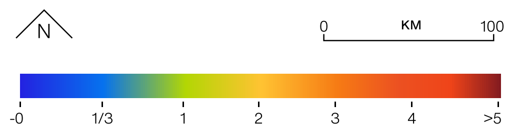

may affect the rate of earthquakes on nearby faults, including the Southern San Andreas Fault, with major earthquakes occurring when the water level is highest. It should be noted that while climate change, or weather, is not considered a significant driver for earthquakes, earthquakes can be a major driver for landslides in areas of steep topography, which is often the case in areas with active faults. Therefore, for JPL in particular, its location astride the frontal toe of the San Gabriel Mountains makes it susceptible to cascading hazards from large (e.g., San Andreas Fault) or local (e.g., San Gabriel frontal faults) earthquakes.

Landslides are among the most common hazards in mountainous regions worldwide (Kirschbaum, Stanley et al. 2015) that are being impacted by climate change (Gariano and Guzzetti 2016). There are many different types, but two large categories are deep-seated landslides, which involve soil and rock that can range in thickness from meters to hundreds of meters, and debris flows, where surface material is carried by water. The mountainous areas of the Los Angeles region have experienced thousands of landslide events over the last 50 years (Figure 2-36) triggered by both rainfall (Biasutti, Seager et al. 2016) (Li, Handwerger et al. 2024) and earthquakes (Harp and Jibson 1996). While deep-seated landslides can occur in large numbers, for example when triggered by earthquakes (Harp and Jibson 1996), rainfall-triggered landslides and debris flows are more frequent on an annual basis and are closely linked to climate. Thus, changes in rainfall patterns, such as the extreme wet periods that are predicted to increase over the next century in California (Persad, Swain et al. 2020) (Swain, Langenbrunner et al. 2018), may increase landslide hazards overall.

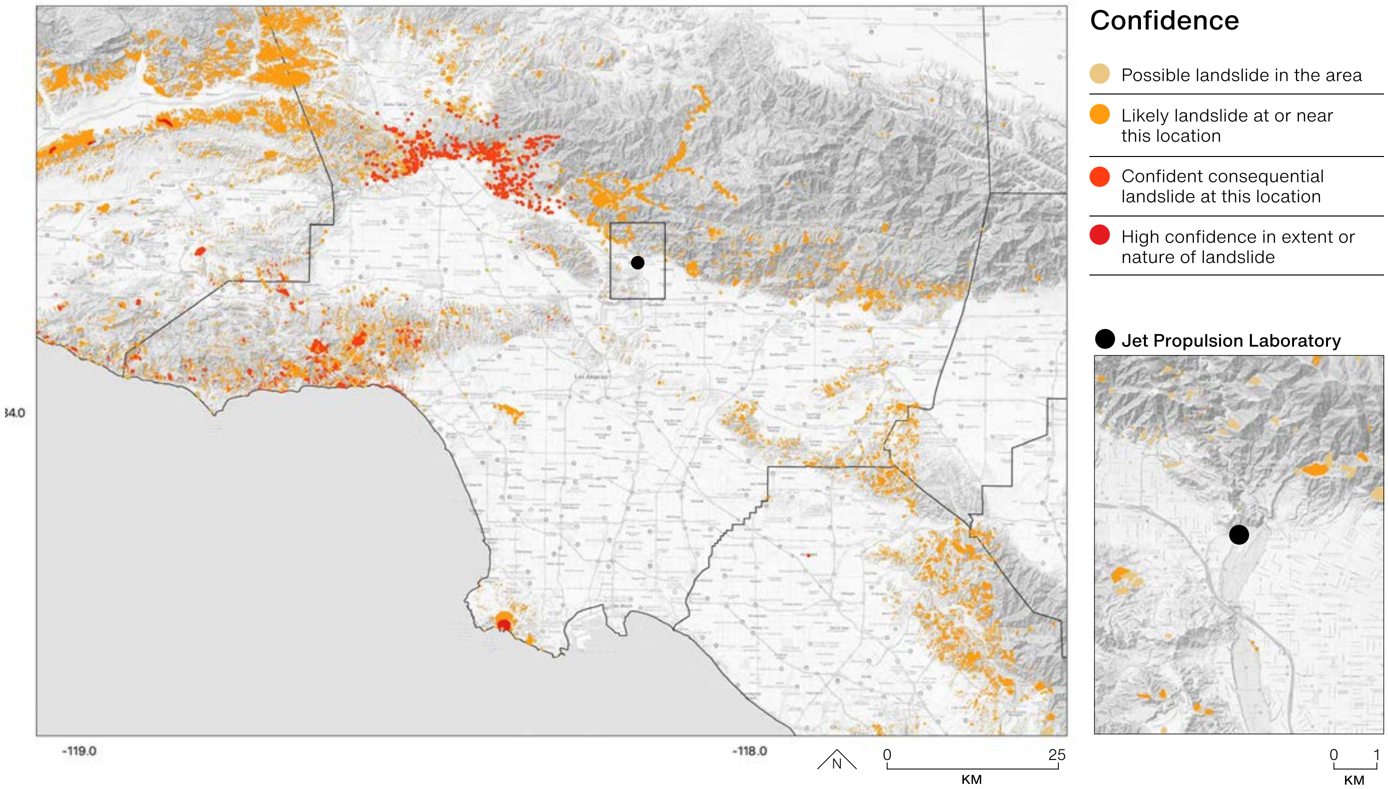

FIGURE 2-36

Landslide inventory for Greater Los Angeles with inset showing the JPL area. The landslide inventory is managed by the USGS and is a compilation of many published landslide databases (Belair, Jones et al. 2022).

Recent work has examined rainfall-triggered landslides in the Los Angeles region and found that the extreme wet years of 2017, 2019, and 2023 all had major impacts on landslide activity and occurrence (Li, Handwerger et al. 2024) (Handwerger, Fielding et al. 2022). The California Geologic Survey inventoried over 1,200 landslides in California, 544 of which were in the Los Angeles region, that were triggered by a parade of ARs during the extreme 2023 wet season (California Department of Conservation 2023). Rancho Palos Verdes, Los Angeles, has experienced some of the most severe landslide events in the Los Angeles region since 2023. In July 2023, 12 homes were destroyed in Rolling Hills Estates (Li, Handwerger et al. 2024) (Figure 2-37). Many others have been damaged or destroyed by the Portuguese Bend landslide between 2023 and 2024, and the area is now under a local state of emergency (City of Rancho Palos Verdes 2025). These recent extreme wet seasons may be representative of the climate conditions, and associated landslide activity, in California over the next century (Swain, Langenbrunner et al. 2018).

As discussed in previous sections, climate change is increasing post-fire debris flows—a type of landslide that occurs after wildfires because fires reduce the soil's capacity to absorb water, leaving more water to flow over the surface and carry debris with it. Figure 2-38 shows examples of post-fire debris flows in southern California, including the 2018 Montecito debris flows after the Thomas Fire and, much closer to JPL, the La Cañada Flintridge debris flows after the 2009 Station Fire (Kean and Staley 2021). Debris flows in the mountains behind JPL caused major accumulation of gravel in the Arroyo Seco after heavy rains in 2010 fell on slopes burned in the Station Fire. Together, the Los Angeles region has high landslide and debris flow susceptibility due to earthquakes, rainfall, and fires combined with steep slopes.

FIGURE 2-37

Photo showing destroyed houses following the 2023 Rolling Hills Estates landslide, Rancho Palos Verdes, California (photo from Robert Gauthier / Los Angeles Times).

FIGURE 2-38

Damage from significant post-fire debris flows in Southern California over the past 20 years includes: (A) Devore in San Bernardino County on December 25, 2003 (following the Old/ Grand Prix Fires); (B) La Cañada Flintridge in Los Angeles County on February 6, 2010 (after the 2009 Station fire); and (C) and (D) Montecito in Santa Barbara County on January 9, 2018 (resulting from the 2017 Thomas fire; photo credits USGS and from Kean and Staley (2021)).

On the JPL campus, the steep hillslopes on the northern side of the Lab are susceptible to landslides. If landslides occur along these slopes, they could easily impact buildings at JPL and cause damages or loss of life. While the landslide susceptibility at JPL has not been modeled under climate change scenarios, the California Geologic Survey has produced basic susceptibility maps that account only for topographic slope angle and material strength properties. Figure 2-39 shows there is relatively high landslide susceptibility along the steeper hillslopes within JPL. More work is needed to better understand specific landslide hazards at these sites and to understand how climate change will affect the landslide and debris flow susceptibility.

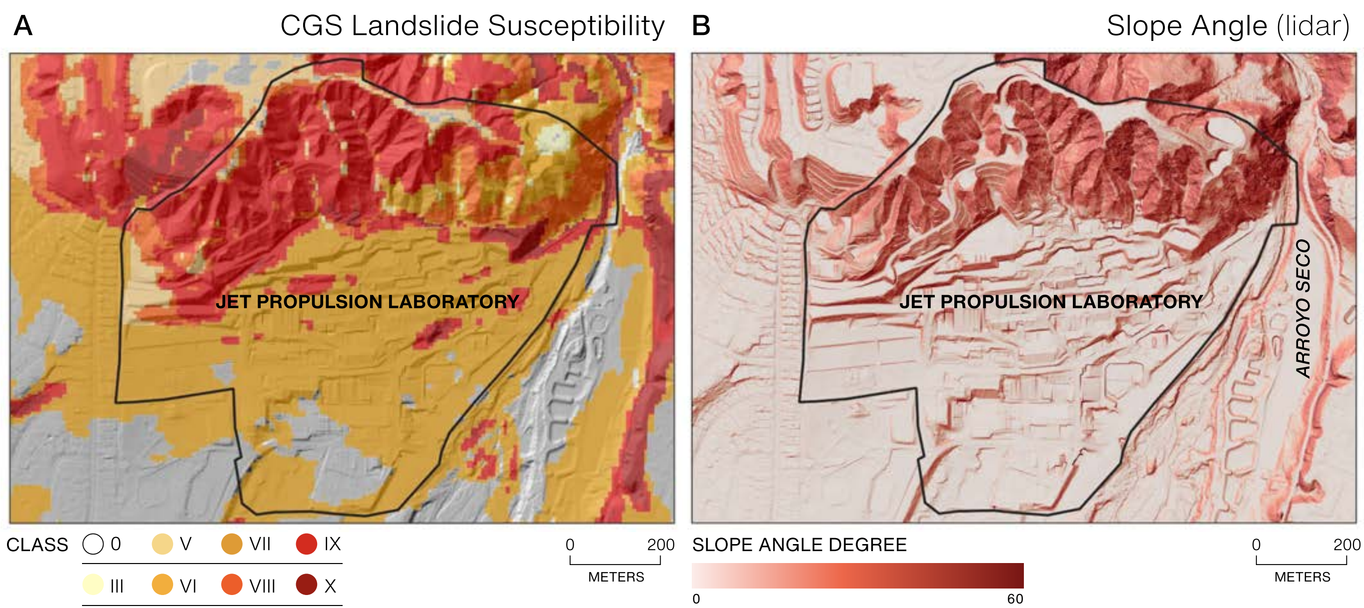

FIGURE 2-39

(A) Map of deep-seated landsliding likelihood based on regional estimates of rock strength and steepness of slopes. Data provided by the California Geologic Survey. (B) Topographic slope angle map draped on a lidar hillshade. (Lidar data provided by the U.S. Forest Service Region 5 Remote Sensing Lab Information Management Staff. (2023). USFS San Gabriel Mountain Lidar, CA 2009. Collected by Dewberry. Distributed by OpenTopography. https://doi.org/10.5069/G9M32T07.)

2.10 Land Use and Land Cover Change

Over the past two decades, the Los Angeles region has undergone significant LULC changes driven by both anthropogenic activities and natural processes. Employing long-term time series analysis of Landsat optical imagery, researchers have developed methodologies to quantify global LULC transformations and discern their causal factors (Potapov, Hansen et al. 2022). As depicted in Figure 2-40, which illustrates LULC dynamics in Southern California from 2000 to 2020, marked urban expansion—highlighted in cyan—is evident in northern Los Angeles County and extends into adjacent counties such as Orange, Riverside, and San Bernardino. This expansion underscores substantial population growth and industrial development within the region.

Natural factors also play a significant role in LULC dynamics, particularly in the rural and mountainous areas surrounding the basin. For instance, the San Gabriel and Santa Monica Mountains have experienced notable vegetation recovery in regions previously disturbed, as indicated by areas marked in brown (tree cover with previous disturbance) and red (short vegetation after tree loss). This recovery highlights the resilience of these ecological systems despite persistent drought conditions during the same period. In contrast, natural LULC changes are less pronounced in highly developed areas, including the immediate vicinity of JPL, as shown in the inset of Figure 2-40.

The San Gabriel Mountains and the 700,000-acre Angeles National Forest, considered a prominent natural asset of the Los Angeles region, are home to wildlife, scenic landscapes, and diverse recreational opportunities. Over the past two decades, increasing frequency and intensity of heat waves—attributable to both natural variability and anthropogenic influences

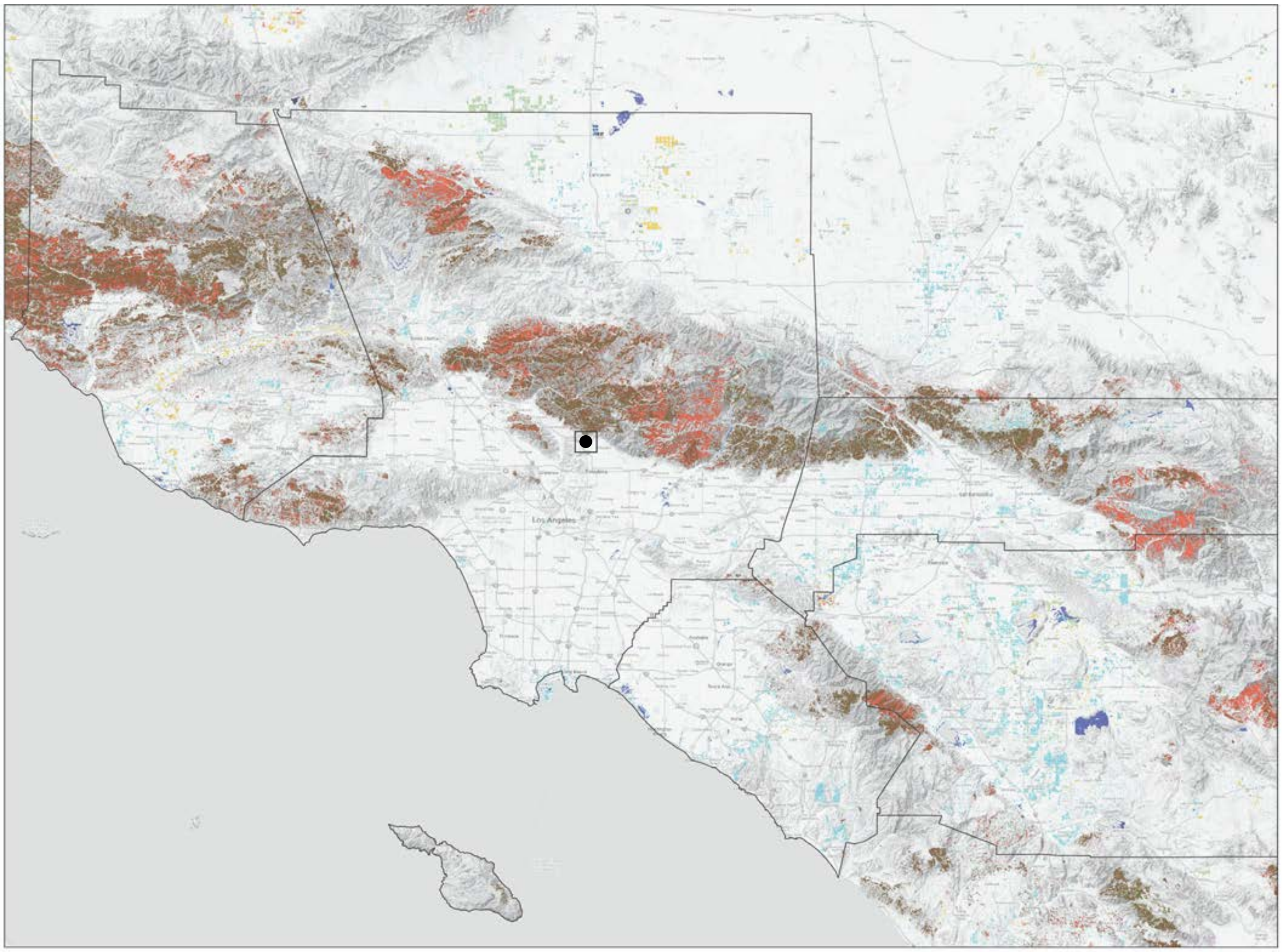

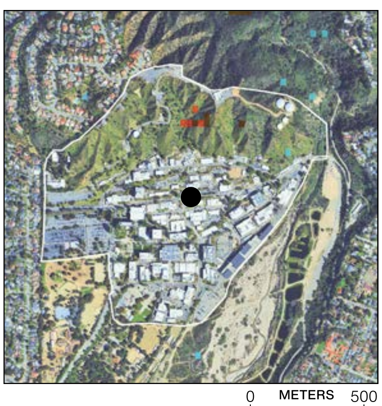

FIGURE 2-40

Land use and land cover change between 2000 and 2020 within the Greater Los Angeles area. (Data credit: Global Forest Change by Global Land Analysis and Discovery (GLAD) Laboratory of the University of Maryland, https://glad.earthengine.app/view/global-forest-change#bl=off;old=off;dl=4;lon=-118.18648323206033;lat=34.23582590817626;zoom=11;.)

such as the urban heat island effect (Section 2.1)—have intensified wildfire risks (Section 2.3), as well as risks of landslides (Section 2.9) and the subsequent debris flows during post-fire rainfall events. This dynamic forest ecosystem, situated a few miles north of JPL, poses substantial risks to surrounding residential areas and the JPL workforce.

Recent advancements in satellite technology have enabled the mapping of global forest change due to wildfire activities (Tyukavina, Potapov et al. 2022). Figure 2-41A illustrates the extent and temporal characteristics of forest disturbance in the Angeles National Forest from 2000 to 2023. This data set provides a means to map the extent and age of forest disturbance due to past wildfires. Areas recently disturbed by wildfires (indicated in light brown to the east of JPL, for example) generally exhibit lower fire risk in subsequent burn events compared to areas disturbed in the more distant past (depicted in red north of JPL, for example), where vegetation may have recovered and become potential burn fuel.

Analysis of the LULC data shown in Figure 2-41B reveals a significant increase in vegetation growth (depicted in green) north of JPL during the decade after the 2009 Station Fire, which advanced to within one meter of JPL's main campus. This increase in vegetation, or accumulating wildfire fuel, necessitates rigorous monitoring to manage the risk of wildfire. Given the proximity of this extensive forested area to JPL, continuous surveillance of fire weather conditions—including relative humidity, temperature, precipitation, and wind speed—is critical. The pristine vegetation untouched by any past wildfires over an area of the foothills northeast of JPL and the seasonal SAWS bringing dry, hot, and rapidly moving air masses over Angeles National Forest further necessitate vigilant wildfire risk management in this region. Analyzing historical wildfire data and potential accumulation/return of vegetation fuel is crucial for informing resource allocation and developing effective wildfire mitigation strategies.

FIGURE 2-41

(A) Fire-driven forest disturbance extent and age and (B) LULC change attributes within the Greater Los Angeles area. (Data credit: Global Forest Change by GLAD Laboratory of the University of Maryland, https://glad.earthengine.app/view/global-forest-change#bl=off;old=off;dl=4;lon=-118.18648323206033;lat=34.23582590817626;zoom=11;.)

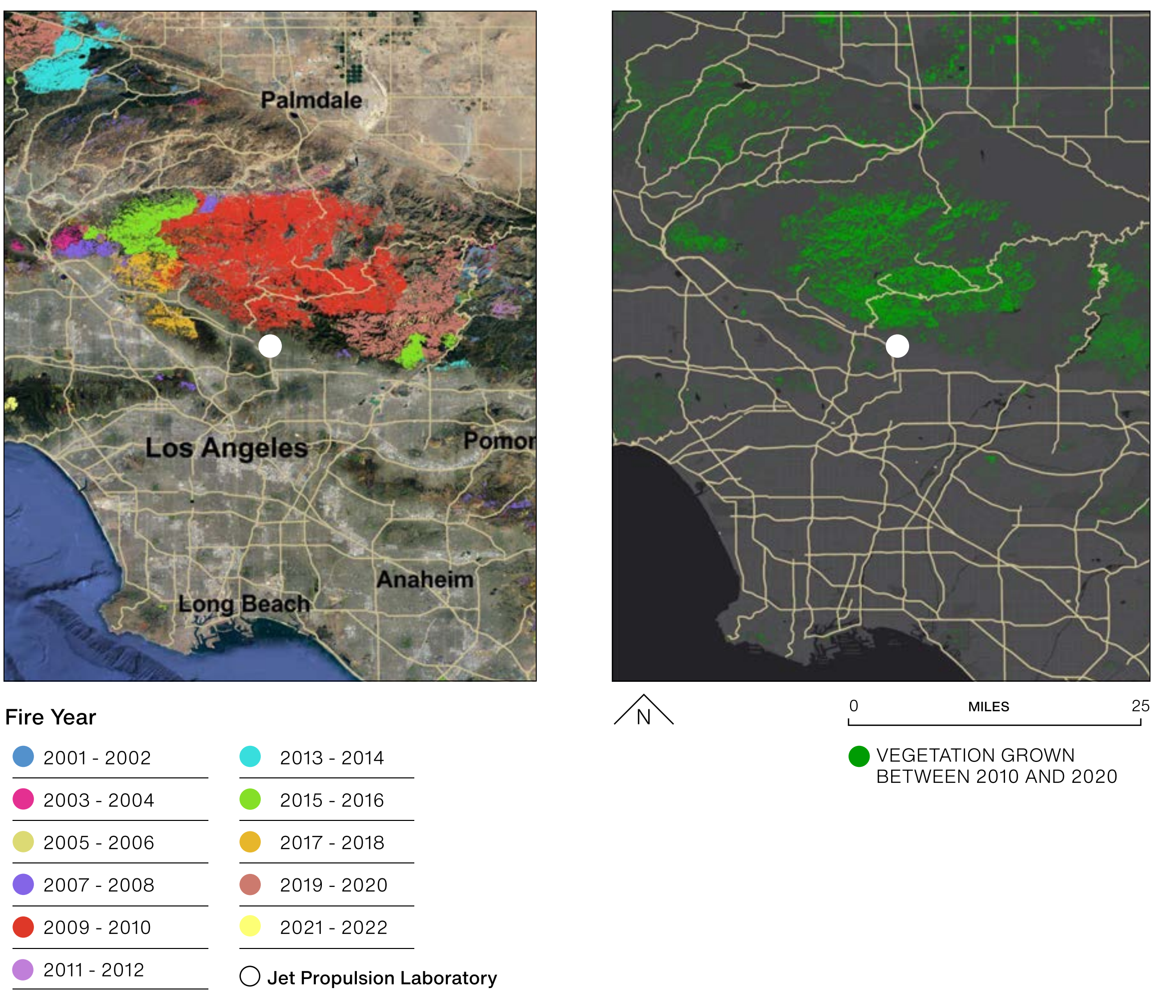

2.11 Carbon and Greenhouse Gas Considerations

JPL and Caltech researchers have developed Los Angeles into the nation's premiere testbed for quantifying urban GHG emissions, deploying an observing system with multiple tiers (Cusworth, Duren et al. 2020). These methods include the Megacities Carbon Project in situ network (Verhulst, Karion et al. 2017); CLARS atop Mt. Wilson (Zeng, Pongetti et al. 2023); Total Carbon Column Observing Network (TCCON) sites at Caltech and NASA's Armstrong Research Flight Center in Palmdale, California, (Schwandner, Gunson et al. 2017) in collaboration with NASA ARC; frequent target mode acquisitions by NASA's OCO-2 satellite and snapshot acquisitions by the OCO-3 instrument on the ISS (Schwandner, Gunson et al. 2017) (Kiel, Eldering et al. 2021) (Roten, Lin et al. 2023); and, most recently, methane and carbon dioxide plume observations from NASA's EMIT instrument on the ISS (Thorpe, Green et al. 2023) and the equivalent airborne instrument AVIRIS-3 (Thorpe, Green et al. 2024). Additionally, aircraft and mobile laboratory campaigns measuring GHGs, their carbon isotopes, and co-emitted species are frequently made in the Los Angeles basin to complement the ongoing measurements (Miller, Lehman et al. 2020). Finally, the availability of the Hestia-LA high-resolution fossil fuel carbon dioxide emissions inventory (Gurney, Patarasuk et al. 2019), the VISTA-LA natural gas infrastructure GIS database (Carranza, Rafiq et al. 2018), and a meter-scale resolution model of the Los Angeles basin biosphere (Parazoo, Coleman et al. 2022) enable accurate GHG emissions estimates from the atmospheric observations. Some of the insights gained from these efforts are highlighted in this section.

These observing system and analysis tools coupled with the length of the time series data records for Los Angeles are now sufficiently mature to help guide and inform city, county, and regional emissions-reduction policies.

2.11.1 High-Resolution Fossil Fuel Emissions Inventories

JPL researchers have been working in collaboration with federal and university partners to develop emissions inventories such as Hestia-LA for understanding GHG mitigation options for the Los Angeles Megacity (Gurney, Patarasuk et al. 2019). The fossil fuel carbon dioxide emissions inventory indicates that human activities concentrated in the Los Angeles megacity generate a significant source of GHG emissions relative to the surrounding less-populated region (Figure 2-42). Vehicles/traffic (43%) and industry (24%) account for two-thirds of area fossil fuel carbon dioxide emissions, with the remaining third being distributed across all other sectors. Los Angeles methane emissions are estimated to account for approximately 20% of California's annual emissions and are thought to be dominated by the natural gas system (Jeong, Newman et al. 2016) (Zeng, Pongetti et al. 2023).

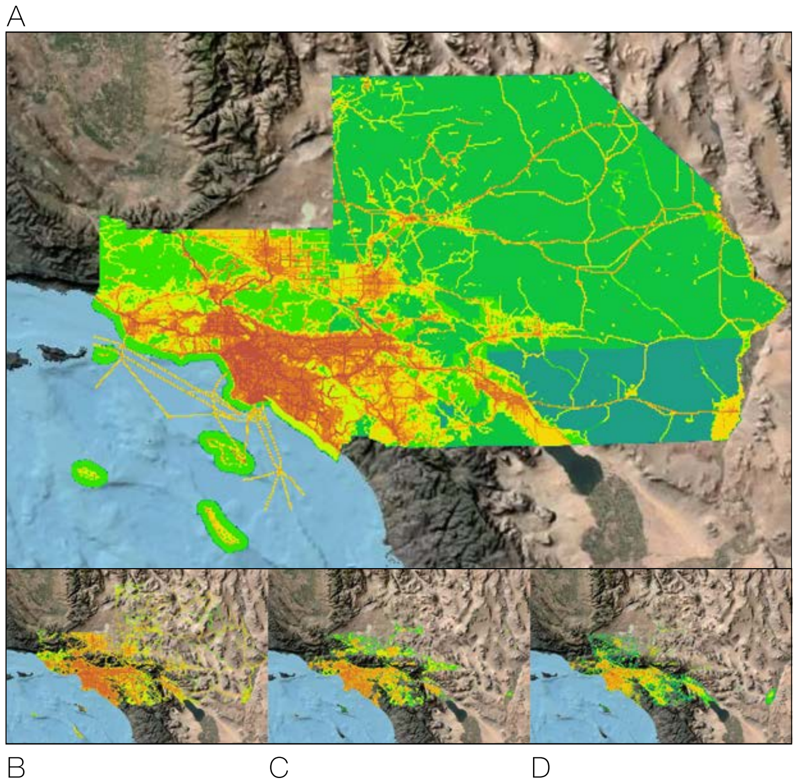

FIGURE 2-42

Hestia-LA v2.5 fossil fuel carbon dioxide emissions for the year 2011 represented on a 1 km x 1 km grid: (A) total emissions, (B) on-road emissions, (C) residential emissions, and (D) commercial emissions. Units: natural logarithm of kgC yr^{-1} (Gurney, Patarasuk et al. 2019).

2.11.2 Identifying and Attributing Los Angeles Emissions

JPL airborne (AVIRIS, AVIRIS-NG) and spaceborne (EMIT, OCO-3) instruments have been used for identifying, quantifying, and attributing variations and trends in methane and carbon dioxide contribution from individual sectors in the Los Angeles region, such as on-road transportation, industry, and marine sectors (Roten, Lin et al. 2023) (Wu, Liu et al. 2022), and from energy, waste, and agriculture sectors (Duren, Thorpe et al. 2019) (Cusworth, Duren et al. 2020) (Jeong, Newman et al. 2016). These instruments have also observed a reduction in carbon dioxide emissions from the transportation sector and methane emissions during COVID-19 (Thorpe, Green et al. 2023) (Roten, Lin et al. 2023).

AVIRIS-3, the most sensitive imaging spectrometer for GHG applications, has provided ongoing observations of methane and carbon dioxide point source emissions in the Los Angeles region, including the South Bay of Los Angeles (Figure 2-43), in support of the United States Greenhouse Gas Center.

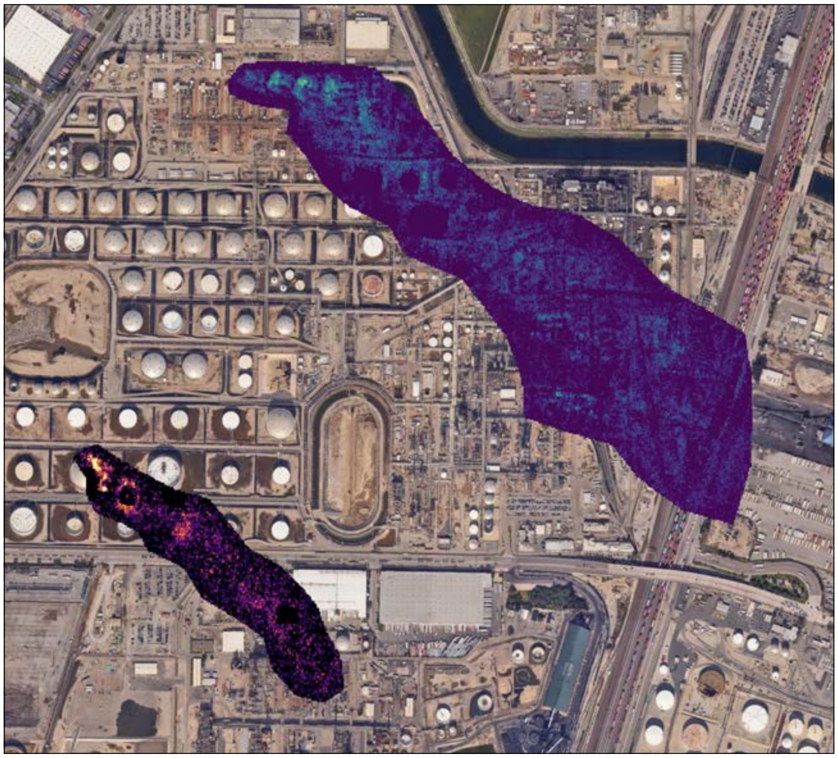

Carbon Dioxide
Conc. Length [ppm m]
— 100,0000
— 80,000
— 60,000
— 40,000
— 20,000
— 0

Methane
Conc. Length [ppm m]
— 1,500
— 1,250
— 1,000
— 750
— 500
— 250
— 0

FIGURE 2-43

When sudden changes in GHG emissions occur, NASA's and JPL's rapid response program is ready to deploy instruments to document and monitor. A methane point source from a storage tank and carbon dioxide emissions from a power generating plant observed with AVIRIS-3 are shown associated with refineries east of Carson in the South Bay of Los Angeles.

2.11.3
Aliso Canyon Natural Gas Well Blowout

When sudden changes in GHG emissions occur, JPL's instruments are ready to document and monitor. On October 23, 2015, a well in the Aliso Canyon natural gas storage facility blew out. Located in Porter Ranch, a suburban area in Southern California, this well vented treated natural gas at a very high rate into the atmosphere for four months. JPL's CLARS-FTS instrument on Mt. Wilson maps the concentrations of methane (the main constituent of natural gas) in the Los Angeles basin every 90 minutes and recorded very high levels of methane from the blowout. While the leaking well itself lay outside the CLARS field of regard, CLARS-FTS measured the excess methane plume when the winds carried the plume from the well into the Los Angeles Basin. Maps showing methane before, during, and after the well blowout are shown in Figure 2-44. The contours in the figure are shown for the ratio of methane to carbon dioxide, which more accurately accounts for aerosol interference. On average, the well blowout increased the excess methane emissions in the Los Angeles Basin by 25%–50% during the leak event. On some occasions, the excess methane concentrations were 10 times larger than normal. JPL researchers also identified the Aliso Canyon natural gas reservoir blowout from space, using the Hyperion imaging spectrometer on board the Earth Observing-1 (EO-1) satellite (Thompson, Thorpe et al. 2016), and quantified Aliso Canyon methane emissions rates using the airborne AVIRIS instrument (Thorpe, Duren et al. 2020).

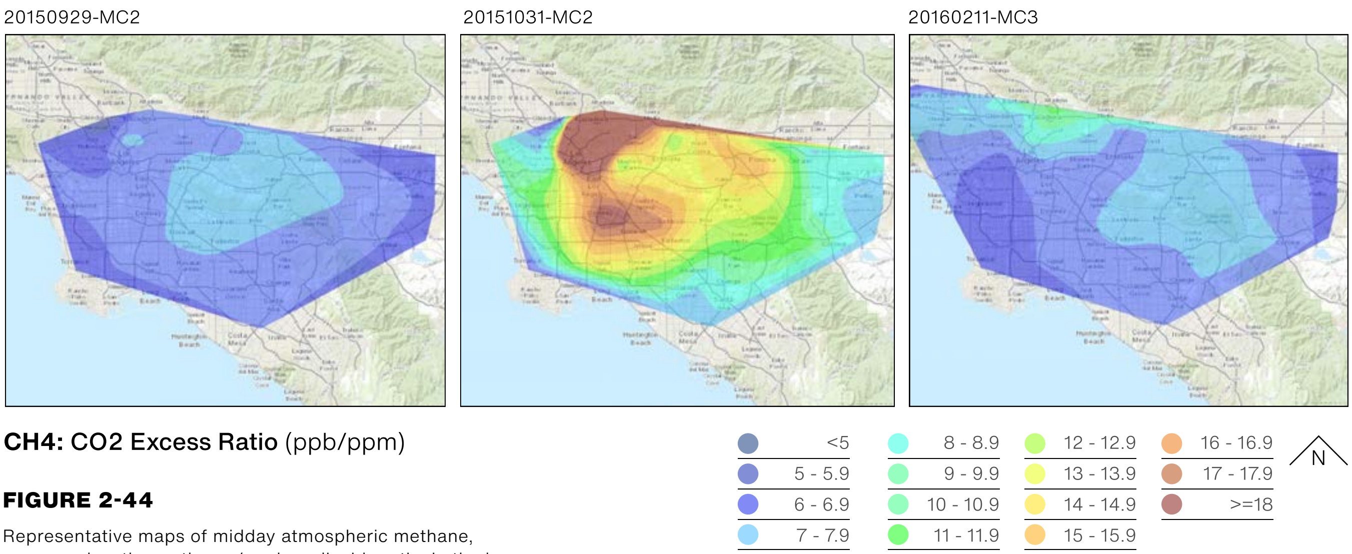

FIGURE 2-44

Representative maps of midday atmospheric methane, expressed as the methane / carbon dioxide ratio, in the Los Angeles Basin. (A) Before the well blowout (September 29, 2015), (B) during the blowout (October, 31 2015), (C) after the well was capped (February 11, 2016).

2.11.4
Tracking Long-Term Trend of Methane Emissions

Methane is a powerful GHG whose global concentrations have been increasing steadily. Methane is relatively short-lived in the atmosphere but has stronger radiative forcing, or warming effect, than carbon dioxide on a per molecule basis, and can therefore do more damage quickly. Efforts to understand and control methane emissions thus pay a large dividend in reducing radiative forcing in the atmosphere compared to other GHGs. JPL plays a large role in this effort in California. In 2014, the California Legislature passed Senate Bill 1371, which required natural gas utilities to avoid, reduce, and repair leaks from their pipelines and equipment. JPL's CLARS-FTS and the Megacity Carbon Project are among the independent, long-term programs verifying progress toward this goal (Fu, Pongetti et al. 2014) (Verhulst, Karion et al. 2017).

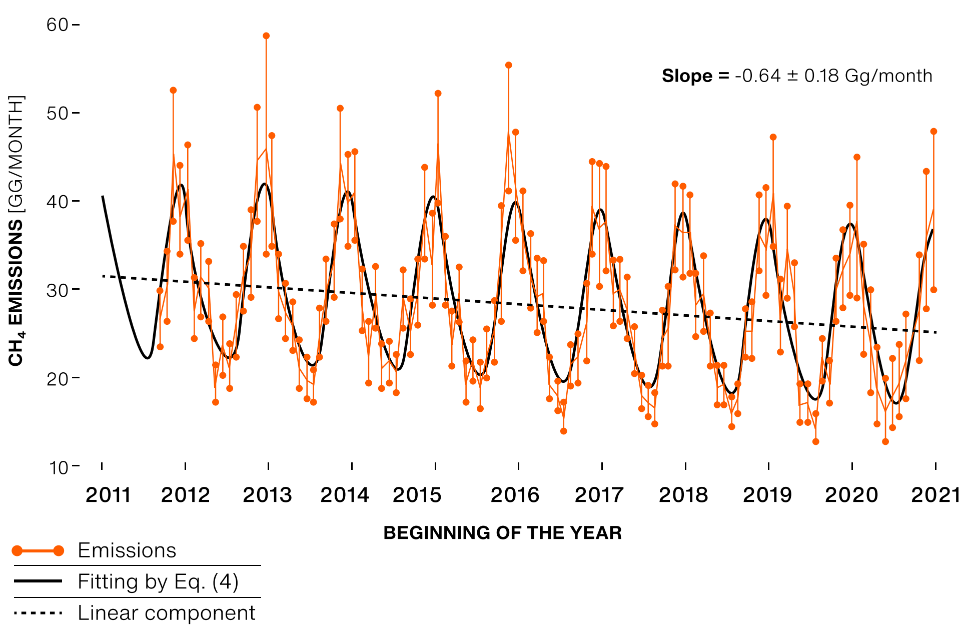

FIGURE 2-45

The seasonal and interannual trends in CH_4 emissions in the Los Angeles basin inferred from measurements from the CLARS-FTS instrument. This illustrates how long-term monitoring from ground-based and satellite instruments is required to discern small, long-terms trends.

From its perch atop Mt. Wilson, CLARS-FTS has been mapping methane emissions in the Los Angeles Basin since 2011. Over that period, some interesting trends have been discovered, as shown in Figure 2-45. Within each year, emissions peak prominently in in the winter and dip in the summer. Natural gas supplied to residential and commercial use should travel via closed pipes that don't emit gas to the atmosphere. But JPL's instruments do detect an increase in emissions when consumption increases, implying there are natural gas leakages occurring primarily in the winter from appliances such as furnaces and water heaters. Second, there is a small overall decline in natural gas (corrected for the long-term increase in methane in the global atmosphere) averaging about 1.5% per year (Zeng, Pongetti et al. 2023). This is likely due to mitigation efforts by the natural gas utility and other operators of facilities that produce natural gas emissions (landfills, wastewater treatment).

Detection and reporting of these cycles and trends is an extremely important element in the goal of reducing natural gas emissions. JPL's monitoring, analysis, and modeling assets are playing a key role in this effort.

2.11.5
Spaceborne Monitoring of the Los Angeles Carbon Dioxide Dome

From its vantage point on the ISS, the OCO-3 instrument scans and measures carbon dioxide over many of the world's cities, including Los Angeles (e.g., Figure 2-46). Since the beginning of the mission in late 2019, the instrument has taken over 100 such snapshots of the Los Angeles region. The majority of snapshots reveal a complex picture of carbon dioxide emissions across the area, with the largest contributions coming from the transportation (especially along the major trucking routes linking the port of Long Beach to various parts of the Los Angeles region) and industrial sectors.

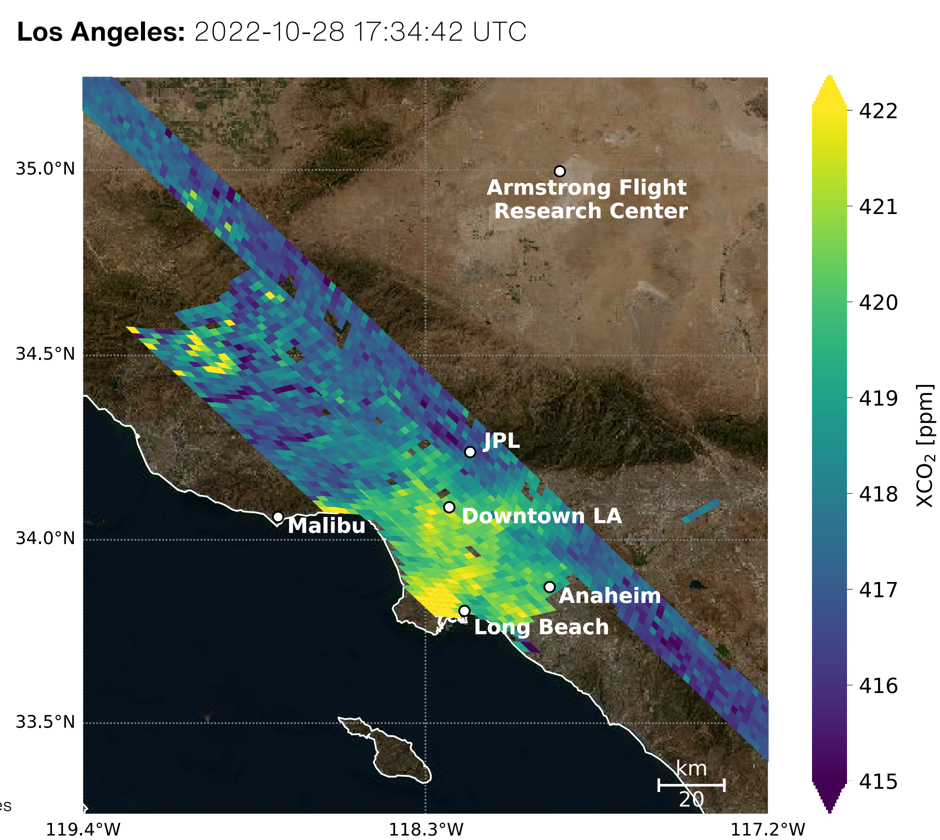

FIGURE 2-46

Representative map of column integrated atmospheric CO_2 concentrations (XCO_2) over the Los Angeles area on October 18, 2022. XCO_2 enhancements of 5–7 ppm in Los Angeles, representing the difference between the Los Angeles metro area and surrounding non-urban areas.

2.11.6 Greenhouse Gas Emissions from JPL Facilities

Activities at JPL and its satellite facilities result in limited onsite GHG emissions (Figure 3-10); however, JPL does generate a significant carbon footprint through emissions directly tied to its electricity use, vehicular commuting, airplane travel, and efforts to relocate fully remote employees back to JPL. Recent trends in the use of high-end computing to process the increasing amounts of data collected from the expanding GHG monitoring network, particularly energy-intensive cloud computing and artificial intelligence systems relying on networks of computers in large data centers, have likely exacerbated JPL's electricity usage. Increased commuting distances, driven by rising home prices across the Los Angeles region, also likely add significantly to JPL's emissions. Considerations for further decarbonizing JPL could include:

- Upgrades from outdated equipment to energy-efficient equipment and optimizing energy-efficient management (occupancy sensors, LED retrofits, and HVAC set timers)
- Incentives for JPL employees and contractors to adopt zero-emissions vehicles
- More stations for charging electric vehicles on Lab
- Encouraging telecommuting when possible
- Increasing the frequency (20 minutes), regularity (morning, midday, afternoon), and quality (new or upgraded vehicles) of the Gold Line shuttle
- Promoting the use of non-airplane work travel, such as the train, by accommodating longer trips and not requiring the use of vacation days
- Separate work advisories for employees who walk or bike to work, and allowing work from home if weather conditions such as high winds, poor air quality, or extreme heat make it unsafe for travel
- Subsidies for people taking public transit but also conducting reviews to ensure subsidies are adequate
- Working with Metrolink, Amtrak, and bus services to provide information for passengers on how their public transit use measurably causes decreases in emissions, as indicated by a World Bank study using data from JPL's OCO-2 satellite (Dasgupta, Lall et al. 2023)

Laboratory Resilience and Perspectives

03

This section provides background on the resilience and continuity-of-operations requirements toward which the Laboratory is working and highlights the weaknesses present in the Laboratory's infrastructure and operations relative to environmental hazards. It offers suggestions for adaptation and addresses further sustainability factors. This section makes the connections between these vulnerabilities, risks, and adaptation considerations with the climate and environmental issues previously mentioned, referring to specific subsections of Section 2.

3.1 Continuity of Operations and Resilience Drivers

Requirements for the resilience of the Lab against environmental and non-environmental hazards have two sources. As a NASA facility, JPL must comply with federal policy related to continuity-of-operations planning for critical infrastructure. And for its own business-continuity reasons, the Lab has policies in place to minimize the impact of external events on the Lab's day-to-day operations. Figure 3-1 shows this hierarchy.

JPL has worked with NASA to define NASA critical infrastructure (NCI) on Lab. Those facilities are known but not shared here. Note that the DSN function as a whole is identified as critical infrastructure the federal government needs to operate spacecraft as part of its minimum functionality. It is supposed to be resilient against a wide range of natural and human-made events.

Plans for improving the Lab's resilience against climate and environmental threats need to be responsive to the priorities and processes identified in these existing federal, NASA, and JPL documents.

FIGURE 3-1

Continuity-of-operations requirements and responding plans and programs from the federal level to the Lab level.

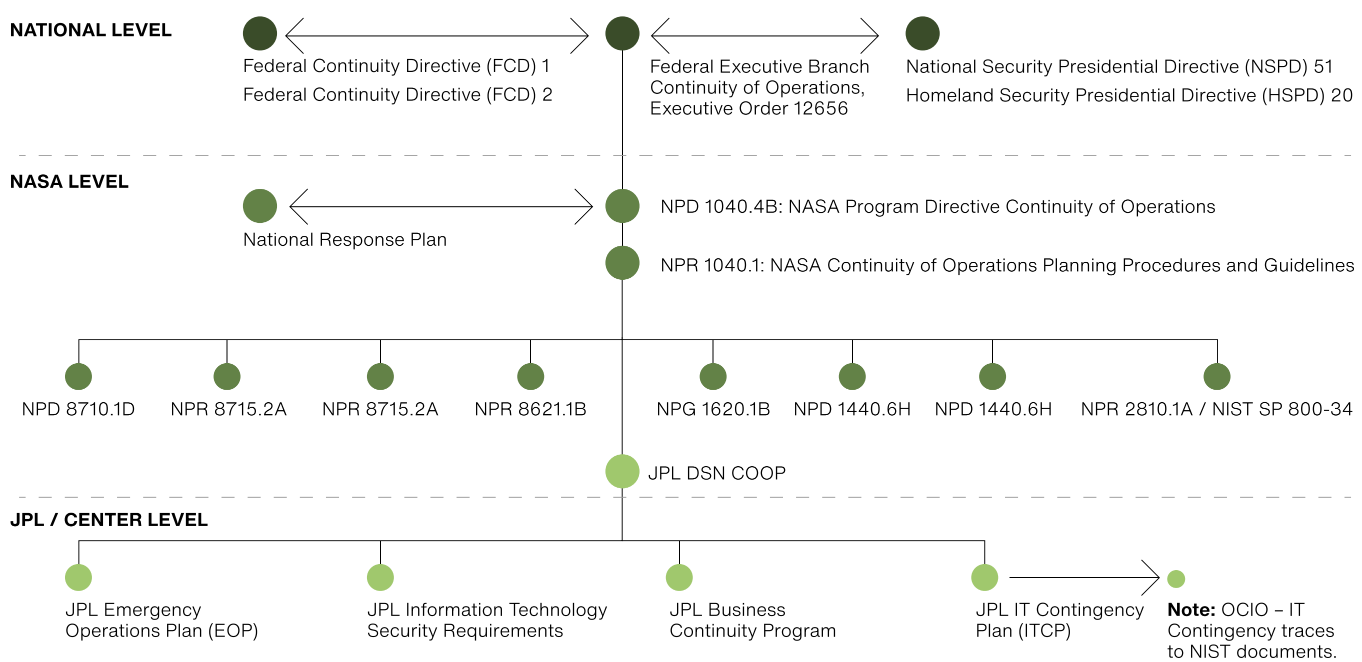

3.2 Summary of Environmental Risks Mapping to Laboratory Infrastructure and Operations

This section outlines the environmental risks and causes that impact JPL's infrastructure and operations. It is essential to address these environmental risks to facilitate informed decision-making regarding mitigation strategies, resilience planning, and sustainability efforts.

Environmental Risks

Heat Waves (Section 2.1): An increase in hot days leads to higher use of HVAC systems, resulting in elevated energy and maintenance expenses.

Wildfires (Section 2.3): An increase in wildfires is due to longer periods of hotter and drier summer and fall seasons. Increased investment in firefighting personnel at JPL is essential. Additionally, deteriorating air and water quality resulting from wildfire contributes to further disruptions. There is also a persistent requirement to monitor weather conditions and issue timely alerts.

Air Quality (Section 2.4): The well-being of employees, particularly those who have pre-existing conditions or commute by biking, walking, or using public transportation, is jeopardized. It is essential to monitor/report air quality on days with elevated pollution levels and wildfires.

Precipitation and ARs (Section 2.5): The Laboratory is susceptible to flooding, and the capacity of the adjacent floodplain to absorb floodwaters has at times been diminished due to debris flows resulting from wildfires. There is a need to alert the Lab of heavy rain that might impact commutes and Laboratory accessibility.

Earthquakes and Landslides (Section 2.9): Natural disasters, such as earthquakes and landslides, could heavily damage the Laboratory and render the nearby roads inaccessible.

Other Environmental and Economic Considerations

GHG Emissions (Section 2.11): The primary source of GHG emissions is the use of fossil fuels for electricity, heat, and transportation. At JPL, buildings and operational energy use account for the largest share of emissions, with employee commuting and work-related air travel also making contributions. Supporting shifts in energy use and commuting habits—such as public transit, cycling, and walking—can help align with evolving emissions and energy strategies.

3.3 Facility-Scale Physical Hazard Risks

Given that CASI's primary purpose is to guide NASA and its centers' facility management decisions regarding climate and environmental risks, this report leverages collaboration with CoreLogic, a company that assesses physical risk to the built environment from natural perils with hazard, vulnerability, and exposure models long recognized in catastrophe bond markets and approved by rating agencies. Here, risk is quantified as a loss rate or monetary loss in current dollars resulting from damage to structures caused by various hazards associated with multiple environmental perils. CoreLogic's models leverage the IPCC climate change scenarios discussed in Appendix D, scientific consensus climate-related phenomenon models from organizations such as NOAA, its own propriety models, vast amounts of parcel and structure information (e.g., construction materials), and proximity information, such as flood zone areas and distances from rivers or earthquake faults. CoreLogic builds 300,000-year event simulation sets of perils in high resolution (property-level resolution), with varying severity and frequency distributions. The climate models dynamically downscale IPCC CMIP6 models, which are then applied to estimate the risk associated with the perils to the properties. CoreLogic routinely incorporates new observations from post-disaster field surveys to calibrate their modeling framework, and their risk modules have undergone stringent review by scientists from multiple organizations (NOAA GFDL, USFS, FEMA, Lawrence Livermore National Laboratory, Stanford University, Texas Tech University, UC Berkeley, and the Insurance Institute for Business and Home Safety [IBHS]).

This section highlights the results of a physical risk analysis of the JPL campus created with tools from CoreLogic that yield model output for current conditions (base scenario) and future conditions at 2040 assuming the IPCC's very high emissions scenario (SSP5-8.5; Appendix D). This section also analyzes results from SSP2-4.5 and presents this in the following text; however, maps focus on the base scenario and very high scenario to show the lower and upper bounds of projections. Earthquake risk measures are provided at the 1-in-200-year return period (0.5% chance annually); inland floods and wildfire are estimated at 1-in-100-year return period (1% chance annually). The common industry metric used to assess these types of losses is the probable maximum loss (PML): the "maximum loss" (worst-case outcome) expected at a given location, for a specific peril, at a specified return time, expressed as a dollar amount or percentage. Each building on campus will have its own PML for each peril, each return time, each scenario, and each horizon. The portfolio loss of the entire campus is a separate computation that accounts for correlations and is also presented in the text. Return time is the frequency at which the maximum loss is measured; for example, once in 100 years is a standard value in insurance and has been widely used for both commercial and non-commercial risks by carriers, owners, and the financial markets. The analysis shows individual maximum values for JPL buildings to identify large damage potential from high-severity events and values for the campus portfolio of buildings.

Given that earthquake, wildfire, and inland floods are the most likely perils to cause losses to the JPL campus, the discussion in this subsection focuses on these risks. These perils are key loss drivers both under current conditions and over the longer term in all climate scenarios.

3.3.1 Earthquake

First, we consider the estimated losses for earthquake peril in Figure 3-2. Using a 0.5%-probability, high-impact metric on a building-specific basis shows that a 1-in-200-year earthquake event can create a large loss of $1.2 million or greater to each of 24 out of 105 buildings analyzed on the JPL campus. PMLs for earthquake for these 24 buildings with the largest projected loss range from 1.2% to 9.6%. Estimated loss dollars equal the product of reconstruction cost (cost to rebuild in a total loss), and the hazard rate of loss for the building. B230, where the DSN operates and many satellite commands are sent, has the largest total loss. Although B230 has a lower loss rate at 3.7% than the campus portfolio rate for all buildings at 4.65%, it has the largest reconstruction cost on campus at $222.4 million. The largest single property earthquake PML on campus is then $8.2 million, or 3.7% of $222.4 million. The earthquake peril does not change by climate scenario in the relatively short time horizons to 2040.

FIGURE 3-2

Earthquake peril
200-year PML
(CoreLogic Climate
Risk Analytics 2024).

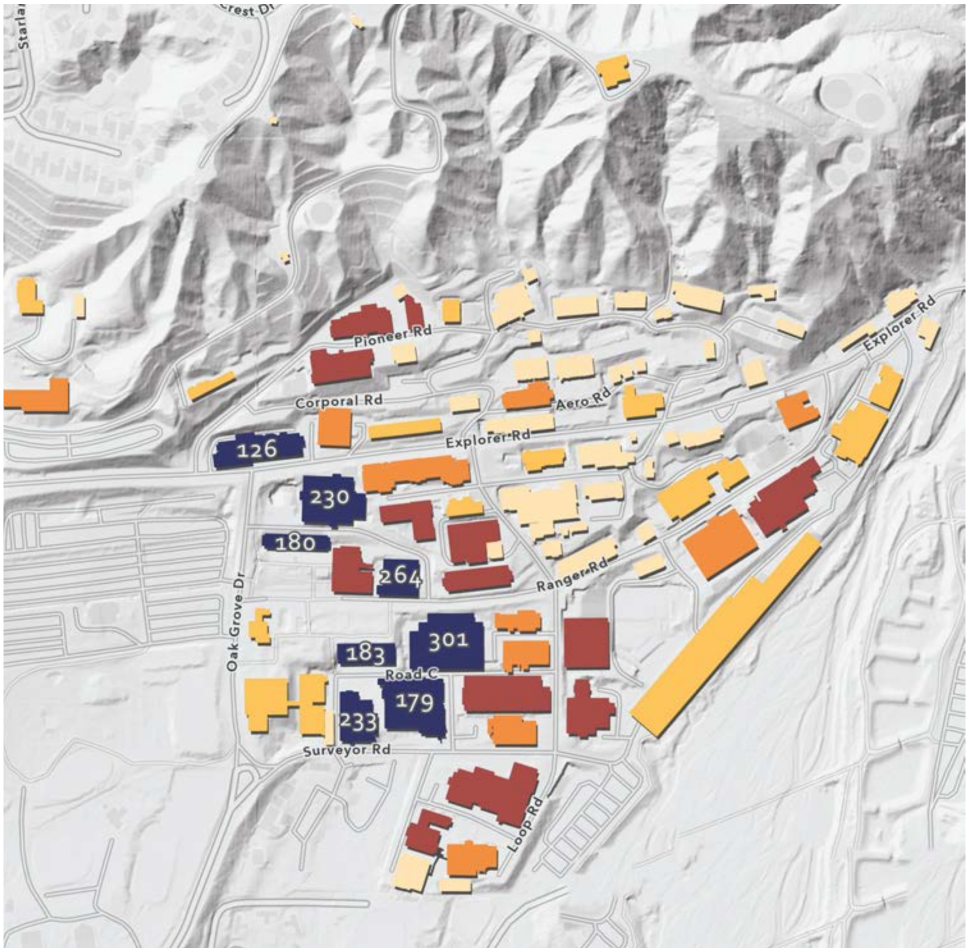

Base Scenario
2024 Horizon

Probable Maximum Loss
200 year return period
($USD)

- 1000 - 200k
- 200k - 500k
- 500k - 1.2M
- 1.2M - 2.5M
- 2.5M - 8.2M

3.3.2
Wildfire

Figure 3-3 shows maps of wildfire risk across JPL campus. On average, PML dollars increase by 3% in the worst-case climate scenario in 2040 compared to today. The portfolio wildfire PML for all of campus is 0.1091% current, 0.1112% in the middle-of-the-road scenario 2040, and 0.1128% in the very high scenario 2040. Although earthquake PML rates are 15 times that of wildfire PML rates, wildfire exposure does present risk, including SAWs, to the JPL campus. Using a 1-in-100-year return on a building-specific basis shows that a wildfire event can create a partial fire loss of $291,749, or 0.131% of $222.4 million, for B230 at current and $298,865, or 0.134% of $222.4 million, in 2040 in the worst case. B310 has a wildfire rate of 0.145% in worst-case 2040 (higher than B230), but its reconstruction cost is only $57,667, yielding a maximum loss of $78, an inconsequential amount. B321, a six-story building where many decisions about mission space flights are made, has the second-largest worst-case wildfire loss at $164,403 in the worst-case 2040 scenario.

Base Scenario
2024 Horizon

Very High Emission Scenario
2040 Horizon

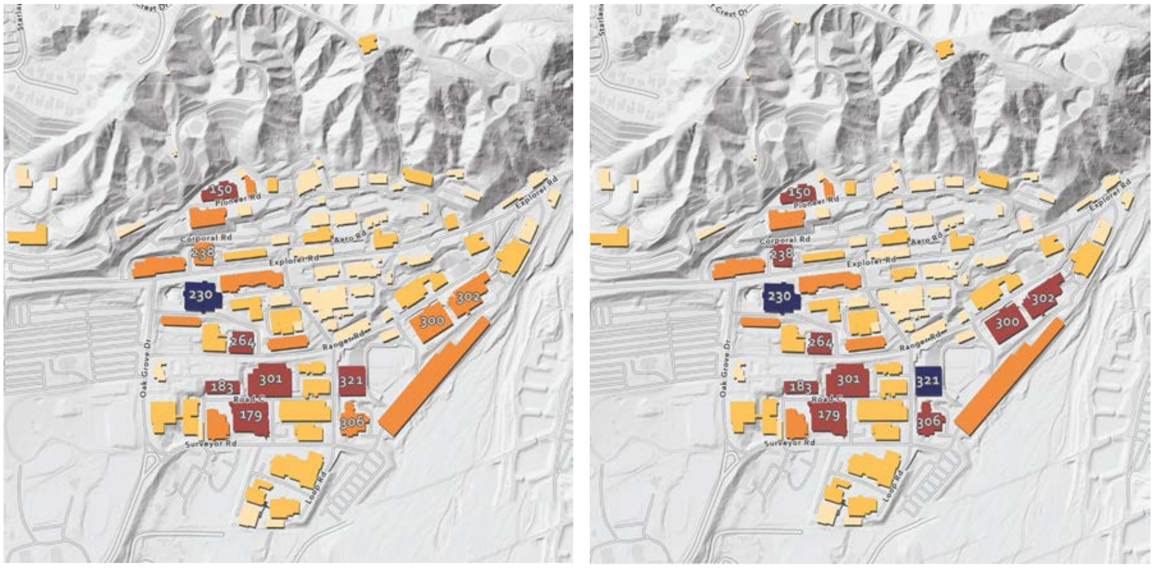

Wildfire Peril

Probable Maximum Loss 200 year return period ($USD)

76 - 10k	80k - 165k
10k - 30k	165k - 292k
30k - 80k	

FIGURE 3-3

Wildfire peril 100-year MPL base scenario (left) and 2040 very high emissions scenario (right) (CoreLogic Climate Risk Analytics 2024).

3.3.3
Inland Flood

Inland flood presents risk to 5% of the JPL campus buildings. Flood risk is a function of weather, soil, proximity to waterways, and the structure of the building, specifically the height of the first floor. Higher first floors have lower flood risk. JPL buildings vary in first floor height with some one or two feet above the minimum of 1.1 feet. Using a 1% probability shows that a high-severity inland flood event can create a loss for B248 of $54,446 at current conditions and increases by 1,200% to $653,357 in worst-case 2040. B161 has no projected inland flood loss at current but has the second-largest inland flood projected loss of $101,740 under the worst-case climate scenario in 2040. These are very large increases in risk for this subset of the JPL campus. The campus portfolio for flood is 0.0342% at base, 0.0749% at SSP2-4.5 2040, and 0.1122% at SSP5-8.5 2040. Figure 3-4 shows building maps of inland flood risk current and in 2040 under the very high emissions scenario.

FIGURE 3-4

Inland flood peril 100-year MPL for base (left) and 2040 very high emissions scenario (right) (CoreLogic Climate Risk Analytics 2024).

Base Scenario
2024 Horizon

Very High Emission Scenario
2040 Horizon

Flood Peril
Probable Maximum Loss 100 year return period ($USD)

●	0
●	54,446
●	2,500 - 10k
●	10k - 163k

3.4 Key Infrastructure Vulnerabilities and Impacts

The many environmental and natural hazards encountered by JPL can temporarily render the Laboratory an unsuitable work environment. Disruptions to electricity, natural gas, potable water, wastewater, transportation services, and other resources may occur in aging buildings and infrastructure throughout the lab. JPL's Facilities Group maintains a comprehensive list of existing infrastructure and improvements related to maintenance of its infrastructure and operations. This maintenance list serves as a baseline for monitoring and enhancing JPL's infrastructure.

The following sections examine potential disruptions to power, gas, potable water, and wastewater services, which may persist for a duration ranging from eight hours to approximately two or three days. If severe enough, these disruptions could lead to the shutdown of the Lab and remote work for the staff. To provide context, a minor flood, earthquake, or wildfire that inflicts relatively limited damage to utility infrastructure could result in such outages, with repairs achievable within hours to days. However, in the event of a more severe earthquake, wildfire, or flood that significantly impacts utility services, outages may extend for a considerably longer period, as immediate repairs may not be feasible. Additionally, it is important to consider that the Laboratory itself could sustain damage rendering it uninhabitable. Finally, this section explores the potential changes to the Lab's energy needs as temperatures rise.

3.4.1
Electricity

JPL primarily depends on external third-party energy suppliers for its electricity needs. While some on-site renewable power generation capability exists, it is insufficient to meet the total energy demands of the campus. Furthermore, JPL is equipped with backup generators to address power outages. Nevertheless, should these backup generators malfunction, the subsequent consequences would occur: A power outage at JPL lasting from one to three hours would require the prompt closure of essential data centers, specifically B230 and B171. During this time, personnel would be unable to use their laptops or computers. Consequently, all activities, virtual or hybrid meetings, and shared applications and documents would be completely suspended. Furthermore, if the outage were to extend beyond a single day, it would lead to the closure of essential environments such as clean rooms, testing chambers, and space simulators, and the suspension of ongoing experiments involving flight hardware. Such disruptions not only compromise the integrity of research activities but could also incur significant delays in project timelines and adversely affect operational efficiency across various departments. Electricity demand as it relates to heating and cooling is discussed more in Section 3.4.7.

3.4.2
Natural Gas

Buildings at JPL are mostly heated by natural gas. Natural gas is used (due to its efficiency) both in the heating systems and boiler. However, back-up systems are limited or nonexistent. This situation is exacerbated by the reliance on a third-party private company that serves as the sole provider of natural gas to the Laboratory. The facility operates with only one connection to this provider, whether it be a fixed or manually operated system. Any disruption in service from this single source could lead to operational challenges and impact overall functionality. Therefore, we recommended exploring alternative supply options and implementing robust redundancy measures to ensure uninterrupted access to this critical resource. Natural gas usage as it relates to heating and cooling demands is discussed more in Section 3.4.7.

3.4.3
Potable Water

Cooling or chilling systems, used to extract heat from spaces by circulating chilled water through pipes for air-conditioning, are the primary consumers of potable water within JPL's buildings. A disruption in water availability for a duration of one to three days would necessitate the complete shutdown of the Lab. In particular, a water outage lasting between one and three hours would necessitate the suspension of operations at the JPL data centers located in B230 and B171, as potable water is essential for air-conditioning and cooling these spaces. A complete shutdown of all restroom facilities and other Laboratory facilities using potable water, including those providing drinking water, will be necessary. If the outage persists for 24 hours, it will lead to the closure of all JPL buildings, including essential areas such as clean rooms, testing chambers, and space simulators. Ensuring a dependable supply of potable water is essential for upholding operational integrity and safety throughout all facilities. The ramifications of a prolonged water outage are dire; fire sprinkler systems, essential for safety, would become inoperative after a week, further heightening the risk of catastrophic incidents.

3.4.4 Wastewater

The cooling tower and chilling plant, restrooms, and some testing operations at JPL are the major consumers of wastewater services, highlighting the critical role of efficient wastewater management within the facility. JPL does not possess its own wastewater treatment operations but instead relies on an external third-party treatment facility for this essential service. The dependence on this connection highlights the vulnerabilities of JPL's infrastructure, as there exists only one line linking the Laboratory to the main off-site wastewater treatment facility. A wastewater disruption lasting eight hours would require the shutdown of HVAC systems, and restroom facilities would become inoperable. An outage lasting a full day would necessitate the evacuation of all (non-critical) Lab buildings until service restoration could be completed. These points highlight the importance of consistent and reliable wastewater services at JPL to ensure the smooth operation of its facilities and the well-being of its workforce.

3.4.5 Communications and Transportation

A disruption in IT communications, DSN Space Flight Operations, emergency management communications, the Lenel life safety system, or radio communications in B35 for even an hour could have consequences for NASA's research and mission support capabilities. It may lead to the loss of crucial research and mission data or hinder the ability to assist other NASA facilities effectively. Furthermore, in terms of transportation, an outage due to events such as an earthquake, wildfires, or flooding lasting between one and three hours would significantly impact various operations. For instance, fire trucks and life safety response teams could be delayed in their critical functions. The transportation of space flight instruments and deliveries would also face disruptions, affecting the overall efficiency of operations. In the event of a 24-hour-long disruption, the consequences escalate further. Reliable access for fire and life safety teams would be threatened, potentially compromising emergency response capabilities. Additionally, the arrivals and deliveries of special instruments essential for space missions could be severely hindered, posing a risk to the overall functioning and preparedness of NASA facilities.

3.4.6 Other Resources

The continuous availability of gaseous nitrogen is essential for the smooth operation of various functions within the lab. This gaseous nitrogen, which is supplied through a third-party vendor, is a crucial component that supports the day-to-day activities and testing procedures conducted at the facility. Any interruptions in the supply of gaseous nitrogen could have a significant impact on the testing chamber work, potentially delaying important experiments and projects. Moreover, the disruption in the supply chains for specialized parts or substances required for specific operations at JPL could also pose challenges for the Laboratory. Maintaining a consistent and reliable source of gaseous nitrogen is vital to ensure the seamless functioning of the Lab.

3.4.7 Building Heating and Cooling Energy Needs

One important consequence of the increasing temperatures in the future climate at JPL (Section 2.1) is the change in energy needed to heat and cool buildings. Heating degree days (HDD) and cooling degree days (CDD) are one set of metrics that quantify heating and cooling demand in buildings. HDD is calculated by subtracting the daily mean temperature from a 65°F (18°C) threshold (this is one of several thresholds used in the building industry) representing a standard for when heating systems are needed. Similarly, the CDD is computed by subtracting a threshold temperature of 50°F (10°C) from the daily average temperature. Negative values are assigned zero-degree days, and the differences calculated for CDD and HDD in degrees Fahrenheit are summed over days to monthly and annual totals. Higher values of HDD and CDD are directly related to higher energy needs for heating and cooling.

To look at HDD and CDD values in the recent past at JPL, NASA MERRA-2 data are analyzed. The annual total of HDD and CDD are unevenly distributed throughout the year. In the last 30 years, the annual sum of HDD and CDD at JPL are 1,843 and 4,876, respectively (Table 3-1). As part of these annual totals, monthly HDD values are highest during the cooler winter and early spring months and are at or near zero from June to October (Figure 3-5). CDD values are non-zero for all months of the year. Monthly total CDD values are small in the winter months, increase in spring, and peak in the summer months of July and August before declining again in the fall.

Quantity	**1994–2024 average annual sum in Fahrenheit degree days** [standard deviation]	**High-emissions scenario projected change in 2035–2055 mean relative to 1994–2024 mean in Fahrenheit degree days** [percentage change]	**Medium-emissions scenario projected change in 2035–2055 mean relative to 1994–2024 mean in Fahrenheit degree days** [percentage change]	**Low-emissions scenario projected change in 2035–2055 mean relative to 1994–2024 mean in Fahrenheit degree days** [percentage change]
HDD	1,843 [256]	-300 [-16%]	-264 [-14%]	-233 [-13%]
CDD	4,876 [382]	598 [+12%]	521 [+11%]	388 [+8%]
Climate Zone	3	No change	No change	No change

TABLE 3-1

Current and future projections of annual total HDD and CDD from MERRA-2 and NEX GDDP, respectively.

Annual totals of the HDD and CDD are utilized by the American Society of Heating, Refrigeration, and Air-Conditioning Engineers (ASHRAE) to define climate zones. These zones are used by municipalities and counties in the United States to define building codes for a building's location. Those building codes define the requirements for building energy systems, including heating and air-conditioning systems. Using the ASHRAE climate zone definitions and the MERRA-2 analysis, an estimate of the current building climate zone for the JPL region is estimated and shown in Table 3-1 as Climate Zone 3. Note that higher climate zone numbers correspond to colder climates, and the smallest number is the warmest.

Climate projections predict increases of CDD and reductions of HDD as calculated from NEX GDDP (Figure 3-6A and 3-6B; See Appendix D for a description of NEX GDDP data set). The changes in CDD and HDD occurring in the next 20 years are not evenly distributed throughout the year. Decreases in the monthly sum of HDD are mostly found in the months of November through May (Figure 3-6C). Increases in the monthly sum of CDD are more evenly spread throughout the year, with a slight peak in May–October (Figure 3-6D). Using those data as input, estimates of future climate zones for the JPL area are made. These changes translate to a transition to a warmer ASHRAE climate zone far in the future (after the year 2070) in the highest-emissions scenario, but not in the period considered here. In the other lower-emissions scenarios, the climate zone at JPL will remain at the current zone. In all scenarios, with increasing CDD and decreasing HDD, cooling systems may need to be larger in future buildings at JPL. As noted in Section 2.1.2, increasing frequency, intensity, and duration of heat waves will also add additional strain on future cooling systems for buildings.

FIGURE 3-5

The 1994–2024 mean value of the monthly sums of HDD (dark green bars) and CDD (light green bars) at JPL, calculated from MERRA-2. The black error bars show plus and minus one standard deviation from the mean.

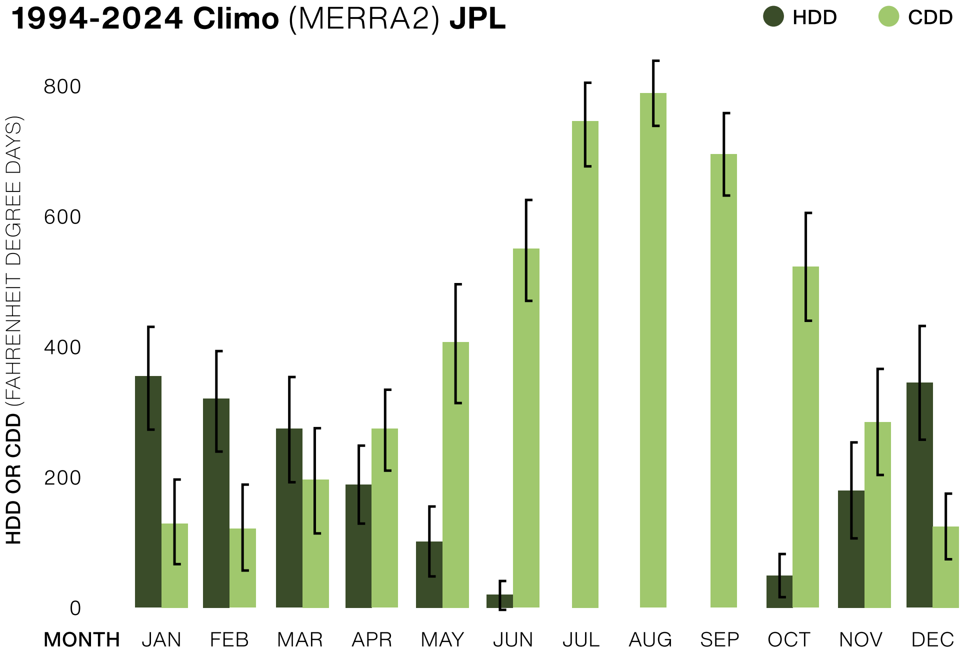

FIGURE 3-6

(A) Time series of CDD at JPL calculated from NEX GDDP data through the year 2055. The three colors represent the projected changes in three different emissions scenarios (low [SSP1-2.6], medium [SSP2-4.5], and high [SSP3-7.0]). The changes shown are an ensemble average of 22 CMIP6 climate models contained in the NEX GDDP downscaled projections. (B) Same as A, but for HDD. (C) The 20-year future projected changes in monthly sums of CDD 2015–2035 and 2035–2055. The three bars, shown for each month, represent the projected changes in three different emissions scenarios (low [SSP1-2.6], medium [SSP2-4.5], and high [SSP3-7.0]). The changes shown are an ensemble average of 22 CMIP6 climate models contained in the NEX GDDP downscaled projections. (D) Same as C, but for HDD.

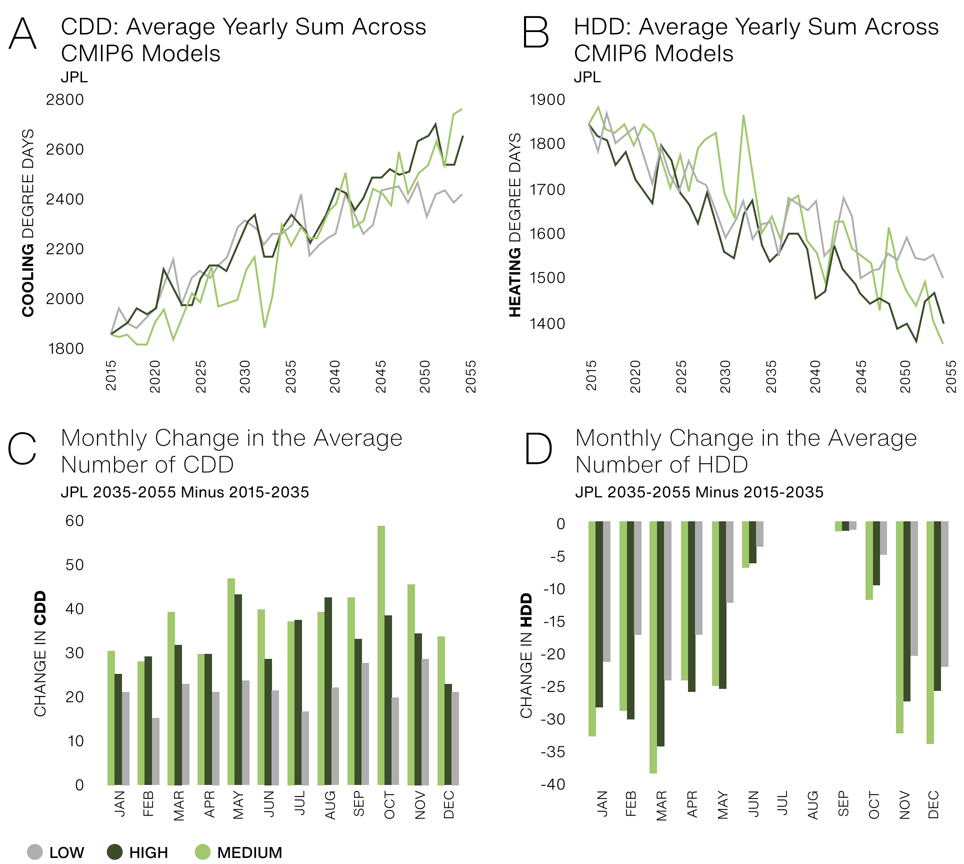

3.5
JPL Buildings, Assets, and Infrastructure: Mitigation and Resilience Plan Considerations

JPL is actively enhancing its resilience in the areas of energy, water, and wastewater diversion while striving to decrease its GHG emissions. The Facilities Group has recognized the various divisions and groups needed to address newly identified vulnerabilities or those for which solutions are not clear, and the subsequent step involves collaborating with these groups to implement mitigation strategies. This section lists the mitigations, resilience plans, and sustainability considerations for the immediately addressable vulnerabilities that the Lab faces. They are organized using a tiered framework consisting of JPL facilities' current plan, tier 1 considerations, and tier 2 considerations. The following provides a detailed explanation of the tiered framework:

Current Plan	JPL is actively implementing plans in response to prevailing weather conditions. A feasibility and cost analysis has been completed to advance this initiative.
Tier 1	JPL is evaluating these plans in light of anticipated weather conditions over the next five years. A feasibility and cost analysis are required to proceed with this initiative.
Tier 2	JPL is assessing these plans concerning weather conditions projected for the next 10 to 20 years. A feasibility and cost analysis are required to proceed with this initiative.

3.5.1
Environmental **Risk**: Rising Temperatures and Heat Waves

Current Plan

JPL is continuing a conservation program based on the varying and limited freshwater supply (Section 2.6). This initiative includes separating the landscaping water supply from potable water sources to ensure efficient usage. JPL's Facilities Design Standard Revision 16, a guideline used for building and site design for facilities, mandates the implementation of drought-resistant native landscaping, the use of drip irrigation systems, and the installation of metering devices. It also stipulates that plumbing fixtures must be designed to reduce water consumption. Currently, smart meters for domestic water usage are being installed across all buildings in phases. JPL's Workplace Planning and Design Principles v1.0 serves as a guideline that outlines the standards for space planning at JPL, encompassing both indoor and outdoor work environments. Additionally, for newly constructed buildings, improvements to the building envelope, such as enhanced insulation and glazing, will contribute to cooling efficiency. Furthermore, the initiative seeks to increase tree coverage for shade and improve air quality, along with the installation of shade structures to reduce the heat island effect (Section 2.1.1; Figure 3-7). The facilities guidelines stipulate that over 90% of the roofs should be equipped with cool polyvinyl chloride (PVC) materials and include plans (Figure 2-3) to treat additional roadways on the Laboratory with "cool" pavement coatings. Furthermore, cool roof coatings are being applied to metal roofs, with plans to replace non-cool roofs.

FIGURE 3-7

An illustrative depiction of future initiatives aimed at enhancing the presence of native plants, trees, and outdoor shade structures to provide occupant comfort, enhance air quality, and mitigate heat island effect.

Tier 1

In the next five years, JPL's Facilities Group is considering a study of the urban heat island effect and potential mitigation strategies. This includes a feasibility study of substituting single-pane windows with heat-reduction windows exhibiting a U-value of 0.30 or lower, along with a solar heat gain coefficient of 0.23 or less, for applicable buildings.

03

Tier 2

In the next 10 to 20 years, as rising temperature and extreme heat continue to increase, providing the option for remote workdays when the NWS issues a heat advisory for the region should be considered for the health and safety of JPL's workforce.

3.5.2
Environmental **Risk**: Wildfires and Santa Ana Wind Conditions

Current Plan

JPL is proactively tackling the challenges anticipated from a changing climate. To mitigate the risk of wildfires (Section 2.3) and enhance overall safety, JPL will continue a routine schedule for clearing brush and pruning existing trees. This not only reduces the potential spread of fires but also helps preserve the surrounding ecosystem. Furthermore, ongoing cross-training initiatives with Facilities, Transportation, Protective Services Division (PSD), and other pertinent groups are aimed at enhancing skills and fostering awareness. Emergency backup generators are in place to supply power to essential buildings in an event a power outage is caused by extreme wind or wildfires. Regular maintenance, including monthly testing and annual inspections for these backup generators, remains a top priority. The JPL Facilities Design Standard Revision 16 also includes the following mitigation methods for wind and wildfires: All maintenance-related replacements of rooftop mechanical equipment, along with the installation of awnings and canopies, must be designed by a licensed structural engineer and submitted for design review. Structural design for wind forces must adhere to Exposure Category C for the main campus and Exposure Category D for the Mesa and the Table Mountain Facility. The calculations should utilize a three-second wind gust speed of 130 mph. Also, the incorporation of non-combustible materials is mandated for new constructions and expansions. In instances where non-combustible materials are impractical, combustible materials treated with fire-retardant can be used for elements such as wood roof nailers, which are used to provide a secure base for nailing or fastening the roofing membrane.

Tier 1

In the next five years, JPL's Facilities Group is considering expediting a current demolition schedule for buildings made from combustible materials. For buildings not included in the demolition list, a possible option is to upgrade building roofs to Class A fire-rated standard. A further evaluation is being considered in the demolition plan for wooden sheds, wooden structures, and combustible materials located on the hillside.

Tier 2

In the next 10 to 20 years, a consideration is a feasibility study to replace window units with windows that are impact-resistant and compliant with SAW standards to help reduce the risk of wildfires spreading through shattered windows. Additionally, there is a possibility of engaging a service for the seasonal application of fire-retardant products from the USDA Forest Service Qualified Product List to the hillside vegetation near buildings, essential infrastructure, and areas at high risk of fire.

3.5.3
Environmental **Risk**: Air Quality

Current Plan

The varying levels of pollution and the rising occurrence of wildfires have heightened concerns about air quality. PurpleAir sensors have been installed at JPL to evaluate air quality and collect data. The Facilities Maintenance and Operations Group addresses air quality concerns by installing new HVAC filters and shutting outside air dampers during wildfire incidents, among other measures. Additionally, plans are in motion to boost the availability of Level 2 electric vehicle chargers, promoting the use of low-emissions and zero-emissions vehicles. This approach aligns with California's legislation that mandates all vehicles sold in the state be classified as low-emissions or zero-emissions by 2035. JPL's rideshare and public transportation programs incentivize carpooling, vanpooling, and using public transit. The JPL Facilities Design Standard Revision 16 enforces regulations from the Antelope Valley Air Quality Management District for the Table Mountain Facility and ensures compliance with the South Coast Air Quality Management District guidelines. Moreover, the ongoing use of low-VOC and no-VOC paints are required to be applied in JPL's buildings.

Tier 1

The integrated response in the forthcoming five years includes the possibility of an online real-time air monitoring dashboard managed by the TFM team. Plans are being considered to establish backup systems for the air quality monitoring devices in the case of power outages. In response to heightened air quality concerns, the Facilities Maintenance and Operation Group is considering the integration of HEPA filters, carbon filters, and ionizing filters into the HVAC systems. Further assessment is needed to evaluate the compatibility of these filters with the current HVAC systems and to analyze the practicality of their implementation.

Tier 2

In the next 10 to 20 years, a consideration is to prepare for optional remote work arrangements for populations at risk due to air quality concerns, as indicated by TFM air monitoring data.

3.5.4
Environmental **Risk**: Precipitation, Atmospheric Rivers, and Flooding

Current Plan

In light of the current weather patterns, maintaining the stormwater drainage systems located near buildings is important to mitigate the risk of flooding. Ensuring the operational efficiency of these drainage systems is essential for flood prevention. A maintenance schedule has been established to facilitate the removal of debris from these systems. According to the JPL Facilities Design Standard Revision 16, site drainage calculations must adhere to the guidelines outlined in the Hydrology Manual of the Los Angeles County Flood Control District. Storm drainpipes should be capable of accommodating a rainfall intensity corresponding to a 10-year return period, while surface flow designs must be prepared to manage the full intensity of a 25-year rainfall event, in accordance with the established standards of Los Angeles County. Additionally, vegetated swales have been implemented at JPL to improve resilience.

Tier 1

In anticipation of potential flooding occurrences over the next five years, JPL's Facilities Group is evaluating a civil engineering analysis to assess the rainfall intensity associated with 50-year and 100-year events. This analysis will also include recommendations for essential improvements to the storm drainage system.

Tier 2

In the coming 10 to 20 years, strategies will be developed to address flooding events, including the exploration of alternative stormwater management solutions. These may involve the implementation of vegetated infiltration basins and the use of permeable pavement or pervious parking areas that are designed to work in conjunction with catch basins.

3.5.5
Environmental **Risk**: Earthquake and Landslides

Current Plan

To mitigate the impact of earthquake occurrences, the JPL Facilities Design Standard Revision 16 specifies seismic coefficients based on findings from a 2017 Seismic Hazard Report. This report highlights site conditions, including the Sierra Madre Fault, a soil site characterized by alluvial fan deposits, and a rock site with shallow basement rock. The standard requires a seismic assessment for mission-critical buildings to attain an immediate occupancy performance level, while all other structures are required to meet a life safety performance level. JPL is committed to adhering to these guidelines, and the seismic retrofitting of structures will be an ongoing process.

Tier 1

In the upcoming five years, there are prospective initiatives to obtain a geotechnical assessment aimed at preventing landslides. Additional evaluations and the implementation of strategies to mitigate landslides and debris flow are currently under consideration to protect the landscape and efficiently conserve water resources (Section 2.6).

Tier 2

In the forthcoming 10 to 20 years, the Facilities Group at JPL will evaluate the integration of retaining walls, the regrading of slopes, vegetation management, structural reinforcement, the installation of subsurface drainage systems, rock bolting, and the establishment of debris barriers.

3.5.6
Other Environmental and Economic Considerations: Greenhouse Gas Emissions

Current Plan

JPL plans include replacing current lighting with energy-efficient LED fixtures. Furthermore, there is a plan to enhance equipment wherever possible with energy-efficient options to reduce energy usage. The installation of high-efficiency HVAC systems will also be given priority. Additionally, JPL is engaged in the deployment of solar panels and batteries through the Energy Savings Performance Contract (ESPC) program. Upon the completion of the ESPC, it is anticipated that solar panels and batteries will meet 7.5% of JPL's energy requirements through photovoltaic systems.

JPL additionally incorporates sustainable building and construction methodologies, with a focus on achieving Leadership in Energy and Environmental Design (LEED) certification. According to the JPL Facilities Design Standard Revision 16, any new construction projects exceeding 5,000 square feet are required to strive for LEED Gold certification, with at least LEED Silver certification as a baseline. Major renovations of existing facilities must comply with the Guiding Principles for Federal Leadership in High-Performance and Sustainable Buildings, as specified by the U.S. Department of Energy, along with the Whole Building Design Guide. These standards emphasize the importance of maximizing energy efficiency, conserving water, implementing assessment and management strategies, improving indoor environmental quality, reducing the environmental impact of materials, and assessing climate-related risks (Section 2.11). Five JPL buildings have successfully attained LEED Gold certifications (B321, B201, B180, B171/202/241, and B111), reflecting adherence to energy and water efficiency standards. The newly built Flight Electronic Integration Facilities (FEIF; B350) is in the process of obtaining LEED certification, meeting sustainable building criteria such as the use of low-emitting materials, locally sourced building materials, waste diversion during construction, and energy and water-efficient systems. In line with JPL's Workplace Planning and Design Principles v1.0, a strategy is being developed to reduce the size of solid exterior walls while increasing the number of windows in new construction projects. This initiative aims to increase airflow and natural daylight, thereby decreasing dependence on artificial lighting and improving energy efficiency (Figure 3-8).

JPL currently operates two electric day buses and electric maintenance carts across the Laboratory, with intentions to enhance the electric vehicle charging station infrastructure to accommodate the future acquisition of electric government vehicles. JPL implemented flexible work arrangements, including some remote work, which would reduce commuting and lower GHG emissions (Figure 3-9). A strategy has been implemented to minimize energy use and greenhouse gas emissions by replacing older, less efficient structures and trailers, and replacing them with more efficient, consolidated buildings. NASA stipulates that, for every square foot constructed, JPL is required to demolish 125% of the existing square footage. This initiative includes retrofitting current structures to meet land zoning regulations and optimizing the basement parking of B301 for better utilization of test beds. Furthermore, there is a plan to consolidate office spaces, which will create additional areas for collaboration and break rooms. This consolidation is crucial for improving operational efficiency and reducing the overall building footprint. It can be achieved through the strategic collocation of functions within areas designed for effective production and operations. Additionally, a strategic plan has been prioritized to reduce operational and maintenance costs by implementing tiered maintenance strategies, which involve upgrading infrastructure and equipment rated from inadequate to viable conditions within a 10-year time frame.

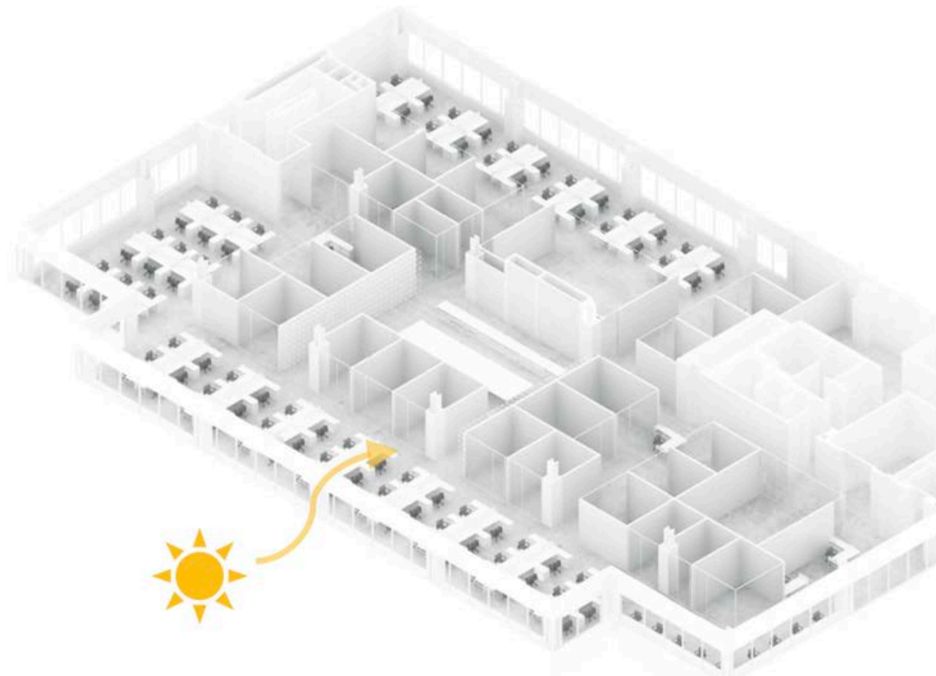

FIGURE 3-8

A schematic representation of a strategy aimed at minimizing solid exterior walls, while increasing the number of windows and reducing the height of workstation panels to promote natural daylight. This method seeks to decrease reliance on artificial lighting and improve energy efficiency.

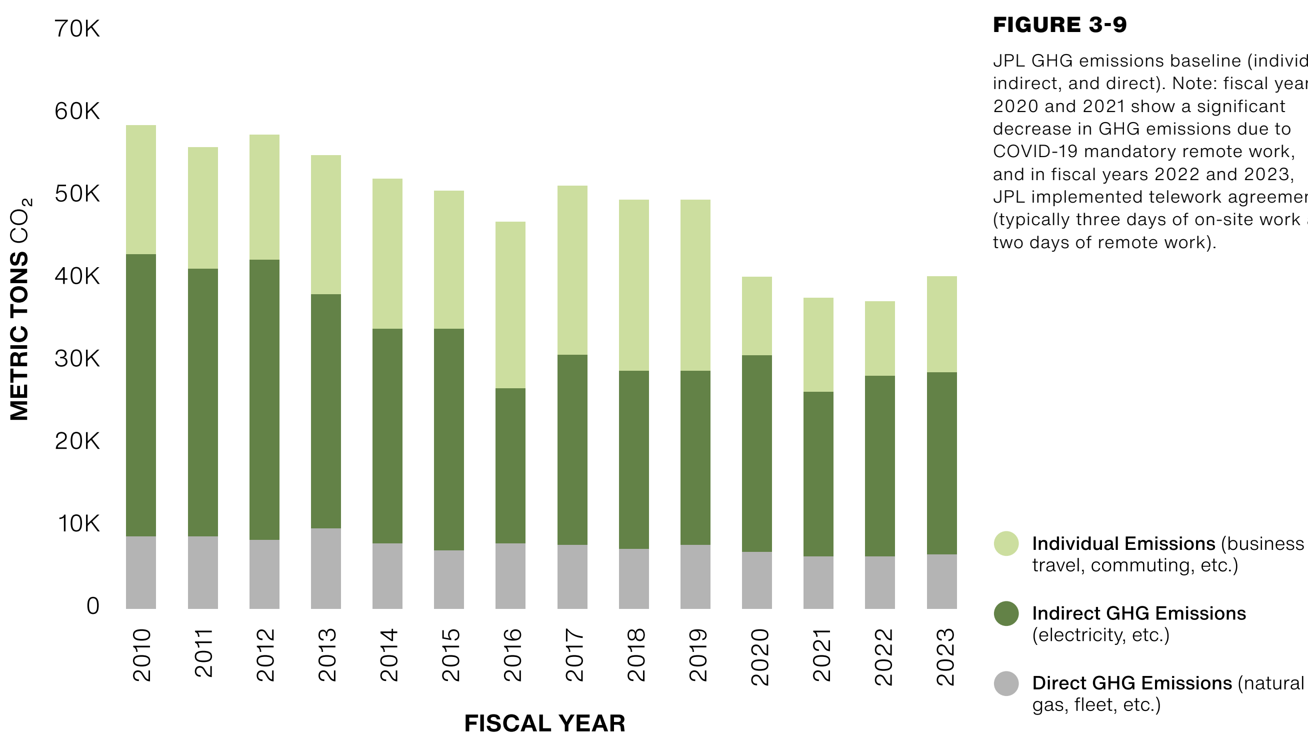

FIGURE 3-9

JPL GHG emissions baseline (individual, indirect, and direct). Note: fiscal years 2020 and 2021 show a significant decrease in GHG emissions due to COVID-19 mandatory remote work, and in fiscal years 2022 and 2023, JPL implemented telework agreements (typically three days of on-site work and two days of remote work).

Tier 1

In the upcoming five years, JPL's Facilities Group will evaluate energy suppliers that offer renewable energy options, referred to as clean or green energy. However, the primary factor in the decision-making process will be the dependability of these energy sources. Additionally, there is a consideration to incorporate a contractual requirement for the use of building materials and equipment obtained from local manufacturers rather than relying on LEED certification for this option.

Tier 2

In the forthcoming decade, JPL is considering a Smart Lab initiative. This initiative seeks to enhance operational energy efficiency via a digital framework that optimizes airflow within the buildings, minimizes pressure drops in HVAC systems, incorporates demand-responsive motion and daylight sensor lighting controls, and improves fault detection capabilities. This initiative is essential in addressing the challenges of GHG emissions and rising temperatures (Section 2.1). Additionally, a further examination of a micro-grid will be essential to fulfill energy needs during emergencies and to address challenges related to disruptions.

3.5.7 All Environmental **Threats** and **Causes**

Current Plan

The Facilities and Logistics Division and Earth Science and Technology Directorate at JPL have investigated the feasibility of developing GIS tools and establishing connections to support various mapping requirements. Engaging with contacts capable of delivering the services necessary to develop this tool will require additional effort.

Tier 1

The strategic plans for the upcoming five years will focus on the application of GIS to consolidate data related to air quality, surface temperatures, and wind conditions at JPL. This methodology will aid in formulating a response plan, pinpointing vulnerabilities, and tracking progress in risk mitigation efforts.

Tier 2

Expanding the GIS mapping tool to analyze facilities maps will be required in 10 to 20 years. This initiative will focus on ensuring that data is easily accessible to facilitate effective and flexible responses. It will also involve the development of interactive mapping specifically designed for mobile applications as well as the mapping of utility meters, shut-off locations, and service points. Furthermore, this effort will encompass the mapping of tree maintenance and the planning of emergency response strategies.

January 2025 Wildfire Event

04

On January 7, 2025, two major wildfires ignited in Los Angeles: the Palisades Fire in the Pacific Palisades neighborhood, and the Eaton Fire in Altadena. The fires began in the midst of a high-wind warning triggered by an exceptionally strong SAW event, with gusts that exceeded 100 mph. The Eaton Fire spread rapidly, reaching an area adjacent to NASA's JPL within hours. This posed a particular disruption to employees as well as to the facility (Figure 4-1). JPL deployed resources and personnel to combat the spread of the Eaton Fire even as mandated evacuations in Altadena and Pasadena affected up to 1,000 Lab employees. Across both fires, at least 200 employees lost their homes, with many more displaced due to smoke and ash damage. Impacts to JPL facilities included the need to shut down the Lab-wide IT infrastructure during the fire, degrading or disrupting JPL computer systems and servers for about 36 hours.

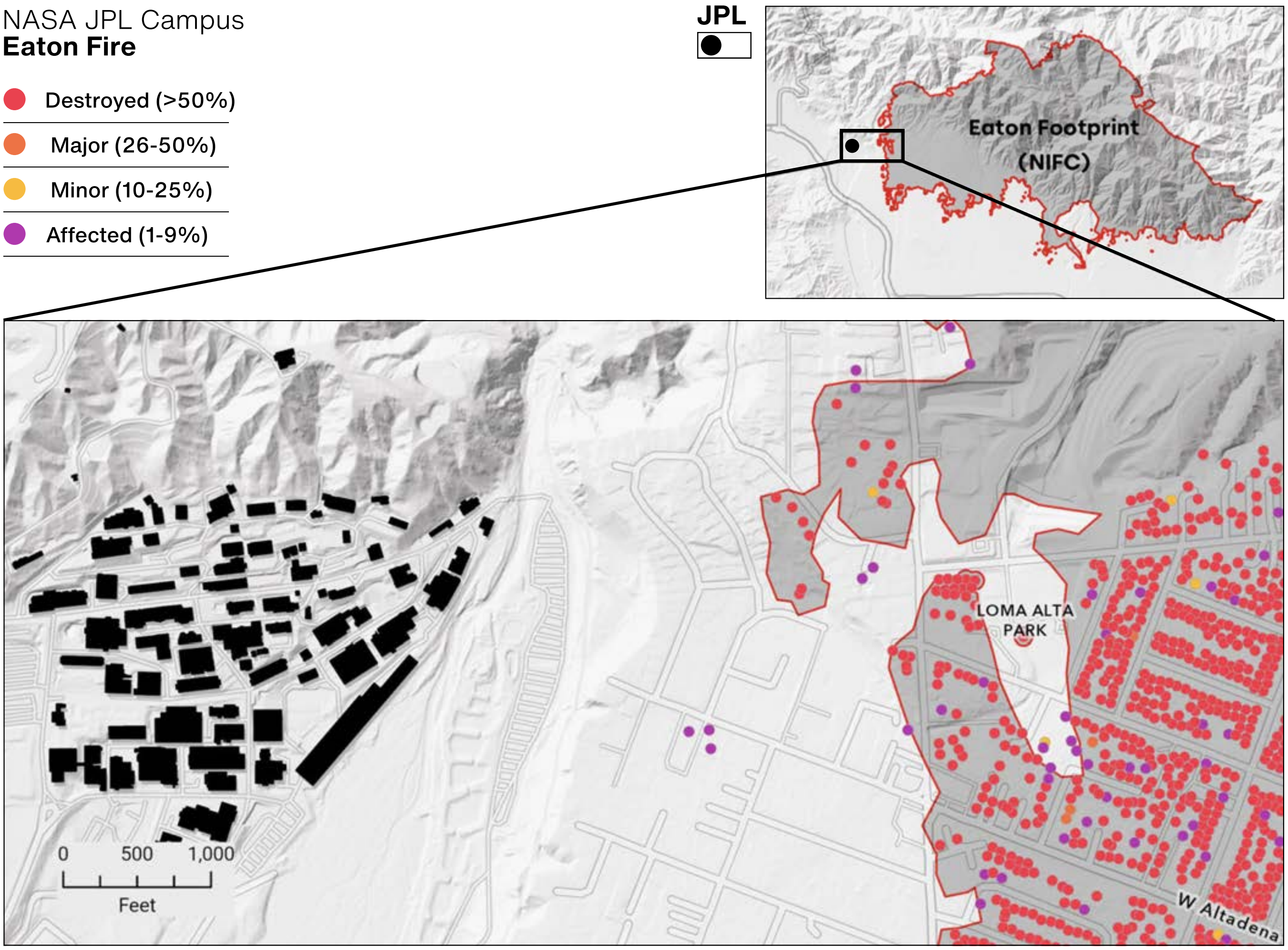

FIGURE 4-1

The extent of damage from the Eaton Fire to structures in proximity to the JPL campus. (Source: CoreLogic, based on the California Department of Forestry and Fire Protection's Damage Inspection Reports and on the National Interagency Fire Center's Eaton Wildfire Footprint.)

04

Climate Context

The January 2025 fires occurred under extreme meteorological conditions—unusually warm, dry, and windy. Figures 4-2, 4-3, and 4-4 illustrate the severity of these conditions in coastal Southern California from a long-term climatological perspective (Madakumbura, Thackeray et al. 2025). In Figure 4-2, the vertical axis represents the number of years from 1895 to 2025 that experienced a given average temperature, with the average temperature shown on the horizontal axis. For example, one year on record had a notably cool June–December average temperature of approximately 60.4°F, (15.8°C) while 15 years recorded an average of around 63.8°F (17.7°C). The graph highlights that the average temperature for the period preceding the 2025 fires, June–December 2024, ranked among the four warmest in the entire 130-year record.

Similarly, Figure 4-3 presents the number of years that experienced a given cumulative precipitation (in inches) from May 1 of each year to January 8 of the following year for Los Angeles, based on a data set extending back to 1877. It reveals that the cumulative precipitation from May 1, 2024, to January 8, 2025, was among the three driest on record.

Figure 4-4 plots the number of Santa Ana days observed at Los Angeles International Airport between November and January since 1944 by maximum hourly average wind speed. It shows that the maximum hourly average wind speed on January 7, 2024, was among the most extreme recorded, while the wind speed on January 8, 2024, also reached the upper range of observed conditions.

In summary, the meteorological conditions leading up to the January 2025 fires were exceptional, marked by a combination of extreme warmth and dryness, and strong winds.

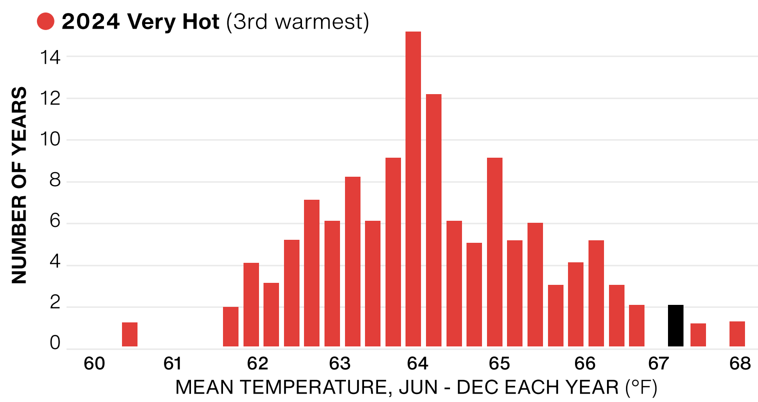

FIGURE 4-2

Frequency distribution of annual mean June–December temperatures for coastal Southern California, represented as the number of years in each temperature bin shown along the horizontal axis. 2024 is included among the years in the black bar. Temperature data are sourced from PRISM Climate Group (Madakumbura, Thackeray et al. 2025).

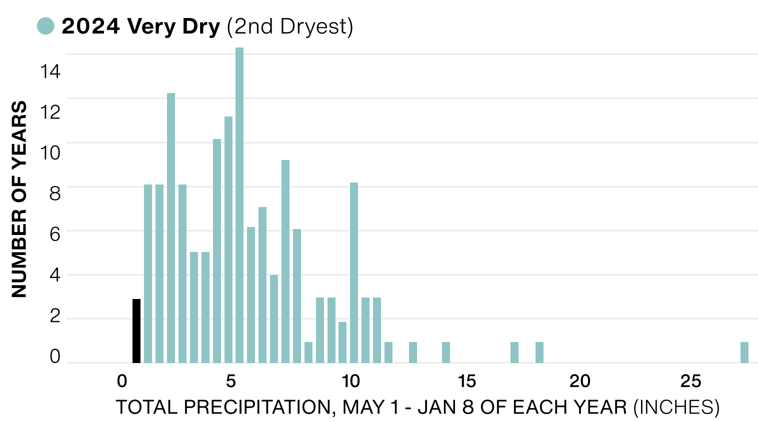

FIGURE 4-3

Frequency distribution of cumulative precipitation totals (in inches) from May 1 through January 8 for downtown Los Angeles, spanning the 1877–2023 period. The number of years corresponding to each precipitation bin is shown on the vertical axis, with the May 1, 2024–January 8, 2025, value counted among the years in the black bar. Precipitation data are obtained from NOAA's Applied Climate Information System (Madakumbura, Thackeray et al. 2025).

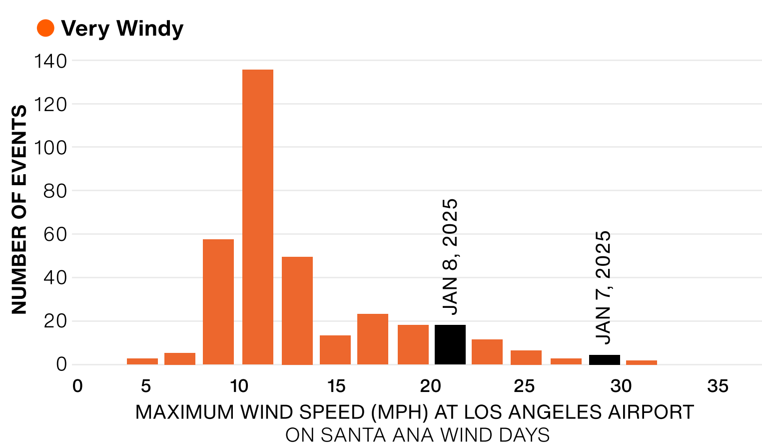

FIGURE 4-4

Frequency distribution of the maximum hourly average wind speed (in miles per hour) on Santa Ana days for the November–January period at Los Angeles International Airport, based on records from 1944–2025. The values for January 7 and 8, 2025, are counted in the black bars. Wind data are sourced from NOAA. Santa Ana days are defined as those when the maximum wind direction falls within a northeast-centered range (330°–360°, 0°–100°) and the daily mean relative humidity is below 35%. Note that these values represent estimates of sustained maximum wind speeds rather than absolute peak gusts (Madakumbura, Thackeray et al. 2025).

Early Warning and Preparedness

The region first received Red Flag and High Wind warnings from the NWS on January 5, 2025, two days before the wildfires started. Red Flag warnings indicate heightened wildfire danger arising from warm temperatures, low humidity, and high winds. In response to these warnings, JPL issued “recommended work-from-home” guidance on the morning of January 7, 2025.

Eaton Fire Event

The Eaton Fire ignited just after 18:00 PST on January 7 and grew rapidly until January 9. The explosive growth stemmed from the strong SAWs that also prevented aircraft from dropping water and fire retardant on the blaze, hampering initial firefighting efforts. Once the winds died down, ground crews were able to make progress in containing the blaze and firefighting aircraft were able to commence their water and retardant drops. After three weeks and an expansion to 14,021 acres, the fire was finally declared fully contained on January 31, 2025. In total, over 2,100 personnel, 10 helicopters, and 149 engines were deployed to fight the Eaton Fire (CAL FIRE 2025).

JPL made its helicopter emergency landing facility available throughout the firefighting effort to the Eaton Fire Incident Management Team. Officials used the facility for helicopter operations to protect the surrounding neighborhoods. JPL continued to assist local and federal agencies after the fire was fully contained, including allowing access to the JPL parking lot for FEMA cleanup crews.

JPL Impact

At the peak of the fire, at least 1,000 JPL employees (or 20% of the Lab’s population) were under mandatory evacuation orders. Fire officials lifted some of those orders within a few days in areas that escaped the flames, enabling some JPL employees to return home. Those who were affected in a more long-term or permanent way included more than 200 employees who lost their homes and over 500 others who could not access potable water, remained without gas or electricity for several days to weeks, or who assisted family or friends who lost homes. JPL’s facilities did not sustain any physical damage from the fires, but they did sustain some damage from the high winds.

During the fire, JPL buildings and hardware were secured and protected, often by people who were impacted at a personal level. DSN operations—normally conducted at JPL 24 hours a day, 7 days a week—were moved offsite on January 8 to a backup operations center at the Goldstone antenna facility near Barstow, California. This ensured that communications with all spacecraft in deep space (beyond the orbit of the moon) continued without pause. While personnel for the DSN and space missions regularly train for this type of scenario, it was the first time in its 60-year history that the DSN did not operate from JPL. DSN operations returned to JPL the following week.

Mandatory telework was put into place for most personnel from January 7 to 17, with leave granted to many employees dealing with property loss and displacement. JPL reopened to in-person work on January 20, although people were encouraged to work remotely if possible. Employees were invited back to resume normal operations on January 27.

Aftermath

The Lab continues to face challenges in the aftermath of the fires. At the time of this writing, many members of the JPL community are still displaced from their neighborhoods due to hazardous conditions, with the cleanup expected to take at least one year, and possibly up to three years. On February 13, 2025, some of the neighborhoods that evacuated for the Eaton Fire had to evacuate again in response to mudslide risks due to heavy rains.

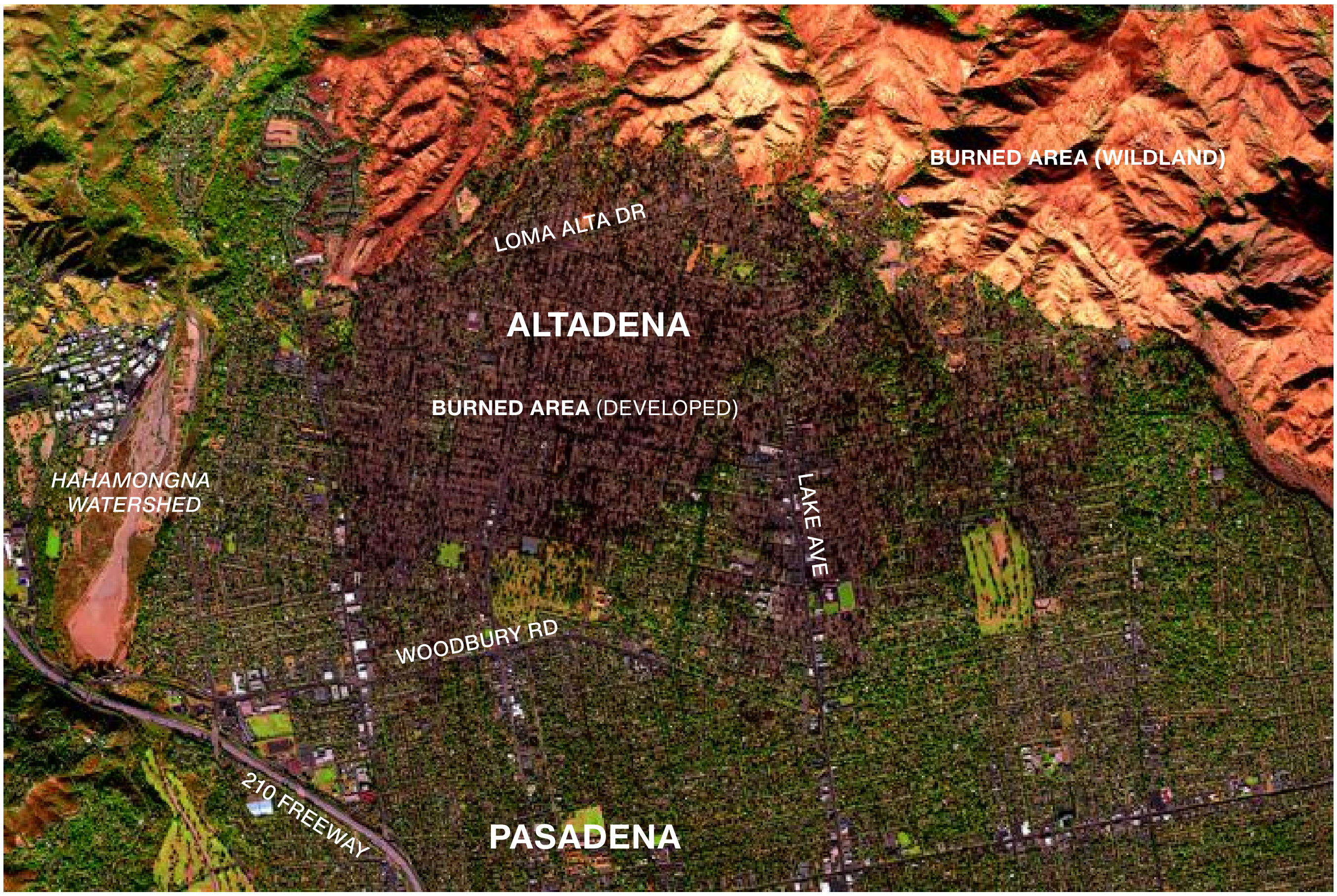

FIGURE 4-5

False-color image of the Eaton Fire's burn area based on images captured by NASA's AVIRIS-3 on January 11, 2025. NASA Earth Observatory image annotated by Lauren Dauphin using data from AVIRIS-3, (https://earthobservatory.nasa.gov/images/153821/eaton-fire-leaves-california-landscape-charred).

Summary and Future Directions

05

This report—which was developed on behalf of CASI and NASA's ESD and OSI, and addresses a number of internal strategic goals and objectives (see About This Report)—underscores the urgency and complexity of environmental challenges faced by the Laboratory and its surrounding areas. Through a detailed review of various environmental risks and hazards, along with considerations of the resilience and sustainability of the Laboratory, this assessment provides an initial/additional foundation for enhancing resilience and sustainability. Key findings follow:

- **Rising Temperatures:** Projections indicate significant increases in both average and extreme temperatures, exacerbating the urban heat island effect. These changes will intensify health risks, modify energy demands, and impact ecosystems and their vulnerabilities.
- **Wildfires:** Increased frequency and severity of wildfires, fueled by drought conditions and changing wind patterns, pose threats to JPL's infrastructure, air quality, and workforce safety. Events such as the January 2025 wildfire highlight the pressing need for comprehensive mitigation and response strategies.
- **Air Quality:** Persistent air quality challenges, driven by local pollution sources and wildfire emissions, emphasize the need for continued monitoring and action to mitigate adverse health impacts on the JPL community.
- **Precipitation and Flooding:** Variability in precipitation patterns and the increased intensity of storms heighten the risk of flooding and infrastructure stress, necessitating enhanced water management and drainage systems.
- **Snowpack and Water Supply:** Projected decreases of the Sierra Nevada snowpack will pose challenges for water management and necessitate the development of strategies to mitigate potential shortages.
- **Facility Vulnerabilities and Sustainability:** Infrastructure analysis identifies critical risks associated with various environmental changes and hazards, underscoring the importance of adaptation measures and sustainable practices.

Recommendations for Immediate Actions

Comprehensive Environmental Resilience Planning:

- Prioritize the integration of Earth system projections into longer-term facility and operational planning.
- Develop a roadmap for adaptive infrastructure that includes flood defenses, energy-efficient cooling systems, more reflective road and roof surfaces, and designs that resist fire and wind damage.

Enhanced Monitoring and Early Warning Systems:

- Expand air quality and heat monitoring networks across the Lab.
- Implement predictive analytics for wildfire and flooding risks using advanced modeling tools.

Community Engagement and Workforce Resilience:

- Establish programs to educate the workforce on environmental risks and personal safety measures.
- Continue to encourage and support remote work capabilities during extreme environmental events to safeguard employee health and productivity.
- Increase support for workers who bike or walk to work, or who use public transit, and issue specific advisories for them during heat waves or storms that account for the additional exposure they face.

Sustainability and GHG Mitigation:

- Accelerate efforts to achieve net-zero emissions through renewable energy adoption and energy-efficient practices.
- Expand water conservation initiatives and sustainable landscaping to mitigate drought impacts.

Next Steps

Conducting Collaborative Assessments and Knowledge Sharing:

- Strengthen collaborations with NASA's CASI and ES2A programs, local government agencies, and academic institutions to enhance regional environmental resilience.
- Through CASI, and its support of NASA's OSI, share findings from this assessment to support broader NASA and regional planning efforts.
- For future efforts along the lines of this report, include engagements with local universities and colleges with Earth science, environmental, and sustainability programs (e.g., Caltech, UCLA, USC, CSU) to foster research partnerships, data-sharing initiatives, and student training opportunities, and overall add to the fidelity of future reports and activities that stem from it.

Developing Scalable Solutions:

- Pilot and evaluate environmental adaptation strategies at JPL that could help to inform sustainability efforts at other NASA centers.
- Scale successful initiatives, such as the use of reflective materials and sustainable landscaping, across other NASA facilities.

Institutionalizing Environmental Resilience:

- Integrate environmental resilience objectives into JPL's strategic goals and operational policies.
- Allocate dedicated resources to implement and sustain resilience efforts.

Conducting Regular Updates and Reassessments:

- Establish a timeline for periodic updates to this assessment report, ensuring that adaptation strategies remain aligned with evolving scientific understanding, technological advancements, and societal needs.
- Leverage new remote-sensing technologies and Earth system modeling to refine future risk analyses.

Leveraging New Data and Technologies:

- Expand the deployment of new airborne assets to acquire high-resolution, near-real-time data on critical environmental variables, such as vegetation health, land motion and landslide potential, wildfire smoke plumes, and hydrological changes. These assets will enhance localized monitoring and early warning capabilities.

- Use new spaceborne assets, including upcoming satellite missions equipped with advanced sensors for land motion (e.g., NISAR), atmospheric composition (e.g., Plankton, Aerosol, Cloud, ocean Ecosystem [PACE], MAIA), land surface temperature and characteristics (e.g., ECOSTRESS, AVIRIS-x, Surface Biology and Geology [SBG]), and sea level measurements (e.g., Surface Water and Ocean Topography [SWOT]). These tools will provide invaluable regional data sets to inform adaptive strategies.

- Incorporate new observation-informed modeling products to improve predictive accuracy. Advances in computational modeling, integrating real-time data from NASA's Earth observation systems, will enable JPL to better anticipate the impacts of extreme weather events and long-term climate trends.

Driving Innovation and Research:

- Invest in research and development for advanced observation platforms, integrating JPL's expertise in Earth sciences and engineering. Develop innovative tools to extract actionable insights from growing data sets.

- Explore collaborations to leverage commercial and international satellite data for comprehensive analysis and multi-source validation of findings.

Developing Partnerships with Civic and Commercial Leaders:

- Foster ongoing collaborations with the City of Los Angeles, Los Angeles County, and California state agencies to integrate JPL's and NASA's scientific insights and information resources into broader regional sustainability and infrastructure plans. Work to align goals with state-, county-, and city-level climate adaptation and resilience efforts.

- Establish a framework for regular dialogues and joint initiatives with civic and commercial leaders, aiming to develop synergistic solutions for environmental challenges. Collaborate on pilot programs for sustainable urban planning, emissions reduction, and community-based adaptation strategies.

- Utilize NASA's ES2A program to ensure JPL's findings and resources actively support the development of actionable environmental resilience strategies within the surrounding community. Create shared platforms for data exchange and joint problem-solving.

Convening Earth/Environment, Space, and Decision Support-Communities:

- In alignment with JPL's Strategic Imperatives, including "Expand JPL's role as a convenor, host, and promoter of Earth- and space-science communities aligned with NASA's missions," integrate the intention for expanded collaborations, regular updatesand engagements, and growing partnerships into a coordinated framework for sustained community engagements, knowledge sharing, and iterative assessment updates.

These next steps will enhance the accuracy and impact of this type of report, benefiting not only JPL but also other NASA centers and the broader community. They will also support NASA's ES2A Strategy, particularly its second objective, "Deliver Trusted Information to Drive Earth Resilience Activities," while leveraging related NASA and non-NASA support opportunities.

This report represents a pivotal step in understanding and addressing environmental risks at JPL. By addressing challenges from environmental changes and hazards, the Laboratory can safeguard its operations and workforce while enhancing its role as a leader in Earth science, and its use for resilience and sustainability planning.

Appendices

06

A. CASI Program

To ensure effective risk management in the face of environmental changes and hazards, NASA established the CASI Workgroup in 2009 (Rosenzweig, Horton et al. 2011). CASI is supported by funding from NASA's Earth Science Division and Applied Sciences Program and is led by Dr. Cynthia Rosenzweig of NASA's Goddard Institute for Space Studies (GISS). The first iteration of CASI lasted until 2014 and aimed to enhance collaboration among NASA's Earth scientists, applications researchers, and institutional stewards (Rosenzweig, Horton et al. 2011). CASI engaged in a range of activities, including:

- Downscaling center-specific environmental hazard information and projections using CMIP models
- Conducting earth and environmental research customized to each center's needs
- Building inventories of each center's existing environment and impact data and research activities
- Co-leading adaptation workshops

CASI's mission is to provide the latest scientific research on Earth system variations and trends to help NASA facilities managers adapt to increasing environmental risks in timely and effective ways. CASI's partnership between scientists and institutional managers brings together NASA's Earth science expertise and its culture of risk management attained through years of experience in space flight and other core missions. CASI workgroups are composed of members from NASA's ESD and the OSI. There are currently seven workgroups:

1. Temperature and Precipitation

2. Extreme Weather Events
- **a**. High temperatures
- **b.** Droughts
- **c.** Inland floods

3. Sea Level Rise and Coastal Flooding
- **a.** Sea level rise projections
- **b.** Coastal inundation maps

4. Fires and Air Quality
- **a.** Wildfire risk, current and future
- **b.** Smoke risk, current and future

5. Energy
- **a.** Energy management tools

6. Water
- **a.** Water demand
- **b.** Surface flooding

7. Ecosystems

CASI activities include focus on the following priorities:

1	Downscaling center-specific environmental hazard risk information using CMIP6 models and updated IPCC methods
2	Assisting with OSI / National Renewable Energy Laboratory (NREL) Center Resilience Assessments
3	Develop CASI Workgroup products as decision aids

Where feasible, NASA's JPL strives to reduce GHG emissions, transition to electricity that reduces carbon pollution, transition to a low-to-zero-emissions fleet, achieve near-zero emissions buildings, increase energy and water efficiency, reduce waste and pollution, achieve sustainable acquisition and procurement, and meet sustainable supply chain efforts. JPL, NASA's only federally funded research and development center (FFRDC), supports not only NASA's overall mission of innovation and development related to space-based science and technology but also NASA's goal of meeting federally mandated sustainability requirements. Specifically, as of this writing, facilities are required to meet NECPA, EPAct, EOs, and EISA.

CASI's primary stakeholder is the OSI. CASI interacts with the Facilities Real Estate, Logistics Management, and Environmental Management divisions (Figure 6-1).

FIGURE 6-1

NASA divisions of the OSI with which CASI interacts.

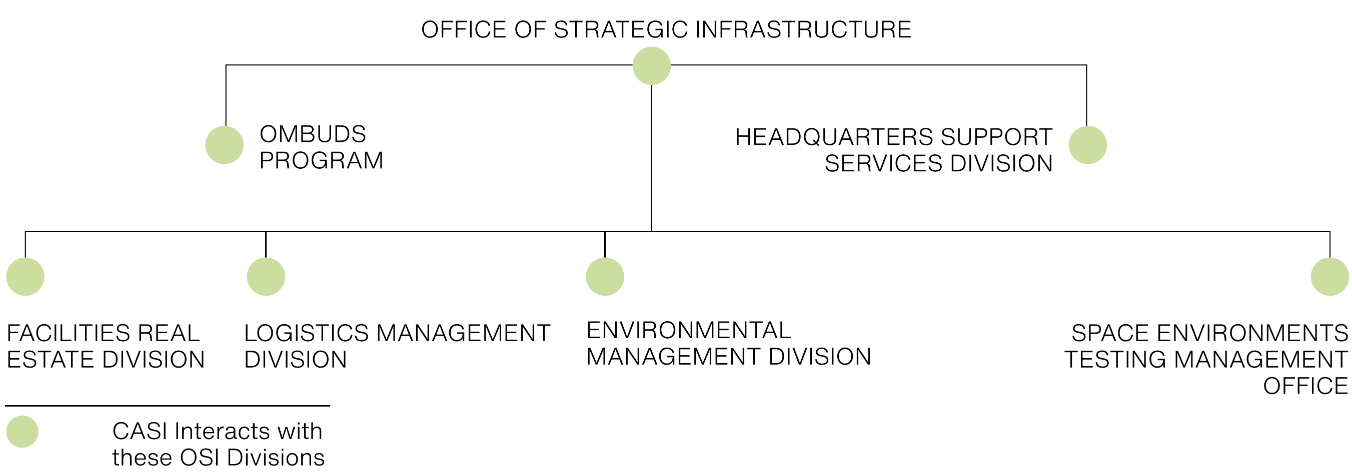

JPL Facilities will use this information in their long-range planning documents. Long-range planning for Facilities rolls up to the NASA OSI at HQ and is managed by the Agency Master Planners in the Strategic Planning Branch of OSI. These planners have been an integral part of the CASI process and are driving the long-range planning deliverables for the Agency. Figure 6-2 shows how CASI products support center and agency climate resilience efforts. An Agency Master Plan was recently approved by the Mission Support Council in 2023 and incorporates planning guidelines that drive the Agency goal of being prepared for environmental changes and risks. Upon approval of the Agency Master Plan in 2023, each center was tasked to create a conceptual 10-year Framework Plan that, among other things, incorporates all large-scale projects that are planned to reduce environmental risks and work to achieve NASA's climate resiliency and sustainability goals. JPL presented its Framework Plan for approval to the Strategic Infrastructure Board of OSI on July 15, 2024. Upon approval of the Framework Plan, JPL and the agency will then move to creating the Center Master Plan, which is a detailed plan showing the feasibility and executability of the Framework Plan. JPL will utilize the CASI and GIS data to help depict some of the risks and vulnerabilities that must be accounted for in the Center Master Plan when considering long-range infrastructure project priorities.

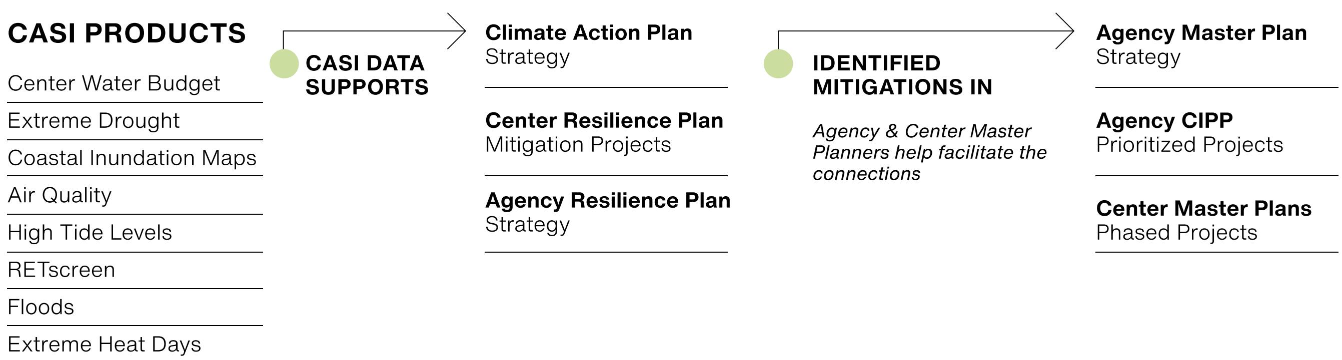

FIGURE 6-2

CASI Workgroup products link to OSI center and agency plans, which inform Master Planners of which environmental risks their centers are most vulnerable to and guides which adaptation efforts will be most effective in protecting facilities and employees from environmental risks and changes.

B. JPL and the Los Angeles Region: Logistic, Demographic, and Geographic Summary

FIGURE 6-3

Map of the Los Angeles region topography and boundary definition as a solid red line, which encompasses Los Angeles, Ventura, and Orange Counties, and adjacent urbanized portions of San Bernardino and Riverside Counties.

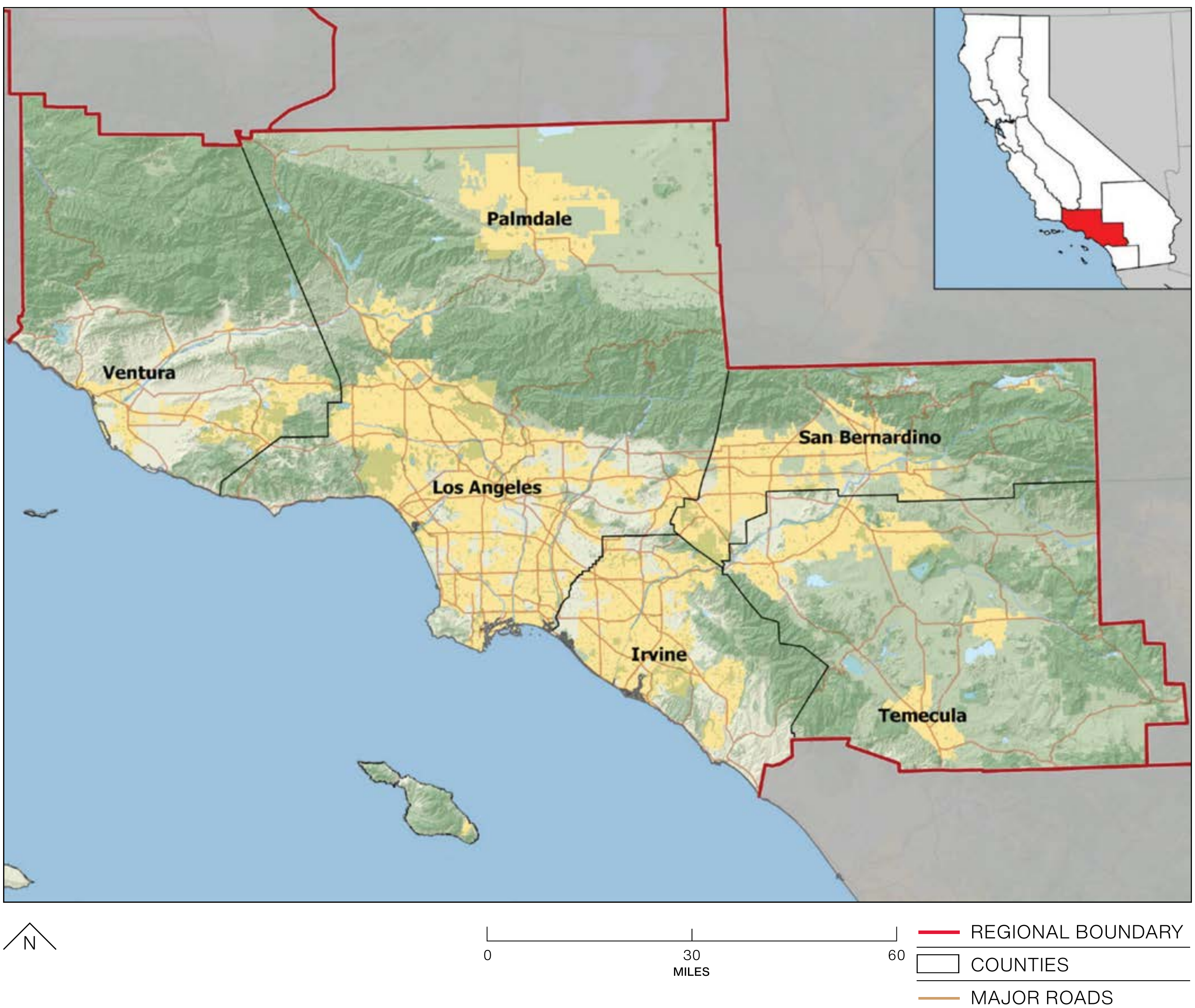

The Greater Los Angeles region is a lowland area in Southern California surrounded by mountain ranges to the east and the Pacific Ocean to the west. It is one of the most populous and economically important regions in the country, encompassing all of Ventura, Los Angeles, and Orange counties, along with urbanized portions of San Bernardino and Riverside counties (Figure 6-3). The region is typified by a semiarid Mediterranean climate with warm, dry summers days and mild, wet winters. The area is seismically active, lying near the San Andreas Fault, a major fault line, which makes the area susceptible to earthquakes. The densely populated region's complex topography and coastal influences result in distinct microclimates and ecological zones, which disproportionately burden low-income residents and communities of color.

The region is home to more than 18 million people and a wide variety of ecosystems throughout the region's coasts, mountains, and desert landscapes (Hall, Berg et al. 2018). The Los Angeles region is also one of the most ethnically and culturally diverse regions in the country, with large Latino, Asian,

FIGURE 6-4

Map of JPL's Southern California sites: the Oak Grove facility, Table Mountain Facility, and GDSCC (AC Martin Partners Inc. 2012a).

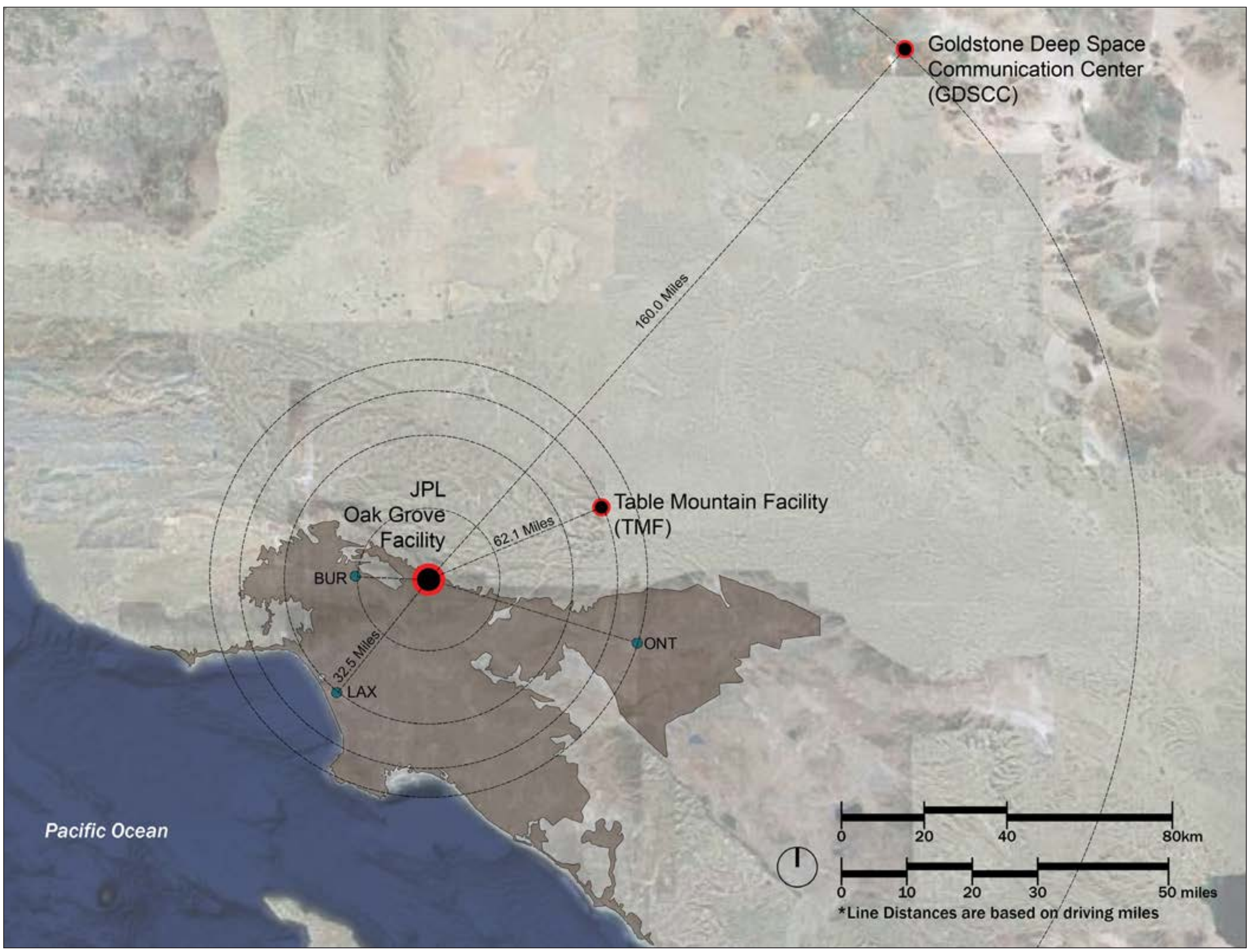

African American, and Caucasian populations. The workforce in the region is highly diverse, with industries ranging from entertainment and technology to manufacturing and logistics.

JPL is an FFRDC owned by NASA and operated by Caltech. JPL is currently NASA's lead center for the robotic exploration of space, and the Lab's primary function is the construction and operation of planetary robotic spacecraft along with the development of Earth and astronomy satellite missions. JPL's campus consists of three main components (Figure 6-4): the main JPL Oak Grove campus (Figure 6-5), the Goldstone Deep Space Communications Complex (GDSCC), and the Table Mountain Facility. The 168-acre Oak Grove campus is in the foothills of the San Gabriel Mountains in the community of La Cañada Flintridge, California, a largely residential region adjacent to Pasadena and at the northern end of the Arroyo Seco watershed system.

JPL's core capacity remains as the ability to formulate, develop, fabricate, and operate spacecraft as well as analyze the returning information pertaining to Earth, the solar system, and space. JPL conducts several important missions for NASA, with a focus on robotic missions to the solar system, including Earth. As of 2025, JPL is responsible for the operation of 35 active spacecraft and instrument missions. JPL is also involved with international space science projects, cooperating with various groups such as the French Space Agency (CNES), the European Space Agency (ESA), ASI, the Japan Aerospace Exploration Agency (JAXA), and the Indian Space Research Organization (ISRO).

JPL Facilities Summary

SUMMARY METRIC	**OAK GROVE**	**GOLDSTONE DEEP SPACE COMMUNICATIONS COMPLEX** (GDSCC)	**MADRID DEEP SPACE COMMUNICATIONS COMPLEX** (MDSCC)	**CANBERRA DEEP SPACE COMMUNICATIONS COMPLEX** (CDSCC)	**TABLE MOUNTAIN FACILITY** (TMF)
Total Land Area Managed (acres)	181.2	33,369	122	322	38
On-site Workforce	5,000 FTE	178	110	112	15
Total Building Area (sf)	2,676,000	185,464	93,295	104,311	28,120
Current Replacement Value (CRV)	$1,042 M	$250 M	$168 M	$155 M	$10.8 M

TABLE 6-1

JPL facilities summary (AC Martin Partners Inc. 2012a).

JPL operates additional facilities located around the world, including maintaining and planning NASA's network of antennas that control and receive scientific data from deep space missions—the DSN. The DSN is a complex telecommunications system that provides tracking and communications for planetary spacecraft, using antenna installations located near Barstow, California; Madrid, Spain; and Canberra, Australia via the Space Flight Operations Command Facility (Table 6-1).

JPL has a large and diverse workforce that is deeply connected to the surrounding communities. JPL employs over 5,500 workers consisting of a dedicated population of scientists, engineers, technologists, developers, communicators, designers, safety experts, business administrators, and more. Approximately 65% of JPL employees and contract personnel live within a 10-mile radius of the Laboratory, which includes the communities of Pasadena, Altadena, La Cañada Flintridge, La Crescenta, Montrose, Tujunga, Sunland, Burbank, Glendale, South Pasadena, San Marino, Alhambra, San Gabriel, Arcadia, Sierra Madre, Temple City, Monrovia, and portions of Los Angeles.

C. JPL's Deep Space Network Facilities

NASA's DSN is an international network of ground-based antennas and communication facilities managed by JPL. The first facility was established in 1958 when JPL selected the Goldstone site to meet the requirements of the Pioneer 3 mission. The network was later expanded in the 1960s to meet the need for constant contact between Earth and spacecraft, and the United States government signed agreements with Australia and Spain to establish additional facilities near Canberra and Madrid.

The DSN's primary role is to support interplanetary spacecraft missions, perform radio astronomy observations, and conduct radar studies for planetary exploration. The network also supports selected Earth-orbiting missions. The DSN ensures two-way communication with spacecraft for data acquisition, transmission of commands, and tracking. The network plays a vital role in advancing scientific exploration and supporting high-profile missions, such as the Voyager spacecraft, the Mars rovers, and the Hubble Space Telescope.

The DSN consists of three major complexes (Figure 6-5):

- **GDSCC:** Located in California's Mojave Desert, GDSCC is NASA's premier communication hub in the United States. It encompasses an area of 44 square miles and houses multiple large antennas within the boundaries of the U.S. Army's Fort Irwin National Training Center.
- **MDSCC:** Situated near Robledo de Chavela, Spain, this facility provides tracking and communication coverage for the Eastern Hemisphere.
- **CDSCC:** Positioned in Tidbinbilla, Australia, CDSCC supports southern hemisphere coverage for constant spacecraft communication as the Earth rotates.

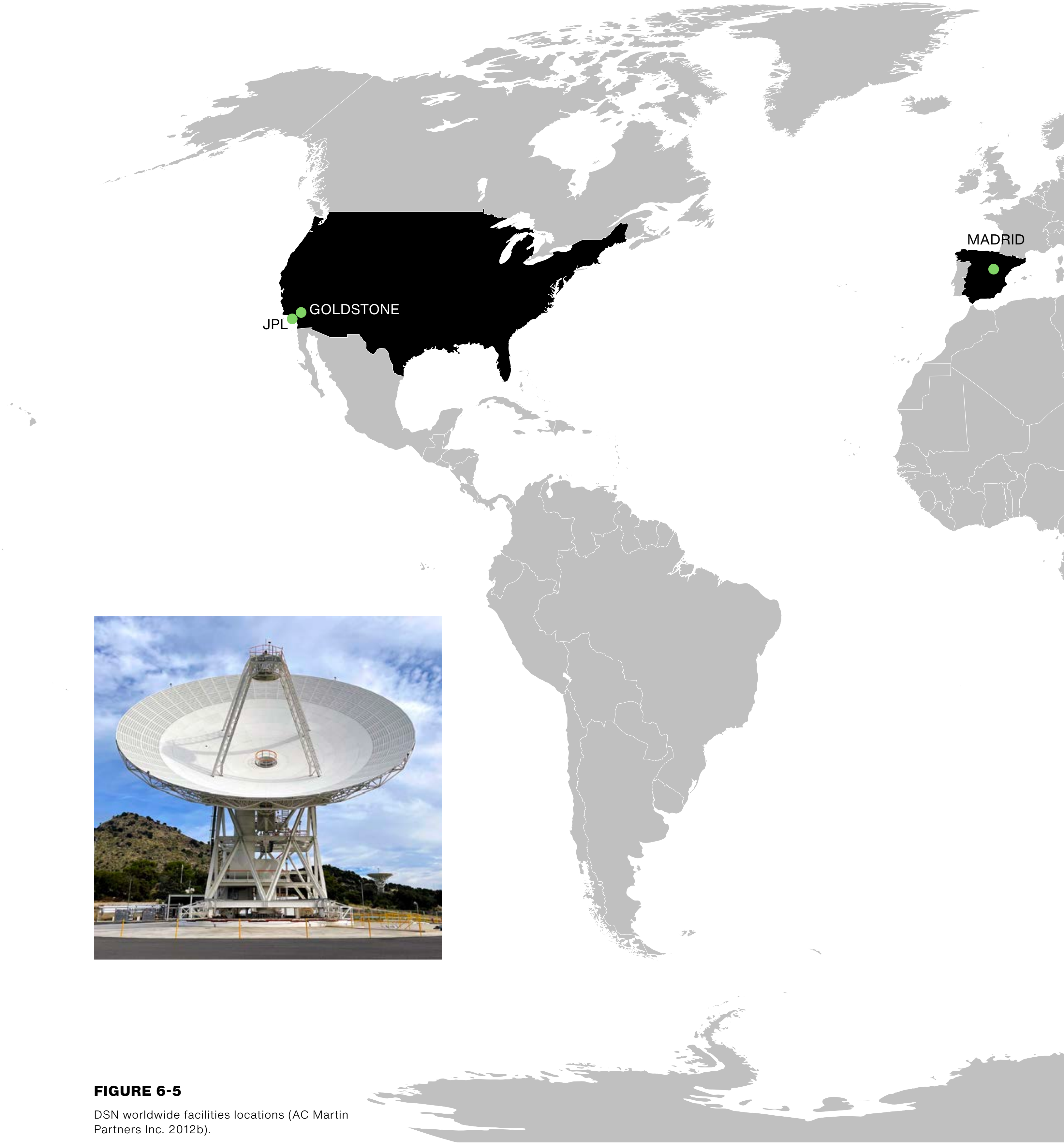

FIGURE 6-5

DSN worldwide facilities locations (AC Martin Partners Inc. 2012b).


CANBERRA

Each DSN facility is placed approximately 120 degrees of longitude apart around the world and hosts 70-meter and 34-meter beam waveguide antennas that are pivotal for tracking spacecraft and retrieving high-volume data from missions exploring the solar system and beyond. The antennas and data delivery systems make it possible to: (1) acquire telemetry data from spacecraft, (2) transmit commands to spacecraft, (3) track spacecraft position and velocity, (4) perform very long baseline interferometry observations, (5) measure variations in radio waves for radio science experiments, (6) gather science data, and (7) monitor and control the performance of the network (AC Martin Partners Inc. 2012b).

The DSN faces several climate change and environmental hazard risks. The primary risk is aging infrastructure. Many DSN facilities and their components were constructed over 40 years ago. Aging systems require significant investment to modernize and ensure operational reliability. Additionally, deferred required preventive and routine maintenance, due to increasing budgetary constraints and unavailability of downtime, have continued to negatively impact critical infrastructure.

High summer temperatures and water scarcity in the Mojave Desert are several climate change challenges facing GDSCC. The climate is typical of open desert with hot, dry summers and mild winters. The mean summer maximum temperature is 106°F (41°C) to a mean summer minimum of 73°F (23°C). High summer temperatures increase cooling demands for antennas and facility buildings, driving up operational costs.

Fort Irwin manages the water supply for the GDSCC for cooling and domestic purposes. There are five major groundwater basins in the vicinity of Fort Irwin: the Irwin, Bicycle, Langford, Nelson, and Coyote basins. Of the five basins, the Irwin, Bicycle, and Langford basins have been developed for use as a water supply for Fort Irwin. A water balance conducted for the three basins by the Army found that more water was being removed from the system than was entering through rainfall recharge, with a net change estimated to be -833 acre-feet per year (AC Martin Partners Inc. 2012b). Fort Irwin estimates that there is a 70-year supply of groundwater available for domestic use from the three basins; however, based on Fort Irwin population projections, and if the Fort Irwin solar electric project is implemented with the proposed water-steam technology, that could be reduced to only about 20 years.

NASA maintains a contractual agreement with Spain's Instituto Nacional de Técnica Aeroespacial (INTA), which contracts with Ingeniería y Servicios Aeroespaciales (INSA), for managing, staffing, and providing maintenance and operation of the MDSCC. The MDSCC facilities are located within a ZEPA (Zona de Especial Protección para las Aves), a special protection area for birds, according to European Executive Council (EEC) Directive 92/43/EEC (Habitats Directive). All activities that may potentially have an impact on the environment are subject to national, regional, local, and European Utilities Requirements (EUR). NASA/JPL works with INSA to ensure compliance with all environmental regulations.

NASA also maintains a series of agreements for the operation of the CDSCC in Australia. NASA has partnered with the Government of Australia's Commonwealth Scientific and Industrial Research Organization (CSIRO) to oversee the maintenance and operation of NASA facilities in Australia. CDSCC must comply with all applicable Australian federal, regional, and local environmental regulations. There are currently no actions required at this time at CDSCC to bring the facility into compliance with environmental regulations.

Using thermal imagery from NASA's ECOSTRESS instrument aboard the ISS, heat maps of LST variations across NASA's Deep Space Communication Complexes located in the United States (Goldstone, California), Spain (Madrid), and Australia (Canberra) were created (Figure 6-6, Figure 6-7, and Figure 6-8). These facilities play a crucial role in supporting interplanetary missions, and understanding their thermal environment can provide insights into land-atmosphere interactions, site-specific microclimates, and potential thermal influences on infrastructure.

The ECOSTRESS data, collected at high spatial and temporal resolution, captures thermal variations influenced by factors such as surface materials, vegetation cover, and local climate conditions. Initial observations indicate distinct temperature differences between the sites due to their unique geographic settings:

- **Goldstone, California:** Exhibits the highest daytime surface temperatures, often exceeding 120°F (50°C) in summer. The arid desert landscape, characterized by sparse vegetation and rocky terrain, absorbs and retains heat, leading to significant thermal stress on infrastructure.
- **Madrid, Spain:** Experiences moderate temperature variations. The surrounding landscape features a mix of natural vegetation and urban infrastructure, which affects heat retention and dissipation. Urban heat island effects may contribute to localized warming around the complex.
- **Canberra, Australia:** Demonstrates the lowest surface temperatures among the three sites. The combination of vegetation cover, a temperate climate, and elevation differences contributes to relatively lower heat retention, reducing cooling demands on infrastructure.

These thermal maps provide some initial information for site management, energy efficiency assessments, and potential climate adaptation strategies. In the event future versions of this report are developed, the climate change and environmental risk challenges associated with these facilities can be explored in further detail.

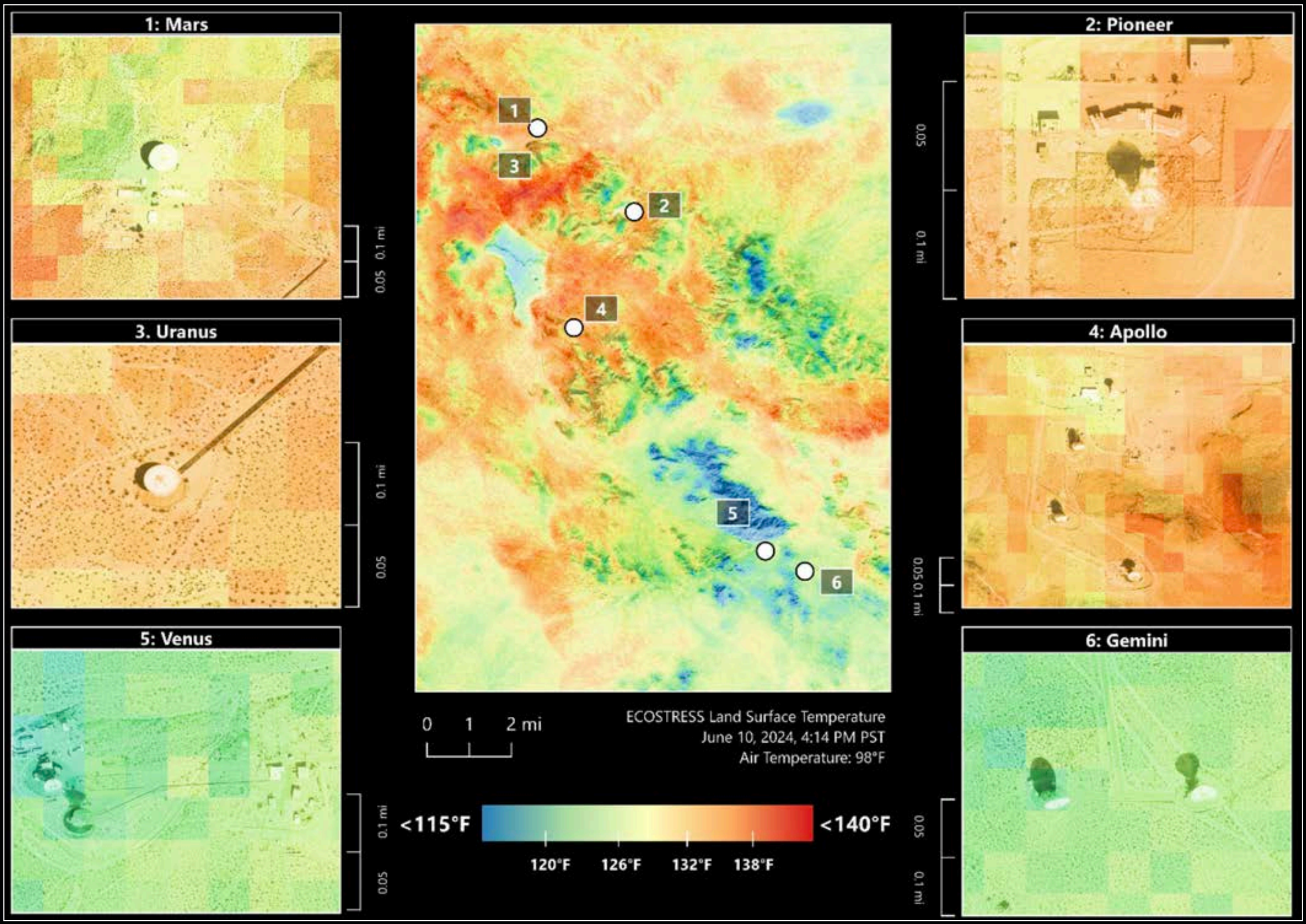

FIGURE 6-6

LST of the GDSCC (United States) based on satellite observations from the ECOSTRESS thermal infrared remote-sensing instrument on the ISS for June 10, 2024.

FIGURE 6-7

LST of the MDSCC (Spain) based on satellite observations from the ECOSTRESS thermal infrared remote-sensing instrument on the ISS for June 22, 2024.

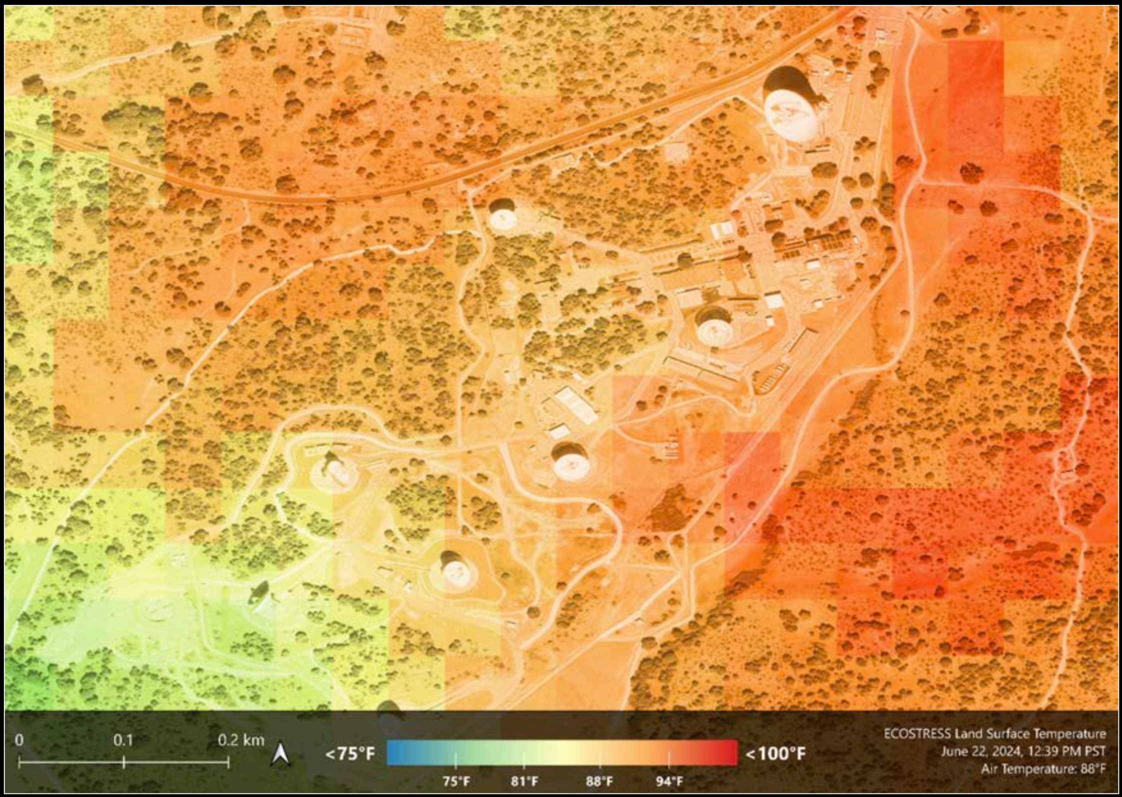

FIGURE 6-8

LST of the CDSCC (Australia) based on satellite observations from the ECOSTRESS thermal infrared remote-sensing instrument on the ISS for January 6, 2024.

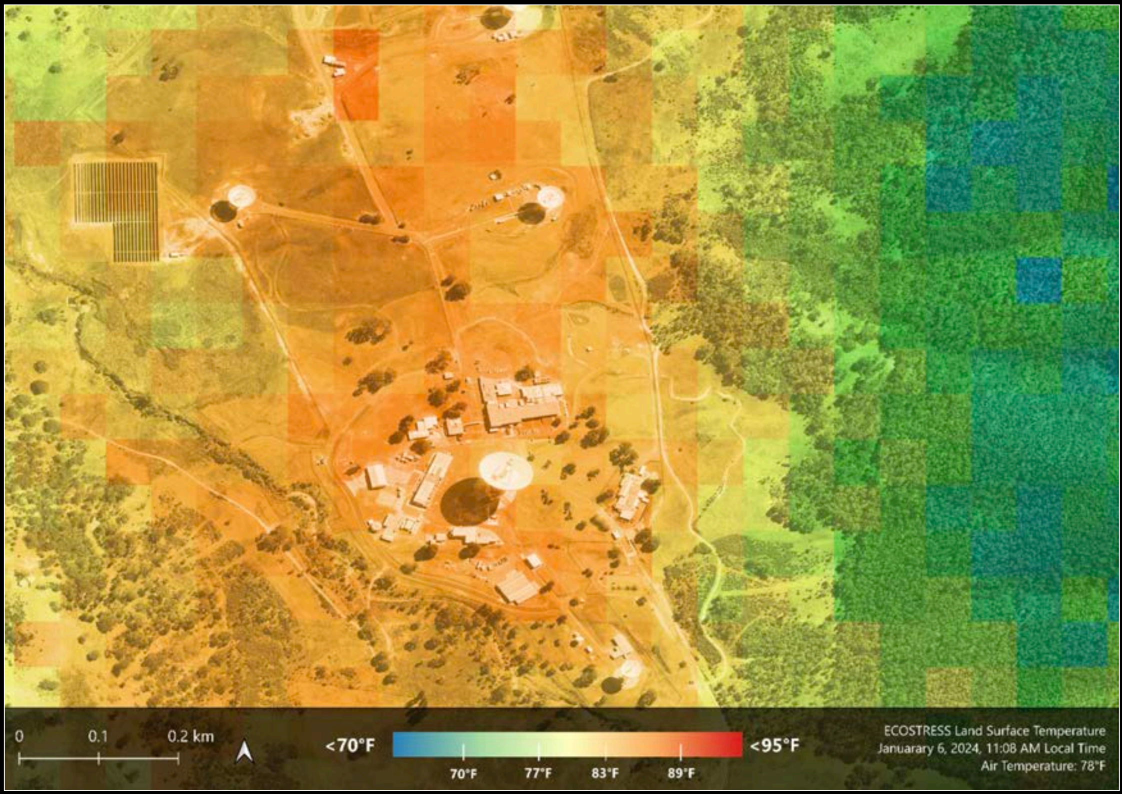

D. Projections and Shared Socioeconomic Pathways

In the IPCC Sixth Assessment Report (AR6), an international team of experts developed a set of five new "pathways," collectively known as the SSPs, as important inputs into the latest Earth system models (CMIP6). The SSPs were created to integrate the understanding of socioeconomic trends and potential climate outcomes by combining them with the Representative Concentration Pathways (RCPs) that were used in the IPCC's Fifth Assessment Report (AR5) (O'Neill, Tebaldi et al. 2016) and that define different trajectories of GHG emissions.

Each SSP describes a potential alternative future society in terms of demographics, economic development, technology, energy use, and political factors. The five pathways—SSP1 (Sustainability), SSP2 (Middle of the Road), SSP3 (Regional Rivalry), SSP4 (Inequality), and SSP5 (Fossil-Fueled Development)—are designed to cover a broad range of future possibilities. Together, the RCPs and SSPs create a new Scenario Matrix Architecture that combines pathways of future radiative forcing and their associated environmental changes with alternative pathways of socioeconomic development.

The combined scenarios can be referred to as SSPx-y, where x represents the specific SSP and y represents the forcing pathway (O'Neill, Tebaldi et al. 2016). Among all the combinations, four "Tier 1" SSP-RCP scenarios were identified:

- **SSP1-2.6 (Sustainability—Taking the Green Road):** This scenario represents an optimistic scenario whereby the world embraces sustainable development and shifts toward a more inclusive, equitable, and environmentally sustainable society. It is characterized by achievement of some of the most ambitious goals set by the Paris Agreement, in which global warming is limited to around 1.5oC by the end of the century.
- **SSP2-4.5 (Middle of the Road):** This scenario represents a future when historical patterns of development continue with a mix of challenges and successes in tackling climate change. It is characterized by moderate progress in reducing GHG emissions; mitigation efforts are significant but not sufficient to meet the most ambitious climate goals, resulting in around 2.7oC of global warming by the end of the century.
- **SSP3-7.0 (Regional Rivalry—A Rocky Road):** This scenario represents a fragmented world characterized by regional rivalry, weak international cooperation, and growing nationalism. It is characterized by little to no effective climate policy; global temperature increases by about 3.2oC to 4.0oC by the end of the century.
- **SSP5-8.5 (Fossil-Fueled Development—Taking the Highway):** This scenario represents a future with high GHG emissions, driven by rapid economic growth that relies heavily on fossil fuels. It is characterized by the highest emissions trajectory of all SSPs, with global temperature rising by more than 4oC by the end of the century. This SSP is often referred to as a "business as usual" scenario.

CASI's climate and researchers provide downscaled projections for key climate variables using NASA's Earth Exchange Global Daily Downscaled Projections (NEX-GDDP-CMIP6), which includes global downscaled climate scenarios derived from 35 General Circulation Model (GCM) runs conducted under the Coupled Model Intercomparison Project Phase 6 (CMIP6) for each emissions scenario. Key climate variables in the NEX data set include minimum, maximum, and average temperatures, precipitation, relative humidity, specific humidity, downwelling longwave and shortwave radiation, and surface wind speed. Of the 35 GCMs, only 22 models are used to avoid including any "hot" models that are outside the IPCC's assessed "Likely" range of transient climate response and are provided for the time spanning from the 2020s to 2100 at a spatial scale of roughly 25 km.

This report includes climate projections for three primary SSP scenarios: low-emissions (SSP1-2.6), medium-emissions (SSP2-4.5), and high-emissions (SSP3-7.0) pathways. These projections extend through 2045 to align with the 20-year planning horizon that JPL's facilities planning and management team uses for essential infrastructure and investment decisions at the Oak Grove campus. The projections cover the following key climate variables:

- Tmax value every year (°F); Figure 2-4A
- Number of extremely hot days per year, with Tmax ≥ 95°F (35°C); Figure 2-4B
- Number of days with frost per year, with Tmin ≤ 32°F (0°C); Figure 2-4C
- Number of days per year where wind speed (m/s) is greater than the 95th percentile from a baseline period (2015–2025); Figure 2-6
- Number of days per year of moderate fire danger, with FWI ≥ N15 for the Greater Los Angeles region (500 km radius around the Laboratory); Figure 2-9A
- Number of days per year of very high fire danger, with FWI ≥ N45 for the Greater Los Angeles region (500 km radius around the Laboratory); Figure 2-9B
- Number of dry days per year, defined as days when precipitation is ≤ .001 inches; Figure 2-14A
- Number of days per year with precipitation greater than the 90th percentile from a baseline period (1995–2014); Figure 2-14B

The figures for the climate change projections for the three primary SSP scenarios feature observed data from 2005 to 2014 and model simulated projections from 2015 to 2025. The gap in the graphs is a visual artifact marking the shift from measured historical data to modeled projections based on climate scenarios.

06

E. NASA Center Vulnerability, Impacts, and Adaptation Worksheet

The latest version of the NASA center climate vulnerability, impacts, and adaptation worksheet (Worksheet 1) provides a broad overview on climate impacts and adaptation strategies for each NASA center. The worksheet contains four main components: (1) environmental hazards, impacts, and vulnerabilities, (2) center Earth model projections, (3) environmental adaptation strategies and metrics, and (4) key environmental risks and adaptation priorities. Climate change projections are based on the IPCC's latest CMIP6 Earth system models for low-emissions (SSP1-2.6), medium-emissions (SSP2-4.5), and high-emissions (SSP3-7.0) scenarios for key environmental variables (e.g., temperature, precipitation, FWI). CASI treats these Worksheets as living documents that will continue to be updated with, for example, new environmental risk variables, model data, and center adaptation efforts as well as continued monitoring and evaluation metrics for climate adaptation efforts.

WORKSHEET 1

NASA Center Climate Change Vulnerability, Impacts, and Adaptation Worksheet for JPL

JET PROPULSION LABORATORY, CA

CLIMATE HAZARDS, IMPACTS, and VULNERABILITIES

Hazards

- Temperature: Increasing temperatures
- Precipitation: Increasing frequency and intensity of atmospheric rivers resulting in flooding
- Drought: Increasing frequency and duration; reduced water availability
- Wildfire: Increasing frequency and intensity
- Wind: Frequency and intensity

Vulnerabilities

- Aging buildings and infrastructure
- Age and health of workforce
- Center substation/distribution system
- Rising utility cost and supply chain uncertainty
- Alternative/renewable energy projects compete poorly against construction and investment options

Impacts

- LAND: More frequent and intense flooding
- STRUCTURES: Structural Damage, Power Supply Damage, Basement Flooding, Electrical System Overload
- OPERATIONS: Water Supply Shortages (Lack of Water for Mission), Power Supply Interruptions and Outages, Indoor Environmental Control, Access to Facilities, Lack of HVAC Cooling Capacity, Building Envelope Heat Gain, Chiller Plant Higher Heat Loads, Increase in Chiller Plant Operational Cost, Tree Falling on Electrical Grid, Access Issues due to Smoke Visibility, Decrease in Labor Productivity due to Heat

CENTER CLIMATE PROJECTIONS[1]

Short term (2030s) / Mid term (2050s) / Long term (2080s)

Temperature

- Hottest Tmax: 34.3C – 34.6C / 34.9C – 35.4C / 35C – 36.8C
- Coldest Tmin: 0.1C - 0.4C / 0.5C - 1.3C / 0.5C - 3C
- # of Tmax days (90th percentile)[2]: 59 - 61 days / 66 – 77 days / 68 – 108 days
- # of Tmax days ≥ 35C: 1 - 1 day / 2 – 3 days / 2 – 9 days
- # of Tmin trop nights ≥ 20C: 6 – 10 days / 10 – 18 days / 12 – 41 days

Rainfall

- # of Prec days (90th percentile)[2]: 5 – 6 days / 5 – 6 days / 5 – 5 days
- # of Dry days (prec ≤0.0001 in): 315 – 316 days / 315 - 317 days / 315 – 318 days

Potential Evapotranspiration

- PET: 280 cm/yr / 297 cm/yr / 315 cm/yr

Air Quality (excluding SSP585)

- Annual Average Surface PM: 7 - 14 $\mu g/m^3$ / 10 - 23 $\mu g/m^3$ / 15 - 38 $\mu g/m^3$

Wildfire (Fire Weather Index)

- FWI N30 JPL: 80 - 86 days / 85 - 92 days / 87 - 105 days
- FWI N30 500km: 137 - 140 days / 139 - 146 days / 139 - 157 days

Cooling Degree Days (CDD):

- CDD Average Annual Sum: 2793-3002 days / 2996 - 3262 days / 3119 - 3715 days

Heat Waves:

- Future heatwaves in California will be more frequent, hotter, more extensive, and more persistent humid nighttime heat waves with a growing daytime signature[3]

Floods:

- Excessive flooding is projected to increase by at least 50% towards the end of the 21st century, with the occurrence of extreme wet events increasing roughly threefold by 2070-2079 from the baseline period (1930-1939)[4]

Wind Intensity:

- Santa Ana winds (SAWs) are projected to decrease, with the trend most pronounced in the early and late season: fall and spring[5]

CLIMATE ADAPTATION STRATEGIES AND METRICS

****Feedback on progress provided by OSI***

CLIMATE ADAPTATION STRATEGIES

- HIGH TEMPERATURE AND HEAT WAVES:
  - Manage JPL's HVAC systems for higher temperatures: *Planned and a few HVAC upgrades completed*
  - Incorporate reflective roofing into new development projects: *Underway*
  - Incorporate light-colored aggregate to improve reflectivity and lower pavement temperatures: *Underway and completed a pilot program Solar Gray installed one roadway at JPL*
  - Improve JPL's building energy efficiency: *Planned - Optimize building operations for appropriate buildings and minimize wasted energy*
  - Energy Savings Performance Contract (ESPC) includes solar PV projects for grid outages and alternative/renewable energy source: *Planned*
- FLOODING:
  - Maintain stormwater drainage systems near buildings: *Planned*
- OTHER:
  - Continue JPL's water conservation program: *Planned and a few adaptation efforts completed such as turf removal, native and drought tolerant plants, drip irrigation, and low flow fixtures*
  - Separate JPL's landscape water supply for potable water supply: *This is not planned*
  - Continue to clear brush from JPL sites to reduce wildfire risk: *Planned*
  - Continue JPL's firefighting training: *Complete and Plan to improve on efforts*
    - Incorporate climate adaptation strategies into JPL's construction and operation & maintenance programs: *Planned by incorporating management strategies to be able to fluctuate building and occupational loads*

ADAPTATION MONITORING AND EVALUATION METRICS

- HIGH TEMPERATURE & HEAT WAVES: Manage/Upgrade JPL's HVAC system for higher temperatures
  - Observed temperature trends and heat waves
  - Electrical System Service Disruptions:
    - Annual Number
    - Center Workforce/Region Population Affected
    - Average Duration
  - Smart Lab: *Underway. Through the process of improving efficiency, adopt Smart Lab practices*
    - Dynamic and digital systems, lowering system pressure drop, air flow optimization, demand-based lighting controls, and fault detection: *Underway*
- DROUGHT:
  - Annual Total Water Demand

KEY CLIMATE RISKS AND ADAPTATION PRIORITIES

Key Climate Risks

- TEMPERATURE: Increasing trend for number of high temperature days and heat waves and impacts on power supply
- RAINFALL: Increasing trend for more heavy rainfall events and increased flooding

Adaptation Priorities

- E.g. Upgrade HVAC system
- Continue JPL's water conservation program

[1] NASA – Climate Adaptation Science Investigator (CASI) Workgroup, 2024 CASI Climate Projections, each time period is calculated by taking the 30-year mean centered around the corresponding decade. The range for each variable includes the range of SSP's including SSP1-2.6, SSP2-4.5, SSP3-7.0, and SSP5-8.5.

[2] 90th percentile calculated using all daily precipitation values (dry days EXCLUDED) or daily maximum temperature values from 1995-2014

[3] Gershunov, A., Cayan, D. R., & Iacobellis, S. F. (2009). The Great 2006 Heat Wave over California and Nevada: Signal of an Increasing Trend. *Journal of Climate*, *22*(23), 6181–6203. https://doi.org/10.1175/2009JCLI2465.1

[4] Yoon, J.-H., Wang, S.-Y. S., Gillies, R. R., Kravitz, B., Hipps, L., & Rasch, P. J. (2015). Increasing water cycle extremes in California and in relation to ENSO cycle under global warming. Nature Communications, 6(1), 8657. https://doi.org/10.1038/ncomms9657

[5] Guzman-Morales, J., & Gershunov, A. (2019). Climate Change Suppresses Santa Ana Winds of Southern California and Sharpens Their Seasonality. *Geophysical Research Letters*, *46*(5), 2772–2780. https://doi.org/10.1029/2018GL080261

06

F. Acronyms

AR atmospheric river

AR6 Sixth Assessment Report

ARC Ames Research Center

ASHRAE American Society of Heating, Refrigeration, and Air-Conditioning Engineers

ASI Italian Space Agency

AVIRIS Airborne Visible / Infrared Imaging Spectrometer

AVIRIS-NG AVIRIS Next Generation

Caltech California Institute of Technology

CASI Climate Adaptation Science Investigators

CDD cooling degree days

CDSCC Canberra Deep Space Communications Complex

CEA California Earthquake Authority

CIPP Capital Investment Program Plan

CLARS California Laboratory for Atmospheric Remote Sensing

CMIP Coupled Model Intercomparison Project

CNES French Space Agency

COOP Continuity of Operations

CSIRO Commonwealth Scientific and Industrial Research Organization (Australia)

CSU California State University

CyAN Cyanobacteria Assessment Network

DPM diesel particulate matter

DSN Deep Space Network

DWR Department of Water Resources

EC elemental carbon

ECOSTRESS ECOsystem Spaceborne Thermal Radiometer Experiment on Space Station

EEC European Executive Council

EHF excess heat factor

EISA Energy Independence and Security Act of 2007

EMIT Earth Surface Mineral Dust Source Investigation

ENSO El Niño-Southern Oscillation

EO Executive Order

EO-1 Earth Observing-1

EOP Emergency Operations Plan

EPAct Energy Policy Act of 2005

ESA European Space Agency

ES2A Earth Science to Action

ESD Earth Science Division

ESPC Energy Savings Performance Contract

EUR European Utilities Requirements

EVS-4 Earth Venture Suborbital

ESM Earth System Model

FCD Federal Continuity Directive

FEIF Flight Electronic Integration Facilities

FEMA Federal Emergency Management Agency

FFRDC federally funded research and development center

FHAB freshwater harmful algal blooms

FTS Fourier transform spectrometer

FWI Fire Weather Index

GCM General Circulation Model

GDDP Global Daily Downscaled Projection

GDSCC Goldstone Deep Space Communications Complex

GFDL Geophysical Fluid Dynamics Laboratory

GHG greenhouse gas

GIS geographic information systems

GISS Goddard Institute for Space Studies

GLAD Global Land Analysis and Discovery

GLDAS Global Land Data Assimilation System

GRACE-FO Gravity Recovery and Climate Experiment Follow-On

GSFC Goddard Space Flight Center

HDD heating degree days

HEPA high-efficiency particulate air

HSPD Homeland Security Presidential Directive

HQ headquarters

HVAC heating, ventilation, and air-conditioning

HyTES Hyperspectral Thermal Emission Spectrometer

IBHS Insurance Institute for Business and Home Safety

INSA Ingeniería y Servicios Aeroespaciales

INTA Instituto Nacional de Técnica Aeroespacial

IPCC Intergovernmental Panel on Climate Change

ISRO Indian Space Research Organization

ISS International Space Station

ITCP IT Contingency Plan

IVT integrated water vapor transport

JAXA Japan Aerospace Exploration Agency

JCSSP JPL Climate Science Strategic Plan

JPL Jet Propulsion Laboratory

JSC Johnson Space Center

LACCE Landslide Climate Change Experiment

LaRC Langley Research Center

LEED Leadership in Energy and Environmental Design

LST land surface temperature

LULC land use / land cover

MAIA Multi-Angle Imager for Aerosols

MDSCC Madrid Deep Space Communications Complex

MERIS Medium Resolution Imaging Spectrometer

MERRA-2 Modern-Era Retrospective analysis for Research and Applications, Version 2

MHHW mean higher high water

MODIS Moderate Resolution Imaging Spectroradiometer

MOMO-Chem multi-model multi-constituent chemical

MSFC Marshall Space Flight Center

MWD Metropolitan Water District

NAAQS National Ambient Air Quality Standards

NASA National Aeronautics and Space Administration

NCI NASA critical infrastructure

NECPA The National Energy Conservation Policy Act

NEX NASA Earth Exchange

NISAR NASA-ISRO Synthetic Aperture Radar

NIST National Institute of Standards and Technology

NLDAS National Land Data Assimilation System

NOAA National Oceanic and Atmospheric Administration

NOS National Ocean Service

NPD NASA Policy Directive

NPR NASA Procedural Requirement

NPG NASA Procedures and Guidance

NREL National Renewable Energy Laboratory

NSPD National Security Presidential Directive NWS National Weather Service

OCIO Office of the Chief Information Officer

OCO-2/3 Orbiting Carbon Observatory 2/3

OLCI Ocean and Land Color Instrument

OPERA Observational Products for End-Users from Remote Sensing Analysis

OSI Office of Strategic Infrastructure

PACE Plankton, Aerosol, Cloud, ocean Ecosystem

PET potential evapotranspiration

PM particulate matter

PML probable maximum loss

PRISM Parameter-elevation Regressions on Independent Slopes Model

PSD Protective Services Division

PVC polyvinyl chloride

PWP Pasadena Water and Power

RCP Representative Concentration Pathway

SAR synthetic aperture radar

SAW Santa Ana wind

SBG Surface Biology and Geology

SCAQMD South Coast Air Quality Management District

SCEC Southern California Earthquake Center

SEDAC Socioeconomic Data and Applications Center

SSP shared socioeconomic pathway

SWE snow water equivalent

SWOT Surface Water and Ocean Topography

TCCON Total Carbon Column Observing Network

TFM Technical Facility Management

Tmax maximum air temperature

Tmin minimum air temperature

TROPESS TRopospheric Ozone and its Precursors from Earth System Sounding

UAVSAR Uninhabited Aerial Vehicle Synthetic Aperture Radar

UC University of California

UCLA University of California, Los Angeles

USC University of Southern California

USDA United States Department of Agriculture

USFS United States Forestry Service

USGS United States Geological Survey

VCP volatile chemical products

VIC variable infiltration capacity

VOC volatile organic compounds

VSWIR Visible to Short Wavelength Infrared

WHO World Health Organization

ZEPA Zona de Especial Protección para las Aves

G. References

AC Martin Partners Inc. (2012a). JPL Oak Grove Master Plan Update 2011-2032, National Aeronautics and Space Administration, Jet Propulsion Laboratory.

AC Martin Partners Inc. (2012b). Deep Space Network Facilities Master Plan Update 2011-2032, National Aeronautics and Space Administration Jet Propulsion Laboratory.

AghaKouchak, A., L. Cheng, O. Mazdiyasni and A. Farahmand (2014). "Global warming and changes in risk of concurrent climate extremes: Insights from the 2014 California drought." Geophysical Research Letters 41(24): 8847-8852.

Amini, H., M. Danesh-Yazdi, Q. Di, W. Requia, Y. Wei, Y. Abu-Awad, L. Shi, M. Franklin, C.-M. Kang and J. Wolfson (2022) "Hyperlocal super-learned PM2. 5 components across the contiguous US." DOI: 10.21203/rs.3.rs-1745433/v2.

Belair, G., E. Jones, S. Slaughter and B. Mirus (2022) "Landslide Inventories across the United States version 2, Geological Survey data release." DOI: 10.5066/P9FZUX6N.

Biasutti, M., R. Seager and D. B. Kirschbaum (2016). "Landslides in West Coast metropolitan areas: The role of extreme weather events." Weather and Climate Extremes 14: 67-79.

CAL FIRE. (2025). "Current Emergency Incidents, Eaton Fire." Retrieved March 11, 2025, from https://www.fire.ca.gov/incidents/2025/1/7/eaton-fire.

California Department of Conservation. (2023). "2023 California Landslide Response." Retrieved March 3, 2025, from https://www.conservation.ca.gov/cgs/landslides/2023.

Carranza, V., T. Rafiq, I. Frausto-Vicencio, F. M. Hopkins, K. R. Verhulst, P. Rao, R. M. Duren and C. E. Miller (2018). "Vista-LA: Mapping methane-emitting infrastructure in the Los Angeles megacity." Earth Syst. Sci. Data 10(1): 653-676.

Cira, M., A. Bafna, C. M. Lee, Y. Kong, B. Holt, L. Ginger, K. Cawse-Nicholson, L. Rieves and J. A. Jay (2022). "Turbidity and fecal indicator bacteria in recreational marine waters increase following the 2018 Woolsey Fire." Scientific Reports 12(1): 2428.

City of Rancho Palos Verdes. (2025). "Land Movement Updates." Retrieved March 6, 2025, from https://www.rpvca.gov/1707/Land-Movement-Updates.

Corbett, S. W. (1996) "Asthma exacerbations during Santa Ana winds in southern California." Wilderness & Environmental Medicine 7, 304-311 DOI: 10.1580/1080-6032(1996)007[0304:Aedsaw]2.3.Co;2.

Cordeira, J. M., J. Stock, M. D. Dettinger, A. M. Young, J. F. Kalansky and F. M. Ralph (2019). "A 142-Year Climatology of Northern California Landslides and Atmospheric Rivers." Bulletin of the American Meteorological Society 100(8): 1499-1509.

Corringham, T. W., F. M. Ralph, A. Gershunov, D. R. Cayan and C. A. Talbot (2019). "Atmospheric rivers drive flood damages in the western United States." Science Advances 5(12): eaax4631.

Cusworth, D. H., R. M. Duren, V. Yadav, A. K. Thorpe, K. Verhulst, S. Sander, F. Hopkins, T. Rafiq and C. E. Miller (2020). "Synthesis of Methane Observations Across Scales: Strategies for Deploying a Multitiered Observing Network." Geophysical Research Letters 47(7): e2020GL087869.

Dasgupta, S., S. Lall and D. Wheeler (2023). "Subways and CO2 emissions: A global analysis with satellite data." Science of The Total Environment 883: 163691.

Dean Runyan Associates (2024). The Economic Impact of Travel in California.

Dettinger, M. (2011) "Climate Change, Atmospheric Rivers, and Floods in California – A Multimodel Analysis of Storm Frequency and Magnitude Changes." JAWRA Journal of the American Water Resources Association 47, 514-523 DOI: https://doi.org/10.1111/j.1752-1688.2011.00546.x.

Duren, R. M., A. K. Thorpe, K. T. Foster, T. Rafiq, F. M. Hopkins, V. Yadav, B. D. Bue, D. R. Thompson, S. Conley, N. K. Colombi, C. Frankenberg, I. B. McCubbin, M. L. Eastwood, M. Falk, J. D. Herner, B. E. Croes, R. O. Green and C. E. Miller (2019). "California's methane super-emitters." Nature 575(7781): 180-184.

EEA. (2024). "Fire weather index." Retrieved July 25, 2024, from https://climate-adapt.eea.europa.eu/en/metadata/indicators/fire-weather-index.

Enayati Ahangar, F., P. Pakbin, S. Hasheminassab, S. A. Epstein, X. Li, A. Polidori and J. Low (2021). "Long-term trends of PM2.5 and its carbon content in the South Coast Air Basin: A focus on the impact of wildfires." Atmospheric Environment 255: 118431.

FEMA (2023). National Risk Index, Federal Emergency Management Agency.

Field, E. H. (2015) "UCERF3: A new earthquake forecast for California's complex fault system." Fact Sheet, 6 DOI: 10.3133/fs20153009.

Fierro, A. O. (2014) "Relationships between California rainfall variability and large-scale climate drivers." International Journal of Climatology 34, 3626-3640 DOI: 10.1002/joc.4112.

Fu, D., T. J. Pongetti, J. F. L. Blavier, T. J. Crawford, K. S. Manatt, G. C. Toon, K. W. Wong and S. P. Sander (2014). "Near-infrared remote sensing of Los Angeles trace gas distributions from a mountaintop site." Atmos. Meas. Tech. 7(3): 713-729.

Gariano, S. L. and F. Guzzetti (2016) "Landslides in a changing climate." Earth-Science Reviews 162, 227-252 DOI: 10.1016/j.earscirev.2016.08.011.

Gershunov, A., J. Guzman Morales, B. Hatchett, K. Guirguis, R. Aguilera, T. Shulgina, J. T. Abatzoglou, D. Cayan, D. Pierce, P. Williams, I. Small, R. Clemesha, L. Schwarz, T. Benmarhnia and A. Tardy (2021) "Hot and cold flavors of southern California's Santa Ana winds: their causes, trends, and links with wildfire." Climate Dynamics 57, 2233-2248 DOI: 10.1007/s00382-021-05802-z.

Guan, B. and D. E. Waliser (2024). "A regionally refined quarter-degree global atmospheric rivers database based on ERA5." Scientific Data 11(1): 440.

Gurney, K. R., R. Patarasuk, J. Liang, Y. Song, D. O'Keeffe, P. Rao, J. R. Whetstone, R. M. Duren, A. Eldering and C. Miller (2019). "The Hestia fossil fuel CO2 emissions data product for the Los Angeles megacity (Hestia-LA)." Earth Syst. Sci. Data 11(3): 1309-1335.

Guzman-Morales, J. and A. Gershunov (2019) "Climate Change Suppresses Santa Ana Winds of Southern California and Sharpens Their Seasonality." Geophysical Research Letters 46, 2772-2780 DOI: 10.1029/2018GL080261.

Hall, A., N. Berg and K. Reich (2018) "Los Angeles Summary Report. California's Fourth Climate Change Assessment."

Handwerger, A. L., E. J. Fielding, S. S. Sangha and D. P. S. Bekaert (2022) "Landslide Sensitivity and Response to Precipitation Changes in Wet and Dry Climates." Geophysical Research Letters 49, e2022GL099499 DOI: https://doi.org/10.1029/2022GL099499.

Harp, E. L. and R. W. Jibson (1996) "Landslides triggered by the 1994 Northridge, California, earthquake." Bulletin of the Seismological Society of America 86, S319-S332 DOI: 10.1785/bssa08601bs319.

Hasheminassab, S., N. Daher, B. D. Ostro and C. Sioutas (2014) "Long-term source apportionment of ambient fine particulate matter (PM2.5) in the Los Angeles Basin: A focus on emissions reduction from vehicular sources." Environmental Pollution 193, 54-64 DOI: 10.1016/j.envpol.2014.06.012.

He, M. and M. Gautam (2016) "Variability and Trends in Precipitation, Temperature and Drought Indices in the State of California." Hydrology 3, 14 DOI: 10.3390/hydrology3020014.

Hill, C. (2024) "Recounting a Harrowing Week at JPL's Table Mountain Facility." JPL Space 2024.

Hill, R. G., M. Weingarten, T. K. Rockwell and Y. Fialko (2023). "Major southern San Andreas earthquakes modulated by lake-filling events." Nature 618(7966): 761-766.

Ho, J. C., A. M. Michalak and N. Pahlevan (2019). "Widespread global increase in intense lake phytoplankton blooms since the 1980s." Nature 574(7780): 667-670.

Holsinger, L., S. A. Parks and C. Miller (2016) "Weather, fuels, and topography impede wildland fire spread in western US landscapes." Forest Ecology and Management 380, 59-69 DOI: 10.1016/j.foreco.2016.08.035.

Holt, B., R. Trinh and M. M. Gierach (2017). "Stormwater runoff plumes in the Southern California Bight: A comparison study with SAR and MODIS imagery." Marine Pollution Bulletin 118(1): 141-154.

Huang, X. and D. L. Swain (2022). "Climate change is increasing the risk of a California megaflood." Science Advances 8(32): eabq0995.

Huang, X., D. L. Swain and A. D. Hall (2020) "Future precipitation increase from very high resolution ensemble downscaling of extreme atmospheric river storms in California." Science Advances 6, eaba1323 DOI: 10.1126/sciadv.aba1323.

Hulley, G. C., B. Dousset and B. H. Kahn (2020) "Rising Trends in Heatwave Metrics Across Southern California." Earth's Future 8, e2020EF001480 DOI: 10.1029/2020EF001480.

Jeong, S., S. Newman, J. Zhang, A. E. Andrews, L. Bianco, J. Bagley, X. Cui, H. Graven, J. Kim, P. Salameh, B. W. LaFranchi, C. Priest, M. Campos-Pineda, E. Novakovskaia, C. D. Sloop, H. A. Michelsen, R. P. Bambha, R. F. Weiss, R. Keeling and M. L. Fischer (2016). "Estimating methane emissions in California's urban and rural regions using multitower observations." Journal of Geophysical Research: Atmospheres 121(21): 13,031-013,049.

Kean, J. W. and D. M. Staley (2021) "Forecasting the Frequency and Magnitude of Postfire Debris Flows Across Southern California." Earth's Future 9, e2020EF001735 DOI: 10.1029/2020EF001735.

Kiel, M., A. Eldering, D. D. Roten, J. C. Lin, S. Feng, R. Lei, T. Lauvaux, T. Oda, C. M. Roehl, J.-F. Blavier and L. T. Iraci (2021). "Urban-focused satellite CO2 observations from the Orbiting Carbon Observatory-3: A first look at the Los Angeles megacity." Remote Sensing of Environment 258: 112314.

Kirschbaum, D., T. Stanley and Y. Zhou (2015) "Spatial and temporal analysis of a global landslide catalog." Geomorphology 249, 4-15 DOI: 10.1016/j.geomorph.2015.03.016.

Knowles, N., M. D. Dettinger and D. R. Cayan (2006) "Trends in Snowfall versus Rainfall in the Western United States." Journal of Climate 19, 4545-4559 DOI: 10.1175/JCLI3850.1.

Lakshmikandan, M., M. Li and B. Pan (2024). "Cyanobacterial Blooms in Environmental Water: Causes and Solutions." Current Pollution Reports 10(4): 606-627.

Leggett, C., N. Scherer, M. Curry and R. Bailey (2014) "Assessing the Economic Benefits of Reductions in Marine Debris: A Pilot Study of Beach Recreation in Orange County, California."

Li, X., A. L. Handwerger, G. Peltzer and E. Fielding (2024) "Exploring the Behaviors of Initiated Progressive Failure and Slow-Moving Landslides in Los Angeles Using Satellite InSAR and Pixel Offset Tracking." Geophysical Research Letters 51, e2024GL108267 DOI: 10.1029/2024GL108267.

Li, Y., V. Ravi, G. Heath, J. Zhang, P. Vahmani, S.-M. Lee, X. Zhang, K. T. Sanders and G. A. Ban-Weiss (2024). "Air quality and public health co-benefits of 100% renewable electricity adoption and electrification pathways in Los Angeles." Environmental Research Letters 19(3): 034015.

Liu, P.-W., J. S. Famiglietti, A. J. Purdy, K. H. Adams, A. L. McEvoy, J. T. Reager, R. Bindlish, D. N. Wiese, C. H. David and M. Rodell (2022). "Groundwater depletion in California's Central Valley accelerates during megadrought." Nature Communications 13(1): 7825.

Madakumbura, G., C. Thackeray, A. Hall, P. Williams, J. Norris and R. Sukhdeo. (2025). "Climate Change a Factor in Unprecedented LA Fires." Retrieved February 26, 2025, from https://sustainablela.ucla.edu/2025lawildfires.

Margulis, S. A., G. Cortés, M. Girotto, L. S. Huning, D. Li and M. Durand (2016) "Characterizing the extreme 2015 snowpack deficit in the Sierra Nevada (USA) and the implications for drought recovery." Geophysical Research Letters 43, 6341-6349 DOI: 10.1002/2016GL068520.

Marshall, A. M., J. T. Abatzoglou, S. Rahimi, D. P. Lettenmaier and A. Hall (2024). "California's 2023 snow deluge: Contextualizing an extreme snow year against future climate change." Proceedings of the National Academy of Sciences 121(20): e2320600121.

Meehl, G. A., C. Tebaldi, G. Walton, D. Easterling and L. McDaniel (2009). "Relative increase of record high maximum temperatures compared to record low minimum temperatures in the U.S." Geophysical Research Letters 36(23).

Miller, J. B., S. J. Lehman, K. R. Verhulst, C. E. Miller, R. M. Duren, V. Yadav, S. Newman and C. D. Sloop (2020). "Large and seasonally varying biospheric CO₂ fluxes in the Los Angeles megacity revealed by atmospheric radiocarbon." Proceedings of the National Academy of Sciences 117(43): 26681-26687.

Miyazaki, K., K. W. Bowman, K. Yumimoto, T. Walker and K. Sudo (2020) "Evaluation of a multi-model, multi-constituent assimilation framework for tropospheric chemical reanalysis." Atmos. Chem. Phys. 20, 931-967 DOI: 10.5194/acp-20-931-2020.

Mizuta, R., H. Yoshimura, H. Murakami, M. Matsueda, H. Endo, T. Ose, K. Kamiguchi, M. Hosaka, M. Sugi, S. Yukimoto, S. Kusunoki and A. Kitoh (2012) "Climate Simulations Using MRI-AGCM3.2 with 20-km Grid." Journal of the Meteorological Society of Japan. Ser. II 90A, 233-258 DOI: 10.2151/jmsj.2012-A12.

Mote, P. W., A. F. Hamlet, M. P. Clark and D. P. Lettenmaier (2005) "Declining Mountain Snowpack in Western North America*." Bulletin of the American Meteorological Society 86, 39-50 DOI: 10.1175/BAMS-86-1-39.

Mote, P. W., S. Li, D. P. Lettenmaier, M. Xiao and R. Engel (2018) "Dramatic declines in snowpack in the western US." npj Climate and Atmospheric Science 1, 2 DOI: 10.1038/s41612-018-0012-1.

O'Neill, B. C., C. Tebaldi, D. P. van Vuuren, V. Eyring, P. Friedlingstein, G. Hurtt, R. Knutti, E. Kriegler, J. F. Lamarque, J. Lowe, G. A. Meehl, R. Moss, K. Riahi and B. M. Sanderson (2016) "The Scenario Model Intercomparison Project (ScenarioMIP) for CMIP6." Geosci. Model Dev. 9, 3461-3482 DOI: 10.5194/gmd-9-3461-2016.

O’Brien, T. A., M. F. Wehner, A. E. Payne, C. A. Shields, J. J. Rutz, L.-R. Leung, F. M. Ralph, A. Collow, I. Gorodetskaya, B. Guan, J. M. Lora, E. McClenny, K. M. Nardi, A. M. Ramos, R. Tomé, C. Sarangi, E. J. Shearer, P. A. Ullrich, C. Zarzycki, B. Loring, H. Huang, H. A. Inda-Díaz, A. M. Rhoades and Y. Zhou (2022). "Increases in Future AR Count and Size: Overview of the ARTMIP Tier 2 CMIP5/6 Experiment." Journal of Geophysical Research: Atmospheres 127(6): e2021JD036013.

Parazoo, N. C., R. W. Coleman, V. Yadav, E. N. Stavros, G. Hulley and L. Hutyra (2022). "Diverse biosphere influence on carbon and heat in mixed urban Mediterranean landscape revealed by high resolution thermal and optical remote sensing." Science of The Total Environment 806: 151335.

Payne, A. E., M.-E. Demory, L. R. Leung, A. M. Ramos, C. A. Shields, J. J. Rutz, N. Siler, G. Villarini, A. Hall and F. M. Ralph (2020) "Responses and impacts of atmospheric rivers to climate change." Nature Reviews Earth & Environment 1, 143-157 DOI: 10.1038/s43017-020-0030-5.

Perkins, S. E. and L. V. Alexander (2013). "On the Measurement of Heat Waves." Journal of Climate 26(13): 4500-4517.

Persad, G. G., D. L. Swain, C. Kouba and J. P. Ortiz-Partida (2020). "Inter-model agreement on projected shifts in California hydroclimate characteristics critical to water management." Climatic Change 162(3): 1493-1513.

Potapov, P., M. C. Hansen, A. Pickens, A. Hernandez-Serna, A. Tyukavina, S. Turubanova, V. Zalles, X. Li, A. Khan, F. Stolle, N. Harris, X.-P. Song, A. Baggett, I. Kommareddy and A. Kommareddy (2022) "The Global 2000-2020 Land Cover and Land Use Change Dataset Derived From the Landsat Archive: First Results." Frontiers in Remote Sensing 3 DOI: 10.3389/frsen.2022.856903.

Ralph, F. M., P. J. Neiman, G. A. Wick, S. I. Gutman, M. D. Dettinger, D. R. Cayan and A. B. White (2006) "Flooding on California's Russian River: Role of atmospheric rivers." Geophysical Research Letters 33 DOI: 10.1029/2006GL026689.

Rosenzweig, C., R. Horton, I. S. Higuchi and C. Hudson (2011) "NASA’s CASI: Building Climate-Resilient NASA Centers." Livebetter Magazine 15.

Roten, D., J. C. Lin, S. Das and E. A. Kort (2023). "Constraining Sector-Specific CO2 Fluxes Using Space-Based XCO2 Observations Over the Los Angeles Basin." Geophysical Research Letters 50(21): e2023GL104376.

Schwandner, F. M., M. R. Gunson, C. E. Miller, S. A. Carn, A. Eldering, T. Krings, K. R. Verhulst, D. S. Schimel, H. M. Nguyen, D. Crisp, C. W. O’Dell, G. B. Osterman, L. T. Iraci and J. R. Podolske (2017). "Spaceborne detection of localized carbon dioxide sources." Science 358(6360): eaam5782.

Siirila-Woodburn, E. R., A. M. Rhoades, B. J. Hatchett, L. S. Huning, J. Szinai, C. Tague, P. S. Nico, D. R. Feldman, A. D. Jones, W. D. Collins and L. Kaatz (2021) "A low-to-no snow future and its impacts on water resources in the western United States." Nature Reviews Earth & Environment 2, 800-819 DOI: 10.1038/s43017-021-00219-y.

South Coast Air Quality Management District (2021). Multiple Air Toxics Exposure Study V (MATES V).

South Coast Air Quality Management District (2022). 2022 Air Quality Management Plan.

Stewart, I. T., D. R. Cayan and M. D. Dettinger (2005) "Changes toward Earlier Streamflow Timing across Western North America." Journal of Climate 18, 1136-1155 DOI: 10.1175/JCLI3321.1.

Swain, D. L., B. Langenbrunner, J. D. Neelin and A. Hall (2018). "Increasing precipitation volatility in twenty-first-century California." Nature Climate Change 8(5): 427-433.

Sweet, W. V., B. D. Hamlington, R. E. Kopp, C. P. Weaver, P. L. Barnard, D. Bekaert, W. Brooks, M. Craghan, G. Dusek and T. Frederikse (2022). Global and Regional Sea Level Rise Scenarios for the United States: Updated Mean Projections and Extreme Weather Level Probabilities along US Coastlines.

Thompson, D. R., A. K. Thorpe, C. Frankenberg, R. O. Green, R. Duren, L. Guanter, A. Hollstein, E. Middleton, L. Ong and S. Ungar (2016). "Space-based remote imaging spectroscopy of the Aliso Canyon CH4 superemitter." Geophysical Research Letters 43(12): 6571-6578.

Thorpe, A. K., R. M. Duren, S. Conley, K. R. Prasad, B. D. Bue, V. Yadav, K. T. Foster, T. Rafiq, F. M. Hopkins, M. L. Smith, M. L. Fischer, D. R. Thompson, C. Frankenberg, I. B. McCubbin, M. L. Eastwood, R. O. Green and C. E. Miller (2020). "Methane emissions from underground gas storage in California." Environmental Research Letters 15(4): 045005.

Thorpe, A. K., R. O. Green, D. R. Thompson, P. G. Brodrick, J. W. Chapman, C. D. Elder, I. Irakulis-Loitxate, D. H. Cusworth, A. K. Ayasse, R. M. Duren, C. Frankenberg, L. Guanter, J. R. Worden, P. E. Dennison, D. A. Roberts, K. D. Chadwick, M. L. Eastwood, J. E. Fahlen and C. E. Miller (2023). "Attribution of individual methane and carbon dioxide emission sources using EMIT observations from space." Science Advances 9(46): eadh2391.

Thorpe, A. K., R. O. Green, D. R. Thompson, P. G. Brodrick, A. Chlus, J. E. Fahlen, R. W. Coleman, K. D. Chadwick and M. L. Eastwood (2024). Attributing Methane and CO2 Plumes by Emission Sector with the EMIT and AVIRIS-3 Imaging Spectrometers. IGARSS 2024 - 2024 IEEE International Geoscience and Remote Sensing Symposium.

Tyukavina, A., P. Potapov, M. C. Hansen, A. H. Pickens, S. V. Stehman, S. Turubanova, D. Parker, V. Zalles, A. Lima, I. Kommareddy, X.-P. Song, L. Wang and N. Harris (2022) "Global Trends of Forest Loss Due to Fire From 2001 to 2019." Frontiers in Remote Sensing 3 DOI: 10.3389/frsen.2022.825190.

USGCRP (2023). Fifth National Climate Assessment. Washington, DC, USA, U.S. Global Change Research Program.

Verhulst, K. R., A. Karion, J. Kim, P. K. Salameh, R. F. Keeling, S. Newman, J. Miller, C. Sloop, T. Pongetti, P. Rao, C. Wong, F. M. Hopkins, V. Yadav, R. F. Weiss, R. M. Duren and C. E. Miller (2017). "Carbon dioxide and methane measurements from the Los Angeles Megacity Carbon Project – Part 1: calibration, urban enhancements, and uncertainty estimates." Atmos. Chem. Phys. 17(13): 8313-8341.

Weber, C., J. Antczak and J. Watson (2024) "Record-setting storm that killed 3 dumps rain on Los Angeles; flash flood alerts still in effect." The Associated Press.

Wiley, D. Y. and R. A. McPherson (2024). "The Role of Climate Change in the Proliferation of Freshwater Harmful Algal Blooms in Inland Water Bodies of the United States." Earth Interactions 28(1): e230008.

Wu, A. X., A. E. Moe and T. P. Enriquez (2024). 2023---2024 Beach Report Card.

Wu, D., J. Liu, P. O. Wennberg, P. I. Palmer, R. R. Nelson, M. Kiel and A. Eldering (2022). "Towards sector-based attribution using intra-city variations in satellite-based emission ratios between CO2 and CO." Atmos. Chem. Phys. 22(22): 14547-14570.

Yoon, J.-H., S. Y. S. Wang, R. R. Gillies, B. Kravitz, L. Hipps and P. J. Rasch (2015). "Increasing water cycle extremes in California and in relation to ENSO cycle under global warming." Nature Communications 6(1): 8657.

Zeng, Z.-C., T. Pongetti, S. Newman, T. Oda, K. Gurney, P. I. Palmer, Y. L. Yung and S. P. Sander (2023). "Decadal decrease in Los Angeles methane emissions is much smaller than bottom-up estimates." Nature Communications 14(1): 5353.

Zhao, Y., Y. Li, Y. Li, A. Kumar, Q. Ying and M. J. Kleeman (2024) "Reducing southern California ozone concentrations in the year 2050 under a low carbon energy scenario." Atmospheric Environment 320, 120315 DOI: 10.1016/j.atmosenv.2023.120315.

Zhu, S., J. R. Horne, M. Mac Kinnon, G. S. Samuelsen and D. Dabdub (2019) "Comprehensively assessing the drivers of future air quality in California." Environment International 125, 386-398 DOI: 10.1016/j.envint.2019.02.007.

’25

National Aeronautics and Space Administration

Jet Propulsion Laboratory
California Institute of Technology
Pasadena, California

www.nasa.gov

4/2025